

University of Windsor

Scholarship at UWindor

Electronic Theses and Dissertations

Theses, Dissertations, and Major Papers

2008

Mechanisms controlling the microchemistry and composition of fish otoliths

Sonia Melancon
University of Windsor

Follow this and additional works at: <https://scholar.uwindsor.ca/etd>

Recommended Citation

Melancon, Sonia, "Mechanisms controlling the microchemistry and composition of fish otoliths" (2008). *Electronic Theses and Dissertations*. 8063.
<https://scholar.uwindsor.ca/etd/8063>

This online database contains the full-text of PhD dissertations and Masters' theses of University of Windsor students from 1954 forward. These documents are made available for personal study and research purposes only, in accordance with the Canadian Copyright Act and the Creative Commons license—CC BY-NC-ND (Attribution, Non-Commercial, No Derivative Works). Under this license, works must always be attributed to the copyright holder (original author), cannot be used for any commercial purposes, and may not be altered. Any other use would require the permission of the copyright holder. Students may inquire about withdrawing their dissertation and/or thesis from this database. For additional inquiries, please contact the repository administrator via email (scholarship@uwindsor.ca) or by telephone at 519-253-3000ext. 3208.

Mechanisms controlling the microchemistry and composition of fish otoliths

By

Sonia Melançon

**A Dissertation
Submitted to the Faculty of Graduate Studies
through the Great Lakes Institute for Environmental Research
in Partial Fulfillment of the Requirements for
the Degree of Doctor of Philosophy at the
University of Windsor**

Windsor, Ontario, Canada

2008

© 2008 Sonia Melançon



Library and
Archives Canada

Bibliothèque et
Archives Canada

Published Heritage
Branch

Direction du
Patrimoine de l'édition

395 Wellington Street
Ottawa ON K1A 0N4
Canada

395, rue Wellington
Ottawa ON K1A 0N4
Canada

Your file Votre référence
ISBN: 978-0-494-42375-2
Our file Notre référence
ISBN: 978-0-494-42375-2

NOTICE:

The author has granted a non-exclusive license allowing Library and Archives Canada to reproduce, publish, archive, preserve, conserve, communicate to the public by telecommunication or on the Internet, loan, distribute and sell theses worldwide, for commercial or non-commercial purposes, in microform, paper, electronic and/or any other formats.

The author retains copyright ownership and moral rights in this thesis. Neither the thesis nor substantial extracts from it may be printed or otherwise reproduced without the author's permission.

AVIS:

L'auteur a accordé une licence non exclusive permettant à la Bibliothèque et Archives Canada de reproduire, publier, archiver, sauvegarder, conserver, transmettre au public par télécommunication ou par l'Internet, prêter, distribuer et vendre des thèses partout dans le monde, à des fins commerciales ou autres, sur support microforme, papier, électronique et/ou autres formats.

L'auteur conserve la propriété du droit d'auteur et des droits moraux qui protègent cette thèse. Ni la thèse ni des extraits substantiels de celle-ci ne doivent être imprimés ou autrement reproduits sans son autorisation.

In compliance with the Canadian Privacy Act some supporting forms may have been removed from this thesis.

Conformément à la loi canadienne sur la protection de la vie privée, quelques formulaires secondaires ont été enlevés de cette thèse.

While these forms may be included in the document page count, their removal does not represent any loss of content from the thesis.

Bien que ces formulaires aient inclus dans la pagination, il n'y aura aucun contenu manquant.


Canada

DECLARATION OF CO-AUTHORSHIP / PREVIOUS PUBLICATIONS

I. Co-Authorship Declaration

I hereby declare that this thesis incorporates material that is result of joint research, as follows:

This thesis also incorporates the outcome of joint research undertaken in collaboration with Stuart Ludsin from NOAA. The collaboration is covered in Chapter 2 of the thesis. In all cases, the key ideas, primary contributions, experimental designs, data analysis and interpretation, were performed by the author, and the contribution of co-authors was primarily through the provision of samples and ideas for the material and methods section.

I am aware of the University of Windsor Senate Policy on Authorship and I certify that I have properly acknowledged the contribution of other researchers to my thesis, and have obtained written permission from each of the co-author(s) to include the above material(s) in my thesis.

I certify that, with the above qualification, this thesis, and the research to which it refers, is the product of my own work.

II. Declaration of Previous Publication

This thesis includes 3 original papers that have been previously published/submitted for publication in peer reviewed journals, as follows:

Thesis Chapter	Publication title/full citation	Publication status*
<i>Chapter 2</i>	Melançon S., B.J. Fryer, J.E. Gagnon, S.A. Ludsin and Z. Yang. 2005. Effects of crystal structure on the uptake of metals by lake trout (<i>Salvelinus namaycush</i>) otoliths. Canadian Journal of Fisheries and Aquatic Sciences. 62 : 2609-2619.	<i>Published</i>
<i>Chapter 3</i>	Melançon S., B.J. Fryer, Z. Yang., J.E. Gagnon and S.A. Ludsin. Biomineralization in fresh water fish: Micro-geochemical tools and approaches to understanding and solving fisheries issues. Accepted to Mineralogical Magazine on 11 April 2008.	<i>Accepted</i>
<i>Chapter 4</i>	Melançon S., B.J. Fryer, and J.L. Markham. Chemical analysis of the endolymph and the growing otolith: fractionation of metals in freshwater fish species. Submitted to Canadian Journal of Fisheries and Aquatic Sciences on 20 February 2008.	<i>Submitted</i>

I certify that I have obtained a written permission from the copyright owner(s) to include the above published material(s) in my thesis. Chapter 2 is reprinted with the permission of National Research Council of Canada (Appendix). I certify that the above material describes work completed during my registration as graduate student at the University of Windsor.

I declare that, to the best of my knowledge, my thesis does not infringe upon anyone's copyright nor violate any proprietary rights and that any ideas, techniques, quotations, or any other material from the work of other people included in my thesis, published or otherwise, are fully acknowledged in accordance with the standard referencing practices. Furthermore, to the extent that I have included copyrighted material that surpasses the bounds of fair dealing within the meaning of the Canada Copyright Act, I certify that I have obtained a written permission from the copyright owner(s) to include such material(s) in my thesis.

I declare that this is a true copy of my thesis, including any final revisions, as approved by my thesis committee and the Graduate Studies office, and that this thesis has not been submitted for a higher degree to any other University of Institution.

ABSTRACT

Understanding the growth and composition of otoliths continues to be a fundamental challenge for chemists and biologists. Since the recognition of the daily increment pattern in the 1970s, there has been a growing interest in otolith microstructure. The purpose of my Ph.D. dissertation was to understand the mechanisms controlling otolith microchemistry and the factors affecting metal uptake in fish otoliths. In Chapter 2, I utilized chemical and spectroscopic analyses of vaterite and aragonite growth in sagittal otoliths of lake trout in an effort to better understand the crystalline growth process. I was also interested in learning about the elemental partitioning of metals. Chapter 3 investigated the nucleation of otoliths to determine how otoliths crystallized and if there was a catalyst that would help the crystallization. I also wanted to see how that affected elemental uptake. A preliminary study, conducted on walleye (*Sander vitreus*) endolymph and otolith composition is also included where the fractionation of metals is investigated. In Chapter 4, metal partitioning between otolith and endolymph of two freshwater species: lake trout (*Salvelinus namaycush*) and burbot (*Lota lota*) is studied. In this chapter I also analyzed blood and surface water to give new insights on the partitioning of metals between these filters. Lastly, Chapter 5 explored the turnover rates of barium and strontium in the blood, bones, whole bodies and otoliths of yellow perch (*Perca flavescens*) using enriched isotope tracers (strontium and barium). The ultimate goal of this research is to improve the ability of scientists to use otolith microchemical investigations for fisheries-related research and management.

ACKNOWLEDGEMENTS

Firstly, I would like to thank my advisor and mentor, Brian J. Fryer, for his guidance over the past 5 years and for always believing in my research abilities. He taught me that there is nothing out of reach in research and you can work towards answering any questions. I am deeply grateful that he took a chance on me as I had never studied in an English environment before. I became his “favourite Francophone/French Canadian student” and the rest is history. I really could have never asked for a better Boss.

I am also grateful to my final committee members: Ken Drouillard, Norm Halden, Iain Samson and Chris Weisener; and the other members who sat on my committee at some point during my Ph.D.: Dan Heath, David Fowle and Peter Sale.

I also thank the following lab members for their assistance in the lab and preparation of otolith samples: my *favorite* American Carrol P. Hand and my summer student Caroline Dennis (a.k.a. Little One). My best friend, Christina “Flashy” Smeaton, deserves a special thank you for her unconditional friendship. She made conferences in Cowboy-land, synchrotron trips and after-hours liquid nitrogen experiments unforgettable. There are a lot of people at GLIER who I will never forget: Zhe (Max) Song, Cara Holcombe, Zhaoping Yang, Joel E. Gagnon, Magda Scarlet, Mohammed Shaheen, Andy Bramburger, Jill Olin and Mary Lou Scratch. I think it is also important to say a big thanks to all the fish that sacrificed their life in the name of research during my numerous Ph.D. projects.

Throughout my education several professors inspired me to go forward with my education and I know I wouldn't be here without them. I would like to acknowledge them here: Davit Zargarian (Université de Montréal), Michel Robitaille (Collège de Maisonneuve) and Clément Timmons (Collège Ville-Marie).

When I chose to move to Windsor for my graduate studies, it was a big decision as I had never lived far away from my family. The calls, letters, care packages and annual visits from my parents made a big difference for me. Je voudrais donc dire un merci tout particulier et en français à mes parents, Monique and Roger, pour tout le support qu'ils m'ont apporté au cours des dernières années.

I would also like to thank my big brother Yannik who has always been an inspiration to me. I admired his drive to succeed in University and wanted to follow in his steps. He was a great example for his little sister.

Lastly, I would like to thank my loyal friend and canine companion, Rocky, for his comforting presence and wet kisses.

TABLE OF CONTENTS

DECLARATION OF CO-AUTHORSHIP / PREVIOUS PUBLICATIONS	III
ABSTRACT	VI
ACKNOWLEDGEMENTS	VII
LIST OF TABLES.....	XII
LIST OF FIGURES.....	XIV
LIST OF ABBREVIATIONS & SYMBOLS	XVII
CHAPTER 1	1
1.1 INTRODUCTION.....	2
1.2 STATEMENT OF PROBLEM.....	4
1.3 OBJECTIVES OF THE DISSERTATION	4
1.4 REFERENCES.....	7
CHAPTER 2	9
2.1 INTRODUCTION.....	10
2.2 MATERIALS AND METHODS	12
2.2.1 Fish and otolith preparation	12
2.2.2 Raman spectroscopy.....	13
2.2.3 Laser ablation-inductively coupled plasma-mass spectrometry (LA-ICP-MS)	14
2.3 RESULTS.....	16
2.3.1 Microscopic observations.....	16
2.3.2. Aragonite and vaterite growth relationships.....	17
2.3.3 Microchemistry of aragonite and vaterite	18
2.3.4 Otolith elemental partitioning	20
2.4 DISCUSSION.....	21
2.4.1 Microchemistry of aragonite and vaterite	21
2.4.2 Possible mechanisms causing vaterite growth.....	24

2.4.3 Implications	27
2.5 REFERENCES.....	29
CHAPTER 3	44
3.1 INTRODUCTION.....	45
3.2 MATERIALS AND METHODS	47
3.3 RESULTS AND DISCUSSION.....	48
3.3.1: Nucleation of otolith growth	48
3.3.2: Flux of metals to the growing otolith.....	52
3.3.3: Effect of crystal structure on element partitioning.....	54
3.4 CONCLUSIONS.....	56
3.5 ACKNOWLEDGEMENTS	56
3.6 REFERENCES.....	58
CHAPTER 4	71
4.1 INTRODUCTION.....	72
4.2 MATERIALS AND METHODS	75
4.2.1 Collection of endolymph and otolith extraction.....	75
4.2.2 Collection of blood and water	76
4.2.3 Inductively coupled plasma-mass spectrometry	77
4.3 RESULTS.....	78
4.3.1 Endolymph and Otoliths	78
4.3.2 Water and Blood.....	81
4.3.3 Partition coefficients (K_{Ds}).....	81
4.4 DISCUSSION.....	83
4.4.1 Endolymph chemistry	83
4.4.2 Otolith-endolymph relationships.....	84
4.4.3 Blood chemistry	85
4.4.4 Fractionation of metals by fish	86
4.4.5 Water versus otolith	87

4.5 CONCLUSIONS	88
4.6 ACKNOWLEDGEMENTS	89
4.7 REFERENCES.....	90
CHAPTER 5	104
5.1 INTRODUCTION.....	105
5.2 MATERIAL AND METHODS.....	107
5.2.1 Laboratory experiment.....	107
5.2.2 Sample extraction and preparation	108
5.2.3 Chemical Analysis.....	110
5.3 RESULTS AND DISCUSSION.....	111
5.3.1 Sr and Ba isotopic ratios in water and blood	111
5.3.2 Otolith, bone and body chemistry	112
5.3.3 Implications	117
5.4 ACKNOWLEDGEMENT	119
5.5 REFERENCES.....	119
CHAPTER 6	133
6.1 INTRODUCTION.....	134
6.2 SUMMARY OF THESIS.....	134
6.3 CHALLENGES FOR THE FUTURE.....	138
6.4 REFERENCES.....	142
APPENDIX A.....	145
VITA AUCTORIS.....	146

LIST OF TABLES

Table 2.1: Mean metal concentrations in the cores and the edges of lake trout (<i>Salvelinus namaycush</i>). Edge results are divided based on the crystal growth: vaterite > aragonite or vaterite < aragonite (units: $\mu\text{g metal}\cdot\text{g}^{-1}$ calcium \pm 1 standard error). Elements are arranged by ionic charges (+1 for Li and Rb; +2 for the rest) and then by cation radii sizes. All edge and core (aragonite only) concentrations were from individuals that spent their entire existence in the hatchery. The vaterite core concentrations were derived from two hatchery-reared fish that were recaptured in Lake Erie (i.e., the core chemistry reflects the hatchery environment) and a single individual that resided solely in the hatchery.	34
Table 2.2: Values of partition coefficients ($K_D \pm$ 1 standard error) for the edge and core of hatchery-reared lake trout. Elements are listed by ionic charges and cation radii sizes.	35
Table 2.3: Metals size differences in ionic radii from calcium (Ca^{2+}) in the CaCO_3 crystal. Elements are classified by ionic charges (+1 at the top of table and +2 at bottom) and cation radii sizes.	36
Table 3.1: Mean metal concentrations (ppm) in the Lake Erie water (western basin), the endolymph and the growing edges of walleye otoliths. Values of partition coefficients $K_{D(E/W)}$, $K_{D(O/E)}$ and $K_{D(O/W)}$ are also shown.	62
Table 3.2: Mean metal concentrations (ppm) in the growing edges of Broodstock lake trout otoliths.	63
Table 4.1: Mean metal concentrations in the endolymph and otoliths of burbot and lake trout (units: ppm \pm 1 standard error). Otoliths are divided by crystalline structure (aragonite and vaterite) for lake trout. Burbot only has one type of CaCO_3 polymorph: aragonite.	96
Table 4.2: Mean metal concentrations for Lake Erie western basin water and the blood of lake trout and burbot (units: ppm \pm 1 standard error).	97
Table 4.3: Partition coefficient values for Lake trout and Burbot fish (KDs). Partition coefficients between: blood and water ($KD(B/W)$), endolymph and blood ($KD(E/B)$), otolith and endolymph ($KD(O/E)$), and otolith and water ($KD(O/W)$), for both polymorphs (Arag: aragonite and Vat: vaterite).	98
Table 4.4: Comparison with literature values of partition coefficients between the otolith and the water $D(O/W)$ for Ba, Sr and Mn in aragonite for different fish species and type of experiments (laboratory versus in the field). The type of water is indicated by the following letters: S for saltwater, F for freshwater and B for	

brackish water. Note that data is for aragonitic otoliths with the only data for vaterite in the table presenting an asterisk (*) and is from this study. 99

Table 5.1: Composition of the injections for Sr and Ba ratios and the amount of enriched ^{84}Sr and ^{135}Ba isotopes injected (μg per g of fish). 122

Table 5.2: Measured values for the average $^{84}\text{Sr}/^{86}\text{Sr}$ and $^{35}\text{Ba}/^{138}\text{Ba}$ ratios in water, fish blood (except for Sr), whole bodies (July and October) and otoliths (July, October and maximum) of yellow perch (*Perca flavescens*). Ratios are calculated considering the sensitivity factor matrix of each isotope and are the average of the number of ratios (\pm standard deviation). N is the number of samples analysed per treatment (except for water where control/low and medium/high were in the same tank). Otolith data was analysed by LA-ICP-MS while all the other parameters were analysed by SO-ICP-MS..... 123

Table 5.3: Average concentrations for Sr and Ba (calculated from ^{86}Sr and ^{138}Ba intensities) in water, fish blood, whole bodies (July and October) and otoliths (July, October and maximum) of yellow perch (*Perca flavescens*) in ppm ($\mu\text{g}/\text{g} \pm$ standard deviation). N is the number of samples analysed per treatment (except for water where control/low and medium/high were in the same tank). Otolith data was analysed by LA-ICP-MS while all the other parameters were analysed by SO-ICP-MS. 125

LIST OF FIGURES

- Figure 1.1: Example of the location and size of the three types of otoliths..... 3
- Figure 2.1: Sagittal otoliths from age-11 lake trout (*Salvelinus namaycush*) that spent their entire existence in captivity. (a) Otolith with vaterite growth being greater than aragonite growth. (b) Otolith with aragonite growth being greater than vaterite growth..... 37
- Figure 2.2: (a) Transition (contact) zone between aragonite and vaterite for an otolith of an 11-yr old hatchery-reared lake trout (*Salvelinus namaycush*) under transmitted light. Notice the 'waviness' of the growth bands in vaterite, as compared to aragonite. The box in (a) is shown in more detail in (b). The arrow in (b) represents the direction of the Raman mapping done on the boundary zone. 38
- Figure 2.3: Vateritic formations in lake trout (*Salvelinus namaycush*) otoliths: (a) Aragonitic core with the transition zone one side and aragonite edge on the other; (b) vateritic and aragonitic core with the transition zone on both sides; and (c) vateritic core with one vateritic and one edge aragonitic edge..... 39
- Figure 2.4: Wave numbers from the Raman spectroscopy analysis of aragonite and vaterite portions of a hatchery-reared lake trout (*Salvelinus namaycush*) that spent its entire existence in the Allegheny National Fish Hatchery (this is the same individual as in Fig. 2a). The patterns presented were typical of 12 other broodstock analyzed with Raman spectroscopy. In arbitrary units plotted against Raman shift in cm^{-1} . Represented are (a) lattice modes, (b) in-plane bending (ν_4) of C-O from carbonate anion bonded to Ca, and (c) symmetric stretching (ν_1) of CO_3^{2-} anions. (d) Raman mapping (symmetric stretching only) through the boundary zone, as shown in Fig. 1b, demonstrating the transition from aragonite to vaterite for the same sample. 40
- Figure 2.5: Transition from aragonite to vaterite in trace metal concentrations perpendicular to the transition zone between aragonite and vaterite boundary like in Fig 2b. of a hatchery-reared lake trout (*Salvelinus namaycush*). Elemental concentrations were quantified along this transect using LA-ICP-MS. Barium is represented by a solid line, magnesium is portrayed by small dashed line (- - - -), manganese by large dashed line (— — —), and strontium is depicted by the following sequence of large and small dashed line (— - - -)..... 41
- Figure 2.6: Concentrations of metal in aragonite versus vaterite from the hatchery-reared lake trout (*Salvelinus namaycush*) otolith edges (units: mg metal/Kg calcium): (a) lithium ($R^2 = 0.99$, $p < 0.001$), (b) magnesium ($R^2 = 0.27$; $p = 0.07$), (c) manganese ($R^2 = 0.09$; $p = 0.32$), (d) zinc ($R^2 = 0.02$; $p = 0.69$), (e) rubidium ($R^2 = 0.26$; $p = 0.08$), (f) strontium ($R^2 = 0.50$; $p < 0.01$), and (g)

barium ($R^2 = 0.35$ $p = 0.03$). Dashed lines, shown on some plots, are one-to-one lines. Regression equations and regression dashed lines are shown. 42

Figure 2.7: Crystallization process of otolith. Arrows portray elements that are mainly incorporated in each crystalline polymorph (vaterite versus aragonite) from the endolymph. Text boxes indicate what is enriched in the residual fluid, after elemental incorporation into the otolith. Differential incorporation of metals into the otolith portions consisting of vaterite versus aragonite would theoretically cause a gradient in the endolymph that might influence future otolith concentration changes. 43

Figure 3.1: Yellow perch (*Perca flavescens*) otolith showing daily growth increments and multiple nucleation sites (primordia) in the core. The core is identified in between the arrows and several primordia have been shown. 64

Figure 3.2: Rainbow trout (*Oncorhynchus mykiss*) otolith showing multiple nucleation sites (primordia) in the core as well as subsequent growth initiated around the individual primordia. Some of the primordia are identified with the arrows. 65

Figure 3.3: Concentration profiles of Mn (ppm) in the otolith cores of (a) Yellow perch (*Perca flavescens*) and (b) cisco (*Coregonus artedii*). Distance is from one edge of the otolith to the other with the laser transect passing through the middle of the core. 66

Figure 3.4: Sagittal otolith from age-11 walleye (*Sander vitreus*). Yearly growth bands are indicated by white dots and LA-ICP-MS analyses were conducted on the edge of the year 11 growth band. 67

Figure 3.5: Comparison of metal concentrations of the endolymph of walleye a) Ca/K, b) Ca/Na, c) K/Na and d) Zn/Cu 68

Figure 3.6: Lake trout (*Salvelinus namaycush*) otoliths showing the simultaneous growth of aragonite and vaterite. The 'waviness' of the vaterite growth bands can be easily differentiated petrographically compared to the regular aragonite growth bands. 69

Figure 3.7: Wave numbers from the Raman spectroscopy analysis of aragonite and vaterite in lake trout otolith edges in arbitrary units plotted against Raman shift in cm^{-1} . Vaterite signal is on top and aragonite is at the bottom. Symmetric stretching (ν_1) values are presented on the Raman graph for both polymorphs. 70

Figure 4.1: Comparison of our proximal endolymph composition (ppm) for Na, Mg, K, Ca and Sr of burbot (black) and lake trout (white) to the literature values for cod's endolymph (horizontal lines) from Kalish (1991), rainbow trout (grey) and turbot (backward slash) proximal endolymph from Payan et al. (1999). 100

Figure 4.2: Relationship between metals (ppm) in the endolymph of burbot (▲) and lake trout (●). (a) Na/K (▲ $R^2 = 0.67$, $p < 0.0001$; ● $R^2 = 0.09$, $p = 0.36$); (b) Rb/K (▲ $R^2 = 0.76$, $p < 0.0001$; ● $R^2 = 0.72$, $p = 0.001$); (c) Na/Ca (▲ $R^2 = 0.03$, $p = 0.49$; ● $R^2 = 0.79$, $p < 0.0001$); (d) Mn/Ca (▲ $R^2 = 0.51$, $p = 0.001$; ● $R^2 = 0.07$, $p = 0.44$); (e) Na/Rb (▲ $R^2 = 0.64$, $p < 0.0001$; ● $R^2 = 0.02$, $p = 0.71$); (f) Zn/Pb (▲ $R^2 = 0.43$, $p = 0.003$; ● $R^2 = 0.29$, $p = 0.09$)..... 101

Figure 4.3: Relationship between metals (ppm) in the endolymph and the otoliths of burbot (▲) and lake trout, aragonitic otoliths (●) and vateritic otoliths (■). (a) Sodium; (b) Mg; (c) K; (d) Mn; (e) Zn; (f) Ba; (g) Sr and (h) Pb..... 102

Figure 4.4: Partition coefficients between: a) blood and water ($K_{D(B/W)}$), b), endolymph and blood ($K_{D(E/B)}$), c) otolith and endolymph ($K_{D(O/E)}$), and d) otolith and water ($K_{D(O/W)}$) for burbot (▲) and lake trout, aragonitic otoliths (●) and vateritic otoliths (■). For a) $K_{D(B/W)}$ and b) $K_{D(E/B)}$ the following symbol (●) is not related to a specific polymorph..... 103

Figure 5.1: Experimental setting of the tanks. Control and low treatment are in the same tank physically separated by a net. The same setting applies to the medium and high level treatments. 127

Figure 5.2: Isotopic ratios: $^{84}\text{Sr}/^{86}\text{Sr}$ (▲) and $^{135}\text{Ba}/^{138}\text{Ba}$ (○) in otoliths of yellow perch (*Perca flavescens*) along the beam transect using laser ablation with inductively coupled plasma mass spectrometry. Distance from the core to the edge of single otoliths from the different treatments a) control, b) low, c) medium and d) high. 128

Figure 5.3: An example from the high level treatment of the isotopic ratios: $^{84}\text{Sr}/^{86}\text{Sr}$ (▲) and $^{135}\text{Ba}/^{138}\text{Ba}$ (○) in otoliths of yellow perch (*Perca flavescens*) against time in days after the injections were administered (Day 0: Inj.). The maximums, fish sampled in July and at the end are shown with appropriate arrows. Dotted line represents average $^{135}\text{Ba}/^{138}\text{Ba}$ ratio in control fish otoliths and full line is the $^{84}\text{Sr}/^{86}\text{Sr}$ ratio 129

Figure 5.4: Fish bone from the high level treatment, the white arrow represents the path of the laser beam on the bone using LA-ICP-MS 130

Figure 5.5: Isotopic ratios: $^{84}\text{Sr}/^{86}\text{Sr}$ (▲) and $^{135}\text{Ba}/^{138}\text{Ba}$ (○) in bones of yellow perch (*Perca flavescens*) along the beam transect using laser ablation with inductively coupled plasma mass spectrometry. Distance is from the one edge of the bone to the other. Each treatment profiled: a) control, b) low, c) medium and d) high. Dotted line represents average $^{135}\text{Ba}/^{138}\text{Ba}$ ratio in control fish bones and full line is the $^{84}\text{Sr}/^{86}\text{Sr}$ ratio. 131

LIST OF ABBREVIATIONS & SYMBOLS

ANOVA	Analysis of variance
DIC	Dissolved inorganic carbon
ICP-MS	Inductively coupled plasma- mass spectrometry
K_D	Partition coefficient between aragonite and vaterite
$K_{D(B/W)}$	Partition coefficient between blood and water
$K_{D(E/B)}$	Partition coefficient between endolymph and blood
$K_{D(O/E)}$	Partition coefficient between otolith and endolymph
$K_{D(O/W)}$	Partition coefficient between otolith and water
LA-ICP-MS	Laser ablation-ICP-MS
LOD	Limits of detection
ppm	Parts per million
R^2	Linear regression coefficient
RBCs	Red blood cells
SD	Standard deviation
SO-ICP-MS	Solution-ICP-MS
Wt%	Weight percent
YOY	Young of the year

CHAPTER 1

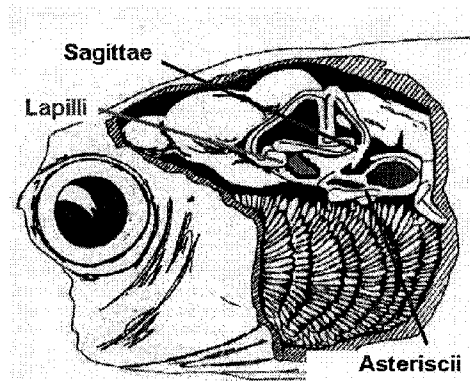
GENERAL INTRODUCTION

1.1 INTRODUCTION

Understanding the influences on growth and composition of otoliths continues to be a fundamental challenge for environmental chemists and biologists. Since the recognition of the daily increment pattern in the 1970s, there has been a growing interest in otolith microstructure examination (Pannella 1971; Campana 1999).

There are three pairs of otoliths: the lapillus, the sagitta and the astericus. (Fig. 1.1). These grow in separate compartments (utricle, saccule and lagena, respectively) filled with a fluid called endolymph. The fact that otoliths grow in compartments differentiate them from other calcified structures (like teeth and bones) as their growth is strictly constrained by the availability of precursors for calcification in the fluid. The endolymph fluid has a simple alkaline chemistry with a pH of 7.8 to 8.2 (Romanek & Gauldie 1996). It predominantly contains calcium, carbonate, bicarbonate ions, dissolved inorganic carbon (DIC), and trace metals (Enger 1964; Payan et al. 1997). Proteins and other organic matrix (proteoglycans, collagens, etc.) are also found, in small proportions, in the endolymph and the otolith (Campana 1999).

Figure 1.1: Example of the location and size of the three types of otoliths



(http://vertebresfossiles.free.fr/otolithes/img/schema_otolith1.gif)

Otoliths are mainly composed of calcium carbonate (CaCO_3). Previous research has demonstrated that otoliths of some fish can be comprised of three different CaCO_3 crystalline structures, aragonite calcite and vaterite which can differ dramatically in their trace elemental composition (Gauldie 1986, 1993, 1997; Casselman and Gunn 1992; Oliveira and Farina 1996, Bowen II et al. 1999, Brown and Severin 1999).

Otoliths play a major role in the fish's body as they are sensitive to gravity, linear acceleration and are responsible for the fish's balance and hearing. Fish can detect sound through vibration of the sensory hair cells in the epithelium which sends a signal by the nerves (Popper & Lu 2000). The continual and daily growth of otolith is recognizable as concentric rings of alternating opaque and translucent zones (somatic growth). Otoliths are believed to not be subject to resorption, due to their acellular nature, which implied that their composition will only vary with fish development state (age) and environmental factors. It has allowed for a range of applications of otolith microchemistry including stock

identification, reconstruction of temperature and salinity of waters, determination of larval dispersion and migratory patterns, differentiation among groups of fish and pollution indicators (Campana 1983, 1999; Arai et al. 2007).

1.2 STATEMENT OF PROBLEM

Despite the recent, widespread use of otolith microchemistry in a wide range of environmental applications and fisheries-related investigations, some unresolved issues remain, which have limited use of this tool to its fullest potential. The purpose of my research is to develop a better understanding of the mechanisms and influences of metal uptake in fish otoliths.

1.3 OBJECTIVES OF THE DISSERTATION

In Chapter 2, I utilized chemical and spectroscopic analyses of vaterite and aragonite growth in sagittal otoliths of lake trout in an effort to better understand the crystalline growth process. I was also interested in learning about the elemental partitioning of metals. I tested the following hypotheses: 1) do both calcium-carbonate polymorphs grow simultaneously in the same otolith (versus sequentially), 2) does vaterite and aragonite growth occur in the same region of the otolith (ontogeny), and 3) do growth rate differences for these polymorphs influence otolith metal composition.

Chapter 3 investigated the nucleation of otolith to determine how otolith crystallized and if there was a catalyst that would help the crystallization. I also wanted to see how that affected elemental uptake. Using a higher spatial

resolution than previous studies on this topic, I investigated the correspondence between elevated Mn concentration and the site (or sites) of initial otolith deposition (primordia). Microscopic observations of the nucleation of otolith (in the core) are reported for several fish species (rainbow trout (*Oncorhynchus mykiss*), yellow perch (*Perca flavescens*) and lake cisco (*Coregonus artedii*)) as well as spectroscopic data for the lake cisco and yellow perch.

A preliminary study, conducted on walleye (*Sander vitreus*) endolymph and otolith composition is also included where fractionation of metals is investigated. I wanted to learn if trace elements were fractionated following the same path from the water to the otolith. In the last part of this chapter I reported the effect of crystal structure (aragonite and vaterite) on the microchemistry of otoliths. This investigation helps understand how the chemical characteristics of the metal ions (i.e., ionic radii) and the crystalline structure interact to cause differential trace metal uptake between the calcium carbonate polymorphs aragonite and vaterite.

In Chapter 4, metal partitioning between otolith and endolymph of two freshwater species: lake trout (*Salvelinus namaycush*) and burbot (*Lota lota*) is studied. Most of the literature on endolymph composition reports analyses for organic compounds (proteins, triglycerides etc.), some metals (Na, Mg, K, Ca, Sr) and non-metals (S). There are no published data for a broad range of metals in endolymph and how they relate to the chemistry of otolith. In this chapter I also analyzed blood and surface water to give new insights on the partitioning of metals between these barriers.

Chapter 5 explores the turnover rates of barium and strontium in the blood, bones, whole bodies and otoliths of yellow perch (*Perca flavescens*) using enriched isotope tracers. I attempt to answer the following questions: 1) are the enriched isotopes of Sr and Ba eliminated/sequestered at the same rate by the fish and 2) are strontium and barium isotope turnover rates in otoliths long enough to be useful as chemical tracers for fish recruitment 3) how rapidly does a fish equilibrate with a new environment and 4) how sensitive is otolith chemistry to environmental change.

This dissertation provides insights on otolith chemistry and increases our understanding of the mechanisms underlying otolith structure, growth and influences on metal uptake. The ultimate goal of this research is to improve the ability of scientists to use otolith microchemical investigations for fisheries-related research and management.

1.4 REFERENCES

- Arai, T., Ohji, M., and Hirata, T. 2007. Trace metal deposition in teleost fish otolith as an environmental indicator. *Water Air Soil Pollut.* **179**: 255-263.
- Bowen II, C.A., Bronte, C.R., Argyle, R.L., Adams, J.V., and Johnson, J.E. 1999. Vateritic sagitta in wild and stocked lake trout: applicability to stock origin. *Trans. Am. Fish. Soc.* **128**: 929-938.
- Brown, R., and Severin, K.P. 1999. Elemental distribution within polymorphic inconnu (*Stenodus leucichthys*) otoliths is affected by crystal structure. *Can. J. Fish. Aquat. Sci.* **56**: 1898-1903.
- Campana, S.E. 1983. Feeding periodicity and the production of daily growth increment in otoliths of steelhead trout (*Salmo gairdneri*) and starry flounder (*Platichthys stellatus*). *Can. J. Zool.* **61**: 1591-1597.
- Campana, S.E. 1999. Chemistry and composition of fish otoliths: pathways, mechanisms and applications. *Mar. Ecol. Prog. Ser.* **188**: 263-297.
- Casselman, J.M., and Gunn, J.M. 1992. Dynamics in year-class strength, growth, and calcified-structure size of native lake trout (*Salvelinus namaycush*) exposed to moderate acidification and whole-lake neutralization. *Can. J. Fish. Aquat. Sci.* **49**(1): 102-13.
- Gauldie, R.W. 1986. Vaterite otoliths from chinook salmon (*Oncorhynchus tshawytscha*). *N.Z. J. Mar. Freshwat. Res.* **20**: 209-217.
- Gauldie, R.W. 1996. Effects of temperature and vaterite replacement on the chemistry of metal ions in the otoliths of *Oncorhynchus tshawytscha*. *Can. J. Fish. Aquat. Sci.* **53**: 2015-2026.

- Gauldie, R.W., Sharma, S.K., and Volk, E. 1997. Micro-Raman spectral study of vaterite and aragonite otoliths of the coho salmon, *Oncorhynchus kisutch*. *Comp. Biochem. Physiol. A Comp. Physiol.* **118**:753-757.
- Oliveira, A.M., Farina, M., Ludka, I.P. and Kachar, B. 1996. Vaterite, calcite, and aragonite in the otoliths of three species of piranha. *Naturwissenschaften.* **83**: 133-135.
- Pannella G., 1971. Fish otoliths: daily growth layers and periodical patterns. *Science*, **173**: 1124-1127.
- Popper, A.N. and Lu, Z. 2000. Structure-function relationships in fish otolith organs. *Fish. Res.* **46**: 15-25.
- Romanek, C.S. and Gauldie, R.W. 1996. A predictive model of otolith growth in fish based on the chemistry of the endolymph. *Comp. Biochem. Physiol.* **114A**: 71-79.

CHAPTER 2

Effects of crystal structure on the uptake of metals by lake trout (*Salvelinus namaycush*) otoliths

2.1 INTRODUCTION

Otoliths are the ear stones of fish and are mainly composed of calcium carbonate (CaCO_3). The continual growth of otoliths is recognizable as concentric rings of alternating opaque and translucent zones. Otoliths are not considered to be subject to resorption, and as such, only ontogenetic and environmental factors should cause changes to their chemical composition (Campana 1999; Halden et al. 2000). Previous work has demonstrated that otoliths of salmonines, including lake trout (*Salvelinus namaycush*), can be comprised of two different CaCO_3 crystalline structures, aragonite and vaterite (Campana 1983; Gaudie 1986; Casselman and Gunn 1992), which can differ dramatically in their trace elemental composition (Brown and Severin 1999).

This study focuses on vaterite and aragonite formation in sagittal otoliths of lake trout. Aragonite is the most common crystalline structure in otoliths of teleosts including lake trout but previous work has shown that both stocked and wild lake trout can have vateritic otoliths (Bowen II et al. 1999). The prevalence of vaterite in lake trout otoliths, however, is much greater for stocked fish than wild fish (59%-86% versus 4%-49%, respectively), possibly owing to a physiological response associated with intense stocking stress (Casselman 1986; Bowen II et al. 1999; Ludsin et al. 2004).

Brown and Severin (1999) have suggested that one or more genes are responsible for switching the production of proteins that facilitate vaterite or aragonite formation in the growing otolith. More recently, Söllner et al. (2003) reported that the starmaker gene might be responsible for the change in the

crystal lattice structure of otoliths in zebrafish (*Brachydanio rerio*). They conducted an experiment in which the activity of starmaker was reduced by the injection of 2 to 40 nanograms of modified antisense oligonucleotides, resulting in concentric daily rings that were star-shaped instead of circular. Quite possibly, another environmentally influenced gene is responsible for vateritic otolith transformation in lake trout.

Gauldie (1986, 1996) showed that aragonite replaced vaterite in chinook salmon (*Oncorhynchus tshawytscha*) sagittal otoliths and found that the degree of transformation varied from partial to total replacement. Further, Gauldie (1986, 1996) frequently observed individuals with one otolith that was comprised completely of vaterite and the other of aragonite, with relatively few individuals having vaterite in both sagittal otoliths. David and Grimes (1994) observed a similar phenomenon in hatchery-reared juvenile red drum (*Sciaenops ocellatus*). By contrast, Brown and Severin (1999) found regions on the otoliths of the inconnu (*Stenodus leucichthys*) that were comprised of a mixture of aragonite and vaterite. Campana (1983) however was the only author to document the co-precipitation of aragonite and vaterite in different zones of the same otolith, but elemental compositions in the two polymorphic structures were not measured.

Herein, we present chemical and spectroscopic analyses of vaterite and aragonite growth in sagittal otoliths of lake trout in an effort to better understand the crystalline growth process. Specifically, we were interested in learning whether 1) both calcium-carbonate polymorphs grow simultaneously in the same otolith (versus sequentially), 2) vaterite and aragonite growth occurs in the same region of the otolith, and 3) growth rate differences exist for these polymorphs,

which might influence otolith shape. To do so, we used Raman spectroscopy to identify the distribution of vaterite and aragonite crystal structures in sagittal otoliths. In addition, we used laser ablation-inductively coupled plasma-mass spectrometry (LA-ICP-MS) to quantify chemical differences between vateritic and aragonitic portions of otoliths, and to determine partition coefficients (K_D) for metals between them, at different growth stages. Ultimately, we discuss potential causal mechanisms to understand differential trace metal uptake between these CaCO_3 polymorphs, including the influence of the metal itself (e.g., ionic radii), the crystalline structure, and the development state of the fish.

2.2 MATERIALS AND METHODS

2.2.1 Fish and otolith preparation

Analyses were conducted on 13 age-11 lake trout that spent their entire existence in the Allegheny National Fish Hatchery in Warren Pennsylvania. All fish were from the same year-class (1992), and sacrificed and collected at the same time. An additional two hatchery-reared lake trout, collected from the eastern basin of Lake Erie via annual assessment surveys conducted by both state and provincial agencies during 1984-2003 (see Ludsin et al. 2004 and Markham 2004 for sampling details), were also analyzed for this study. Sagittal otoliths from this suite of individuals were provided dry, stored in envelopes.

Sagittal otoliths were embedded in epoxy resin (West Coast Marine®) and transverse sections (~350 μm wide) were cut using a Buehler ISOMET™ saw, such that each section contained the full growth chronology (including the core).

After mounting sections to a piece of an overhead transparency sheet with Krazy Glue®, the upper surface was polished using a combination of 20-, 12-, 1-, and 0.3- μm aluminum-oxide 3M® lapping film to improve optical quality and to ensure the otolith core was at the exposed surface of the section. Sections were then randomly mounted (with a small piece of the transparency sheet) to acid-washed glass slides with Krazy Glue® (n = 12-14 otoliths per slide) and left to dry for 24 h. Slides were then sonicated for 10 min in ultra-pure Milli-Q water, rinsed three times in Milli-Q water, dried for 24 h in a HEPA-filtered laminar flow hood in a Class 100 clean room, and then stored in a covered Petrie dish until analysis. These last steps (sonication, rinsing, drying) were repeated between Raman and LA-ICP-MS use. All post-polishing processing (including storage) occurred in a Class 100 clean room, and only non-metallic instruments were used to handle otoliths.

2.2.2 Raman spectroscopy

Calcium carbonate is found in otoliths in three polymorphic crystalline structures: calcite, vaterite, and aragonite (Truchet et al. 1995; Oliveira and Farina 1996; Tomás and Geffen 2003). The crystal structures are, respectively, rhombohedral, hexagonal, and orthorhombic. Crystal structures of CaCO_3 in the otoliths can be determined using X-Ray diffraction and Raman spectroscopy (Gauldie 1986; Tomás and Geffen 2003). We used Raman spectroscopy, which is the measurement of the wavelength and intensity of scattered light from molecules (Hollas 1998). The Raman scattered light occurs at wavelengths that

are shifted from the incident light by the energies of molecular vibrations and rotations which are unique for all chemical complexes. It is a non-destructive technique that quantitatively determines where vaterite and aragonite are located in the otolith (Gauldie et al. 1997). The Raman spectra of each mineral structure are the same, independent of where they are taken, core or edge. The best way to differentiate aragonite from vaterite is the 1000-1200 cm^{-1} portion of the spectrum. Raman analyses were conducted on the edges (last 1-2 years of life) of all hatchery-reared lake trout ($n = 13$), and the cores (first 18 months) of three lake trout (one pure hatchery lake trout and the two Lake Erie recaptures), using a Renishaw® inVia Reflex Raman spectrometer. The exciting source was a He:Ne laser operating at 633 nm with a power of about 27 mW with a focus of 3.5 mW on the sample. The system was equipped with a charged-coupled device (CCD) detector. Calibration was performed using a static spectral acquisition on a silicon plate positioned at 520 cm^{-1} . Because otolith cores are dark (i.e., difficult to see under our microscope), whereas the edges are clear (almost transparent for some), Raman spectra taken on otolith edges were done at higher resolution (50X) than the cores (20X). Mapping of the transitional zone between aragonite and vaterite growth zones was done at a magnification of 50X.

2.2.3 Laser ablation-inductively coupled plasma-mass spectrometry (LA-ICP-MS)

Elemental concentrations were quantified using a purpose-built system comprised of a Continuum® Surelite® I solid state Nd:YAG laser (wavelength:

266 nm; maximum power: 40mJ; pulse rate: 20 Hz; pulse width: 4-6 ns; laser spot diameter: 15 μm) coupled to a Thermo-Elemental® X7® ICP-MS (peak-jumping mode, 10 ms dwell time per isotope). A glass reference standard (NIST 612) with known concentrations of elements was analyzed before and after every 16 samples ($n = 2$ replicates before and after), which allowed for quantification and correction of instrumental drift. This same standard also was used to determine precision in estimating elemental concentrations. The Ar carrier gas and instrument noise (i.e., background) were analyzed for 60 sec before every sample.

Concentrations of the elements were calculated by measuring the following isotopes: ^7Li , ^{25}Mg , ^{43}Ca , ^{44}Ca , ^{55}Mn , ^{66}Zn , ^{85}Rb , ^{86}Sr , ^{88}Sr , ^{137}Ba and ^{138}Ba . Each of these elements met a rigorous set of criteria before use in this study. Specifically, for an element to be included in our analyses, it had to be precisely measured; i.e., the average coefficient of variability (i.e., standard deviation/mean*100%) for at least one measured isotope, as determined from our NIST samples, had to be $< 10.5\%$ (Gillanders and Kingsford 1996). In addition, its concentration had to be above the LOD for 90% of the samples. Details concerning measures of precision, limits of detection (LODs), and percentages of samples of above LODs are reported elsewhere (Ludsin et al. 2004). A series of ablations were performed at the growing edges which represent the last 1-2 years of life (last rings). Otolith core concentrations were determined by a single transect of about 200 μm that was approximately equidistant on each side of the core (Ludsin et al. 2004). Calcium was used as an internal standard to correct for variations in the amount of material ablated (i.e., ablation yield). The two

polymorphs of CaCO_3 , vaterite and aragonite, do not have the same structure but their chemical composition is identical. Therefore, calcium concentration is the same in both polymorphs (~40% wt.).

2.3 RESULTS

2.3.1 Microscopic observations

Microscopic observations of individual sagittal otoliths demonstrated that aragonite and vaterite grow simultaneously in the otolith, but in different locations that are separated by an easily identifiable transition zone. Interestingly, growth rates of these polymorphs differed, even in the same growth rings. In most instances, vaterite growth rates exceeded that of co-precipitating aragonite, as evidenced by larger vateritic areas (Fig. 2.1a). Although relatively uncommon, it also was possible for aragonite growth to be greater than vaterite growth (Fig. 2.1b). In addition to these growth-zone and growth-rate differences, clear differences in the structure of growth bands were evident microscopically. In general, vateritic portions of the otolith demonstrated excessive waviness, which made aging impossible (Figs. 2.2a, 2.2b). By contrast, growth bands in the aragonitic zone of the otolith were less wavy and more uniform, making aging easier (Figs. 2.2a, 2.2b). These two crystalline polymorphs also had different optical properties, as the opacity of vaterite was greater than that of aragonite (Fig. 2.2a). Further, the contact (transition) zone between aragonite and vaterite growth, over 20-30 μm , did not optically look like pure aragonite or pure vaterite (Fig. 2.2b).

Sagittal cores were of three different types: pure aragonite (the most dominant case), pure vaterite, and a combination of the two (Figs. 2.3a-2.3c). Under transmitted light, aragonitic and vateritic cores are quite dark and microscopic observations could not help distinguish their crystal composition. Sketches of the different otolith types are presented beside the photographs to facilitate identification (Figs. 2.3a-2.3c).

2.3.2. Aragonite and vaterite growth relationships

The characteristics of the transition zone and vateritic cores were investigated by Raman spectroscopy and LA-ICP-MS. Raman study on the structural forms of CaCO_3 in lake trout sagittae substantiated the microscopic analyses, which indicated aragonite and vaterite growing at the same time in otoliths (Fig. 2.4a-c). Three distinct characteristics associated with group vibration, a change in the dipole moment of the molecule, (Gans 1971; Truchet et al. 1995) were used by Gauldie et al. (1997) to distinguish vaterite from aragonite. We used the same ones here, which were lattice mode, symmetric stretching, and in-plane bending. Lattice modes of vaterite were characterized by two peaks in closer proximity to one another (peaks at 152 cm^{-1} and 205 cm^{-1}) relative to aragonite with peaks at 106 cm^{-1} and 302 cm^{-1} (Fig. 2.4a). Second, ν_4 , the in-plane bending of CO_3^{2-} , was characterized by a narrow doublet instead of a broader doublet for the Raman spectrum of aragonite (Fig. 2.4b). Finally, vaterite was characterized by triplet bands (1075 cm^{-1} , 1081 cm^{-1} and 1090 cm^{-1}) for symmetric stretching, ν_1 , of C-O from carbonate anion bonded to calcium (Fig.

2.4c), whereas aragonite had only a single band (1084 cm^{-1}). The bands ν_2 and ν_3 were not visible as their intensities are too weak and fluorescence overshadowed their peaks. In any case, they were not needed to differentiate the two polymorphs. Analysis of the transition zone, dividing areas of aragonite and vaterite growths, demonstrated that a thin zone (20-30 μm) comprised of a mixture of aragonite and vaterite separates the crystal polymorphs. This was evident from a gradual shift from a single peak to broad triplet in symmetric stretching as one moved from aragonite into vaterite (Fig. 2.4d). Additional Raman analysis of otoliths from the remaining 12 lake trout demonstrated that most cores were comprised entirely of aragonite. In one instance, however, the entire core was vaterite, while two others had cores that were half aragonite and half vaterite.

2.3.3 Microchemistry of aragonite and vaterite

The microchemistry of aragonite and vaterite growing simultaneously in sagittae was quantified using LA-ICP-MS. This technique is very sensitive, detecting low concentrations of trace metals (parts per billion) in environmental matrices and permits determination of temporal concentrations (Bellotto and Miekeley 2000). Vateritic core data were obtained from two types of fish: (1) two hatchery-reared fish that were released and recaptured in Lake Erie (note, the core is representative of hatchery existence, given that these individuals spent their first 18 months in the hatchery; see Ludsin et al. 2004); and (2) one

individual that spent its entire existence in the hatchery. Microchemical analyses of otolith edges were from fish that resided in the hatchery since birth (n = 13).

To quantify differences in average concentrations between aragonitic and vateritic edges in our hatchery lake trout (n = 13), paired t-tests were conducted for each element. Significant differences existed between mineral types for all elements (paired t-test: all $|t| \leq 3.5$; all $p < 0.004$) but Zn ($t = -0.07$; $p = 0.94$). In the core, Mg levels in vaterite were 30-fold higher and Mn levels were five times higher than in aragonite, whereas Sr levels were 10-fold and Ba levels were 20-fold higher in aragonite than vaterite (Table 1). There was a similar trend for the edges; concentrations of Mg were 40-fold higher in vaterite and about 20-fold lower for Sr as compared to aragonite. Manganese was 10-fold more abundant in vaterite and Ba 40-fold more concentrated in aragonite (Table 2.1).

A LA-ICP-MS transect through the transition zone demonstrated chemical differences (Fig. 2.5) that correspond well with the Raman results (see Fig. 2.4d). There was a gradual but not abrupt transition from one mineral type to the other. Pure aragonite was characterized by high Sr and Ba and low Mg and Mn, whereas vaterite demonstrated the opposite trend (also see Table 2.1). The arrow in Fig. 2.2b shows the perpendicular trajectory of the Raman and ICP-MS laser transects through the aragonite-vaterite boundary zone separating simultaneous growth of aragonite and vaterite. Some variation within each polymorph may be due to the fact that we passed through two annuli while analyzing this portion of the otolith.

2.3.4 Otolith elemental partitioning

Partition coefficients represent the concentrations of elements in one phase as compared to the concentration in a coexisting phase. Typically, researchers calculate the ratio between elemental concentrations in water relative to those in the otolith, generally aragonite crystals (Bath et al. 2000; Elsdon and Gillanders 2003). However, with aragonite and vaterite growing simultaneously, and separately, in the same otolith, we were provided with the unique opportunity to calculate partition coefficients for the two mineral types using the following equation:

$$(1) \quad K_D = [\text{metal}/\text{Ca}]_{\text{aragonite}} / [\text{metal}/\text{Ca}]_{\text{vaterite}}$$

wherein K_D is the partition coefficient between the concentration of a metal in aragonite relative to its concentration in vaterite. For this determination, all metals were standardized against Ca before analysis. The average partition coefficients determined for the edges and the cores are presented (Table 2.2). As expected, based on mean concentrations in Table 2.1, uptake rates of Sr and Ba were higher in aragonite than vaterite (i.e., coefficients greater than one), in both the edge and core of aragonitic portions of the otolith, whereas the opposite was true for Mg and Mn (Table 2.2). These trends also were evident from plots of metal concentrations in vaterite versus aragonite (Fig. 2.6). Specifically, those elements with slopes greater than one indicate preferential uptake by aragonite relative to vaterite. Both Sr and Ba had slopes in excess of six (Figs. 2.6f and 2.6g, respectively). By contrast, both Mg and Mn had slopes much less than one (both less than 0.07), indicating preferential uptake by vaterite relative to aragonite (Figs. 2.6b and 2.6c, respectively). Lithium demonstrated near equal partitioning

between mineral types (slope = 1.42; Fig. 2.6a). Also, with the exception of Zn, which demonstrated no obvious relationship between aragonite and vaterite (Fig. 2.6d), all elements were positively (but not necessarily significantly) related in vaterite and aragonite which makes sense given that these minerals were reflecting the same water chemistry.

2.4 DISCUSSION

Previous investigations involving salmonines, including lake trout, have documented the existence of vaterite in otoliths that also contain aragonite. Our investigation is unique because we demonstrate through both elemental and spectroscopic analyses that both vaterite and aragonite can grow in otoliths simultaneously. Interestingly, these two minerals grow at different locations within the otolith, separated by a well demarcated transition zone that consists of a blend of these two crystalline polymorphs. Further, from microscopic observations, there are growth rate differences between vateritic and aragonitic portions of the otolith with vaterite growth being generally greater than aragonite growth. Below, we explain the likely mechanisms responsible for differences in chemical composition, as well as growth rates.

2.4.1 Microchemistry of aragonite and vaterite

Two primary factors should influence the incorporation of elements into aragonite versus vaterite. First, we would expect less substitution of metals with a +1 ionic charge (e.g., Li, Rb) in the CaCO₃ matrix of otoliths than metals with a +2

ionic charge (e.g., Mn, Mg, Zn, Sr, Ba), given that calcium is a +2 cation and crystals must be electrically neutral. Second, the relationship between the ionic radii relative to calcium versus potential replacement ions also should be important, with ions whose ionic radii is most similar to calcium (e.g., Mg, Sr) being favored over those that are not (e.g., Rb; Table 2.3).

The co-precipitation of aragonite and vaterite in otolith cores and edges allowed us to directly measure concentrations in both polymorphs and then calculate the partition coefficients (uptake rates) at different development stages (core = larval to fry; edge = adult). Regardless of relative growth rates between vaterite and aragonite, Sr and Ba were higher in edges comprised of aragonite than vaterite, whereas the opposite was true for Mg and Mn. By contrast, the variation in Rb and Zn between these two polymorphs was minimal. Similar differences (and non-differences) were evident in otolith cores.

Aragonitic otoliths preferentially ($K_D > 1$) incorporated large cations such as Sr^{2+} (1.32 Å), Ba^{2+} (1.49 Å), and Rb^{1+} (1.66 Å) whereas smaller cations like Mg^{2+} (0.86Å) and Mn^{2+} (0.81Å) were favored ($K_D < 1$) in vaterite. These results can be explained by the crystal structure of vaterite and its reduced ability to incorporate larger cations (i.e., Sr, Ba) without serious crystal distortion (Casanova et al. 2004). In addition, the length of the metal-oxygen bond in MCO_3 in both crystal structures supports this conclusion: an average of 2.46 Å is found in vaterite compared to approximately 2.53 Å for aragonite (Taylor 1993; Hasse et al. 2000). Zn and Li partition coefficients were close to one for both the core and the edge, indicating that their uptake was the same in both crystal structures and is largely independent of the age of fish. As expected, the concentrations of

trace metals in both CaCO_3 polymorphs also were strongly influenced by differences in their ionic radii relative to that of calcium, with the closest +2 metals to calcium being preferentially incorporated. These quantitative results for pure vaterite and pure aragonite follow the same trends as obtained by previous researchers using whole otoliths that were dominantly vaterite or aragonite (Gauldie 1986, 1996; Tomás and Geffen 2003).

Trace metal abundances of otoliths from fish raised in the hatchery environment can vary significantly with ontogeny. Specifically, Ludsin et al. (2004) reported significant concentration differences between the edge (age-2 to age-11) and core (first few months) of these same hatchery-reared individuals for both Zn and Mn. These authors were uncertain of the causal mechanisms, but suggested the potential role of a changing crystal structure or perhaps a shift in diet or metabolism (physiology).

An additional possibility that needs to be explored for changing element concentrations is whether element concentrations are affected by the growth rate of the crystals. The results for vaterite>aragonite and vaterite<aragonite are similar for most elements. Lithium, which had similar partition coefficients for both crystal growth rate groups, showed distinctly different concentrations for the two groups (two times the concentration of Li in vaterite growth greater than aragonite compared to vaterite growth less than aragonite). Except for this element, the dimensional differences of CaCO_3 crystals are not influencing the concentrations results. One explanation for this difference is that Li may have a different mechanism of incorporation in otoliths than the other elements studied. The Li

uptake may differ for the two polymorphs, owing to metals being trapped in the CaCO_3 crystal structure as opposed to substituting for Ca^{2+} . Indeed, previous work with aragonitic otoliths has demonstrated that metals can bind to proteins or be trapped in the growing crystal lattice (Milton and Chenery 2001). To date, however, no similar work has been conducted with vateritic otoliths.

2.4.2 Possible mechanisms causing vaterite growth

The role of extrinsic factors

Discrimination of calcium carbonate polymorphs can be done qualitatively, given that vaterite growth zones have bands that are optically relatively 'wavy' relative to the more evenly-spaced and uniform co-precipitating aragonite growth zones. We also observed that vaterite and aragonite are deposited in the normal growth increments as the layers crystallize chronologically, which is what would be expected given the basic model of otolith growth. In contrast, Brown and Severin (1999) documented regions comprised of a mixture of aragonite and vaterite that were not limited to growth bands, as they diagonally crossed otolith daily increments. These authors explained that their results did not follow the basic model of otolith growth based on their assumption that some genes switched production of proteins causing a mixture of aragonite and vaterite. Other researchers have found that otoliths of fish regularly grow vaterite around an aragonitic core following normal otolith increment deposition (Gauldie et al. 1997; Bowen II et al. 1999; Tomás and Geffen 2003). One vateritic and one aragonitic otolith have also frequently been observed in the same fish (Gauldie 1986; David and Grimes 1994).

As for the cause of vateritic growth, we are not certain. Presently, it is assumed that stocking stress or possibly residing in a hatchery environment is responsible for this change in the crystal structure of the otolith (Casselman 1990; Casselman and Gunn 1992; Bowen II et al. 1999). However, determining whether it is the hatchery environment itself or the act of stocking that caused vaterite to form in otoliths has remained elusive. Clearly, based on the fact that we found vaterite in adult lake trout that never left the hatchery, as well as in the cores of recaptured fish deposited before they left the hatchery, indicates that stocking itself might not be the root cause. The fact that several investigators (Casselman 1986; Ludsin et al. 2004) have documented vaterite formation in lake trout fingerlings and adults that were of wild origin also demonstrates that the hatchery environment is not solely responsible for vaterite formation. As such, perhaps it is not the specific environment (e.g., hatchery versus wild) that is so important, but how stressed that individual is in that environment. Natural environments can be relatively more stressful for some individuals than others, which may explain the occurrence of vaterite in some wild individuals. The fact that vaterite is more typical of hatchery-reared individuals than wild ones (Casselman 1990; Casselman and Gunn 1992; Bowen II et al. 1999) only indicates that a hatchery environment (or the act of stocking) may be more stressful than a natural setting. Clearly, this is a research area deserving more attention. Perhaps additional research might identify an environmentally influenced gene similar to *starmaker*— which controls crystal lattice formation in zebrafish (Söllner et al. 2003)—that triggers vaterite otolith transformation in salmonines such as lake trout.

The role of intrinsic factors

Previous hypotheses on vaterite formation were always related to hatchery stress (Gauldie 1986; David and Grimes 1994; Bowen II et al. 1999). The presence of a vateritic core and two mixed vaterite-aragonite cores suggest that causes of vaterite crystallization is more complicated than previously described, as it is occasionally found early in the larval stage. Pote and Ross (1991) found that each otoconia polymorph, from several species of vertebrates, had unique proteins associated with it. Researchers also have suggested that a gene could influence the production of some proteins facilitating the production of vaterite or aragonite in a growing otolith (Oliveira and Farina 1996; Brown and Severin 1999). If specific proteins control vaterite or aragonite formation, we should expect to find only vaterite or aragonite crystals precipitating at one time in the endolymphatic sacs. In this study both phases were found to form simultaneously on either side or wing of the otolith.

One possibility to explain the simultaneous growth of aragonite and vaterite in otoliths is the possibility of organic matrix to differ from one zone of the otolith to the other (Williams 1984, Strong et al. 1986). From these observations, it is believed that the presence of a gradient in the endolymph chemical composition influences the uptake of metals by the otolith and perhaps the crystal structure as well. Indeed, ionic (K^+ , Na^+) and proteomic gradients has been observed within the endolymph along the proximal-distal axis (Payan et al. 1999; Borelli et al. 2001). Further, Payan et al. (1999) documented that nonuniformity in the composition of the endolymph of trout (*Oncorhynchus mykiss*) and turbot (*Psetta maxima*) can influence the biomineralization process of the otoliths. They

concluded that the chemical gradient is partially maintained through the sagittal otolith acting as a physical barrier to the diffusion of ions and proteins. This new information on endolymph composition needs to be taken into consideration as a factor in determining otolith concentration changes. Such a scenario is portrayed in Figure 2.7.

2.4.3 Implications

This study identified vaterite and aragonite growing separately, but simultaneously, on the edges and the cores of lake trout otoliths. This characteristic had only been documented once before (Campana 1983) and raises several questions concerning their origin(s) and highlights the need to investigate the partitioning of trace metals between endolymph and otoliths for a better understanding of uptake mechanisms. Stocking stress might be a cause of vaterite replacing aragonite during otolith growth, but cannot explain what causes vateritic or half aragonitic/half vateritic cores, nor the two phases growing simultaneously. Is a mixture of proteins responsible for the occurrence and geometry of calcium carbonate? Is the endolymph gradient (ionic and proteomic) influencing the crystallization process? These questions are unanswered and complicate the understanding of polymorphic growth mechanisms in otoliths.

Our work also has implications for future otolith microchemistry work involving salmonines such as lake trout. Based on our research, otoliths can vary considerably in crystalline structure, which in turn, will cause variation in otolith elemental composition. Given the lack of a proportional (linear) relationship

between the chemistry of co-precipitating vaterite and aragonite for some elements, it is clear that aragonite and vaterite do not incorporate all elements from the water in the same way. Previous work has demonstrated that aragonitic otolith chemistry reflects that of the water (e.g., Thorrold et al. 1998; Bath et al. 2000; Gillanders and Kingsford 2000). If this is always true, it appears that vateritic portions of the otolith likely do not reflect water chemistry equivalently. Thus, the use of vateritic portions of otoliths in traditional microchemical studies (e.g., stock discrimination, migration history tracking) would be limited. As such, care must be taken when dealing with otoliths that contain vaterite. Certainly, the criteria for discriminating between these two crystalline polymorphs would be valuable to future otolith microchemistry efforts by allowing investigators to avoid vateritic areas.

2.5 REFERENCES

- Bath, G.E., Thorrold, S.R., Jones, C.M., Campana, S.E., McLaren, J.W., and Lam, J.W.H. 2000. Strontium and barium uptake in aragonitic otoliths of marine fish. *Geochim. Cosmochim. Acta.* **64**: 1705-1714.
- Bellotto, V.R., and Miekeley, N. 2000. Improvements in calibration procedures for the quantitative determination of trace elements in carbonate material (mussel shells) by laser ablation ICP-MS. *Fresenius J. Anal. Chem.* **367**: 635-640.
- Borelli, G., Mayer-Gostan, N., De Pontual, H., Bœuf, G., and Payan, P. 2001. Biochemical relationships between endolymph and otolith matrix in the trout (*Oncorhynchus mykiss*) and turbot (*Psetta maxima*). *Calcif. Tissue Int.* **69**: 356-364
- Bowen II, C.A., Bronte, C.R., Argyle, R.L., Adams, J.V., and Johnson, J.E. 1999. Vateritic sagitta in wild and stocked lake trout: applicability to stock origin. *Trans. Am. Fish. Soc.* **128**: 929-938.
- Brown, R., and Severin, K.P. 1999. Elemental distribution within polymorphic inconnu (*Stenodus leucichthys*) otoliths is affected by crystal structure. *Can. J. Fish. Aquat. Sci.* **56**: 1898-1903.
- Campana, S.E. 1983. Feeding periodicity and the production of daily growth increment in otoliths of steelhead trout (*Salmo gairdneri*) and starry flounder (*Platichthys stellatus*). *Can. J. Zool.* **61**: 1591-1597.
- Campana, S.E. 1999. Chemistry and composition of fish otoliths: pathways, mechanisms and applications. *Mar. Ecol. Prog. Ser.* **188**: 263-297.

- Casanova, D., Cirera, J., Lluell, M., Alemany, P., Avnir, D., and Alvarez, S. 2004. Minimal distortion pathways in polyhedral rearrangements. *J. Am. Chem. Soc.* **126**: 1755-1763.
- Casselman, J.M. 1986. Scale, otolith, and growth characteristics of juvenile lake trout—criteria for discriminating between indigenous and hatchery fish from the natural environment. Great Lakes Fishery Commission Completion Report, Ann Arbor, MI.
- Casselman, J.M. 1990. Research project: lake trout rehabilitation studies. Chapter 17 *in* Lake Ontario Fisheries Unit 1989 Annual Report. Ontario Ministry of Natural Resources, LOA 90.1, Toronto, ON.
- Casselman, J.M., and Gunn, J.M. 1992. Dynamics in year-class strength, growth, and calcified-structure size of native lake trout (*Salvelinus namaycush*) exposed to moderate acidification and whole-lake neutralization. *Can. J. Fish. Aquat. Sci.* **49**(1): 102-13.
- David, A.W., and Grimes, C.B. 1994. Vaterite sagittal otoliths in hatchery-reared juvenile red drums. *Prog. Fish-Cult.* **56**: 301-303.
- Elsdon, T.S., and Gillanders, B.M. 2003. Relationship between water and otolith elemental concentrations in juvenile black bream (*Acanthopagrus butcheri*). *Mar. Ecol. Prog. Ser.* **260**: 263-272.
- Farrell, J., and Campana, S.E. 1996. Regulation of calcium and strontium deposition on the otoliths of juvenile tilapia, *Oreochromis niloticus*. *Comp. Biochem. Physiol.* **115**: 103-109.

- Gans, P. 1971. General considerations *In* Vibrating molecules. An introduction to the interpretation of infrared and raman spectra. Edited by Williams Clowes & Sons Limited. London, Colchester and Beccles. pp. 1-25.
- Gauldie, R.W. 1986. Vaterite otoliths from chinook salmon (*Oncorhynchus tshawytscha*). N.Z. J. Mar. Freshwat. Res. **20**: 209-217.
- Gauldie, R.W. 1996. Effects of temperature and vaterite replacement on the chemistry of metal ions in the otoliths of *Oncorhynchus tshawytscha*. Can. J. Fish. Aquat. Sci. **53**: 2015-2026.
- Gauldie, R.W., Sharma, S.K., and Volk, E. 1997. Micro-Raman spectral study of vaterite and aragonite otoliths of the coho salmon, *Oncorhynchus kisutch*. Comp. Biochem. Physiol. A Comp. Physiol. **118**:753-757.
- Gillanders, B.M., and Kingsford, M.J. 1996. Elements in otoliths may elucidate the contribution of estuarine recruitment to sustaining coastal reef populations of a temperate reef fish. Mar. Ecol. Prog. Ser. **141**: 13-20.
- Gillanders, B.M., and Kingsford, M.J. 2000. Elemental fingerprints of otoliths of fish may distinguish estuarine 'nursery' habitats. Mar. Ecol. Prog. Ser. **201**: 273-286.
- Halden, N.M., Mejia, S.R., Babaluk, J.A., Reist, J.D., Kristofferson, A.H., Campbell, J.L., and Teesdale, W.J. 2000. Oscillatory zinc distribution in Arctic char (*Salvelinus alpinus*) otoliths: the results of biology or environment? Fish. Res. **46**: 289-298.
- Hasse, B., Ehrenberg, H., Marxen, J.C., Becker, W., and Epple, M. 2000. Calcium carbonate modifications in the mineralized shell of the freshwater snail *Biomphalaria glabrata*. Chem. -A Eur. J. **6**: 3679-3685.

- Hollas, J.M. 1998. Spectroscopie Raman rotationnelle. *In* Spectroscopie. Edited by DUNOD. Paris, France. pp. 107-119.
- Ludsin, S.A., Fryer, B.J., Yang, Z., Melançon, S., and Markham, J.L. 2004. Exploration of the existence of natural reproduction in Lake Erie lake trout using otolith microchemistry. Fisheries Research project completion report, Great Lakes Fisheries Commission, Ann Arbor, MI.
- Markham, J. 2004. Report of the Coldwater Task Group to the Standing Technical Committee of the Lake Erie Committee. Great Lakes Fishery Commission, Ann Arbor, MI.
- Milton, D.A., and Chenery, S.R. 2001. Sources and uptake of trace metals in otoliths of juvenile barramundi (*Lates calcarifer*). *J. Exp. Mar. Biol. Ecol.* **264**: 47-65.
- Oliveira, A.M., and Farina, M. 1996. Vaterite, calcite, and aragonite in the otoliths of three species of piranha. *Naturwissenschaften.* **83**: 133-135.
- Payan, P., Edeyer, A., De Pontual, H., Borelli, G., Bœuf, G., and Mayer-Gostan, N. 1999. Chemical composition of saccular endolymph and otolith in fish inner ear: lack of spatial uniformity. *Am. J. Physiol.: Reg. Int. Comp. Physiol.* **277**: R123-R131.
- Pote, K.G., and Ross, M.D. 1991. Each otoconia polymorph has a protein unique to that polymorph. *Comp. Biochem. Physiol.* **98B**: 287-295.
- Shannon, R.D. 1976. Revised effective ionic radii and systematic studies of interatomic distances in halides and chalcogenides. *Acta Crystallogr.* **A32**: 751.

- Söllner, C., Burghammer, M., Busch-Nentwich, E., Berger, J., Schwarz, H., Riekel, C., and Nicolson, T. 2003. Control of crystal size and lattice formation by starmaker in otolith biomineralization. *Science*. **302**: 282-286.
- Strong, M.B., Neilson, J.D., and Hunt, J.J. 1986. Aberrant crystallization of Pollock (*Pollachius virens*) otoliths. *Can. J. Fish. Aquat. Sci.* **43**:1457-1463.
- Taylor, M.G., Simkiss, K., Greaves, G.N., Okazaki, M., and Mann, S. 1993. An X-ray absorption spectroscopy study of the structure and transformation of amorphous calcium carbonate plant cystoliths. *Proc. R. Soc. Lond. B.* **252**: 75-80.
- Thorrold, S.R., Jones, C.M., Swart, P.K., and Targett, T.E. 1998. Accurate classification of juvenile weakfish *Cynoscion regalis* to estuarine nursery areas based on chemical signatures in otoliths. *Mar. Ecol. Prog. Ser.* **173**: 253-265.
- Tomás, J., and Geffen, A.J. 2003. Morphometry and composition of aragonite and vaterite otoliths of deformed laboratory reared juvenile herring from two populations. *J. Fish. Biol.* **63**: 1383-1401.
- Truchet, M., Delhaye, M., and Beny, C. 1995. Identification des carbonates de calcium, calcite, aragonite et vaterite par microsonde Raman-Castaing. Application aux biominéralisations. *Analisis.* **23**: 516-518.
- Williams, R.J.P. 1984. An introduction to biominerals and the role of organic molecules in their formation. *Philos. Trans. R. Soc. Lond. B Biol. Sci.* **304**: 411-424.

Table 2.1: Mean metal concentrations in the cores and the edges of lake trout (*Salvelinus namaycush*). Edge results are divided based on the crystal growth: vaterite > aragonite or vaterite < aragonite (units: $\mu\text{g metal}\cdot\text{g}^{-1}$ calcium \pm 1 standard error). Elements are arranged by ionic charges (+1 for Li and Rb; +2 for the rest) and then by cation radii sizes. All edge and core (aragonite only) concentrations were from individuals that spent their entire existence in the hatchery. The vaterite core concentrations were derived from two hatchery-reared fish that were recaptured in Lake Erie (i.e., the core chemistry reflects the hatchery environment) and a single individual that resided solely in the hatchery.

Cation radii ¹	Edge						Core		
	Vaterite > aragonite (n = 7)		Vaterite < aragonite (n = 6)		Arag. > vaterite (n = 25)		Vaterite < aragonite (n = 3)		
	Arag.	Vat.	Arag.	Vat.	Arag.	Vat.	Arag.	Vat.	Vat.
Li	1.1 \pm 0.8	1.0 \pm 0.5	0.5 \pm 0.2	0.5 \pm 0.1	0.18 \pm 0.03	0.6 \pm 0.2			
Rb	0.05 \pm 0.01	0.027 \pm 0.005	0.05 \pm 0.01	0.027 \pm 0.002	0.12 \pm 0.01	0.09 \pm 0.03			
Mn	0.26 \pm 0.03	3.4 \pm 0.2	0.34 \pm 0.05	4.6 \pm 0.4	2.0 \pm 0.2	6.3 \pm 0.1			
Mg	20 \pm 5	757 \pm 32	21 \pm 4	768 \pm 38	19 \pm 2	514 \pm 54			
Zn	4.4 \pm 0.5	4.5 \pm 0.9	5 \pm 1	4.6 \pm 0.8	34 \pm 2	51 \pm 6			
Ca	1000000	1000000	1000000	1000000	1000000	1000000			
Sr	202 \pm 12	11 \pm 1	170 \pm 16	11 \pm 2	666 \pm 32	60 \pm 5			
Ba	1.3 \pm 0.1	0.03 \pm 0.01	1.5 \pm 0.1	0.03 \pm 0.01	14.7 \pm 0.6	0.89 \pm 0.05			

¹Shannon R.D., 1976

Table 2.2: Values of partition coefficients ($K_D \pm 1$ standard error) for the edge and core of hatchery-reared lake trout. Elements are listed by ionic charges and cation radii sizes.

K_D (Arag./Wat.)	Ionic charge	Cation radii ¹	Edge (n = 13)	Core (n = 3)
Li	+1	0.90	0.79 \pm 0.09	1.1 \pm 0.6
Rb	+1	1.66	2.0 \pm 0.3	3 \pm 1
Mn	+2	0.81	0.08 \pm 0.01	0.46 \pm 0.01
Mg	+2	0.86	0.027 \pm 0.004	0.043 \pm 0.006
Zn	+2	0.88	1.2 \pm 0.2	0.8 \pm 0.1
Sr	+2	1.32	17 \pm 1	10 \pm 1
Ba	+2	1.49	42 \pm 7	13.0 \pm 0.8

¹Shannon R.D., 1976

Table 2.3: Metals size differences in ionic radii from calcium (Ca^{2+}) in the CaCO_3 crystal. Elements are classified by ionic charges (+1 at the top of table and +2 at bottom) and cation radii sizes.

Metal	Radii differences from Ca^{2+} (Å)
Li	0.24
Rb	0.52
Sr	0.18
Zn	0.26
Mg	0.28
Mn	0.33
Ba	0.35

Figure 2.1: Sagittal otoliths from age-11 lake trout (*Salvelinus namaycush*) that spent their entire existence in captivity. (a) Otolith with vaterite growth being greater than aragonite growth. (b) Otolith with aragonite growth being greater than vaterite growth.

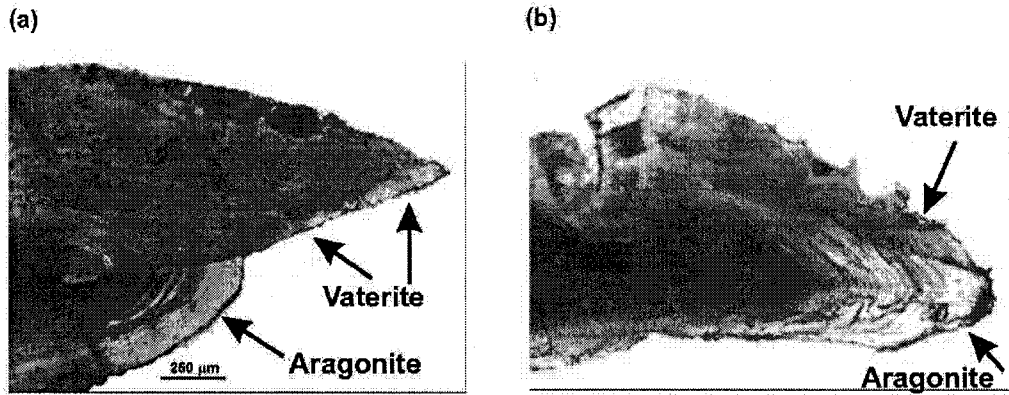


Figure 2.2: (a) Transition (contact) zone between aragonite and vaterite for an otolith of an 11-yr old hatchery-reared lake trout (*Salvelinus namaycush*) under transmitted light. Notice the 'waviness' of the growth bands in vaterite, as compared to aragonite. The box in (a) is shown in more detail in (b). The arrow in (b) represents the direction of the Raman mapping done on the boundary zone.

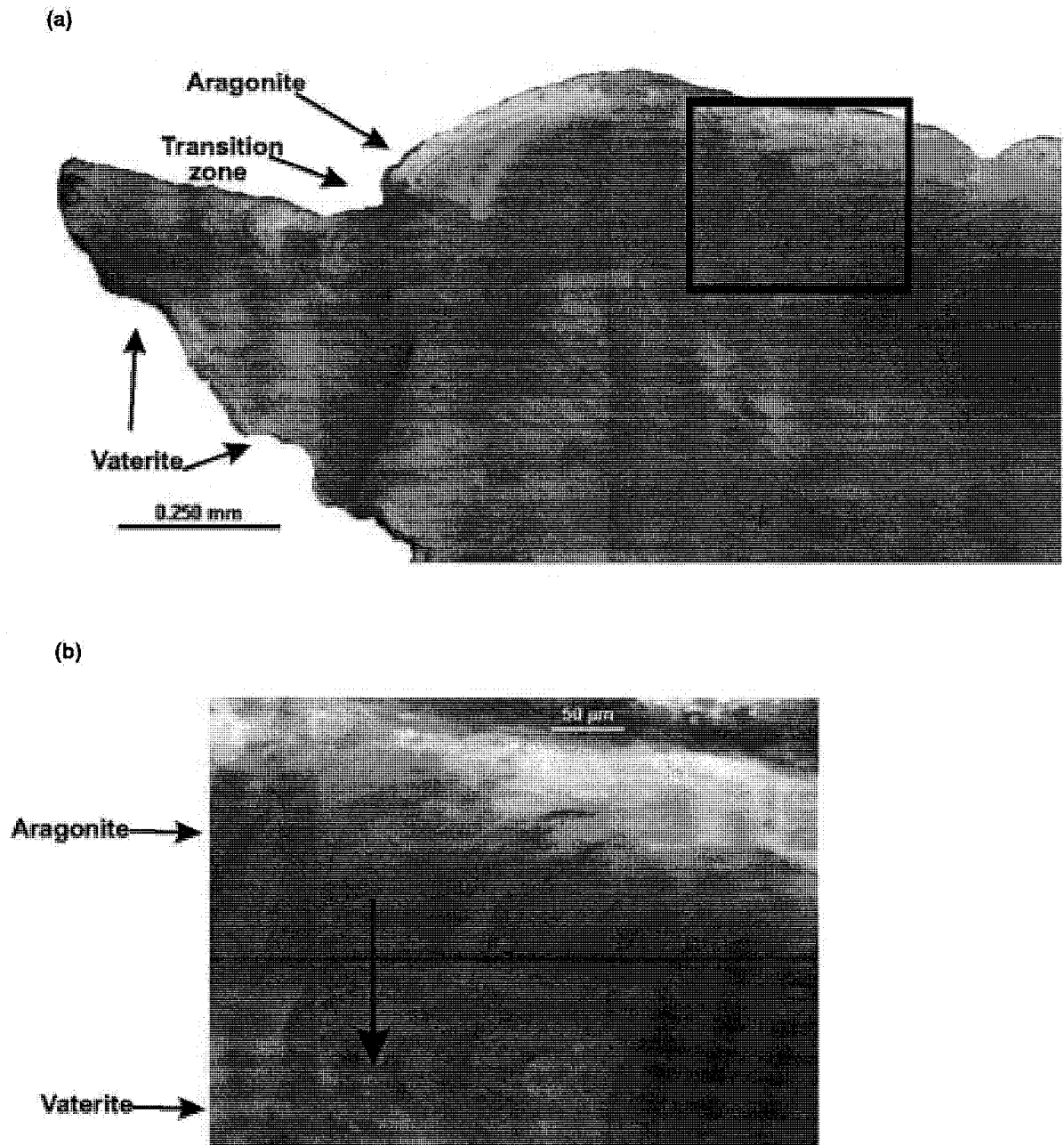
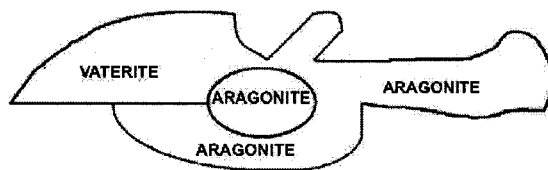
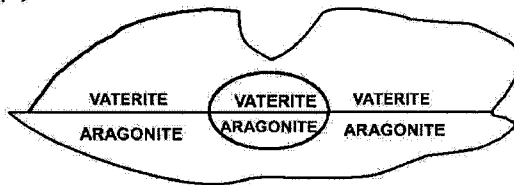


Figure 2.3: Vateritic formations in lake trout (*Salvelinus namaycush*) otoliths: (a) Aragonitic core with the transition zone one side and aragonite edge on the other; (b) vateritic and aragonitic core with the transition zone on both sides; and (c) vateritic core with one vateritic and one edge aragonitic edge.

(a)



(b)



(c)

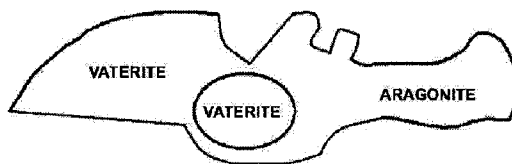


Figure 2.4: Wave numbers from the Raman spectroscopy analysis of aragonite and vaterite portions of a hatchery-reared lake trout (*Salvelinus namaycush*) that spent its entire existence in the Allegheny National Fish Hatchery (this is the same individual as in Fig. 2a). The patterns presented were typical of 12 other broodstock analyzed with Raman spectroscopy. In arbitrary units plotted against Raman shift in cm^{-1} . Represented are (a) lattice modes, (b) in-plane bending (ν_4) of C-O from carbonate anion bonded to Ca, and (c) symmetric stretching (ν_1) of CO_3^{2-} anions. (d) Raman mapping (symmetric stretching only) through the boundary zone, as shown in Fig. 1b, demonstrating the transition from aragonite to vaterite for the same sample.

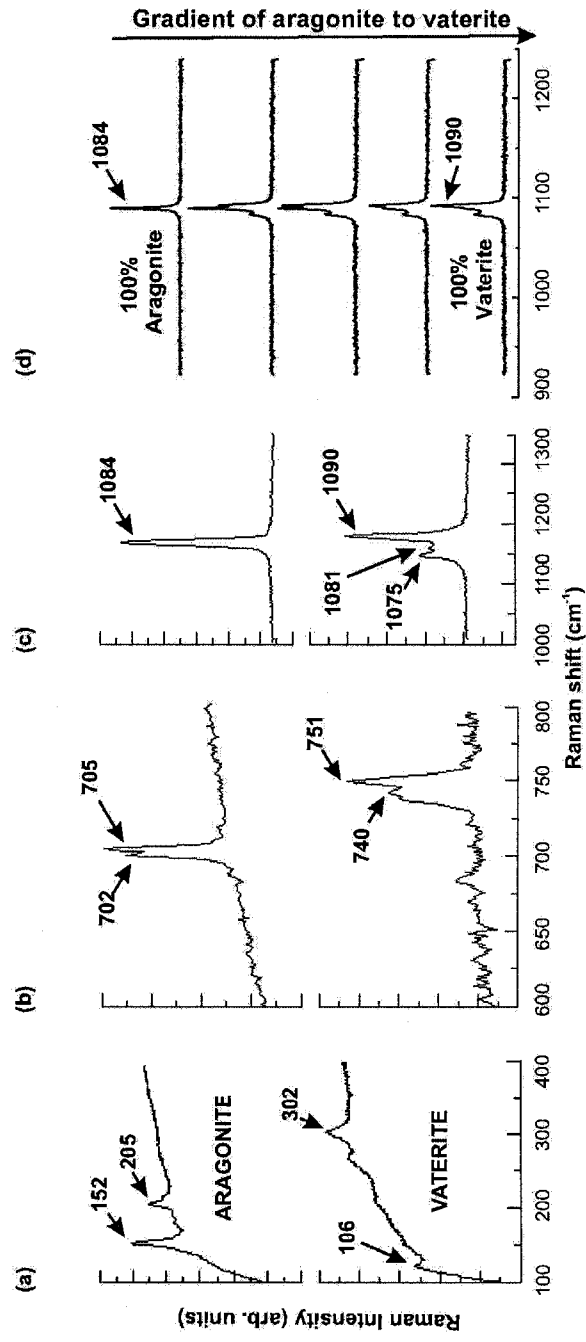


Figure 2.5: Transition from aragonite to vaterite in trace metal concentrations perpendicular to the transition zone between aragonite and vaterite boundary like in Fig 2b. of a hatchery-reared lake trout (*Salvelinus namaycush*). Elemental concentrations were quantified along this transect using LA-ICP-MS. Barium is represented by a solid line, magnesium is portrayed by small dashed line (-----), manganese by large dashed line (———), and strontium is depicted by the following sequence of large and small dashed line (— - - -).

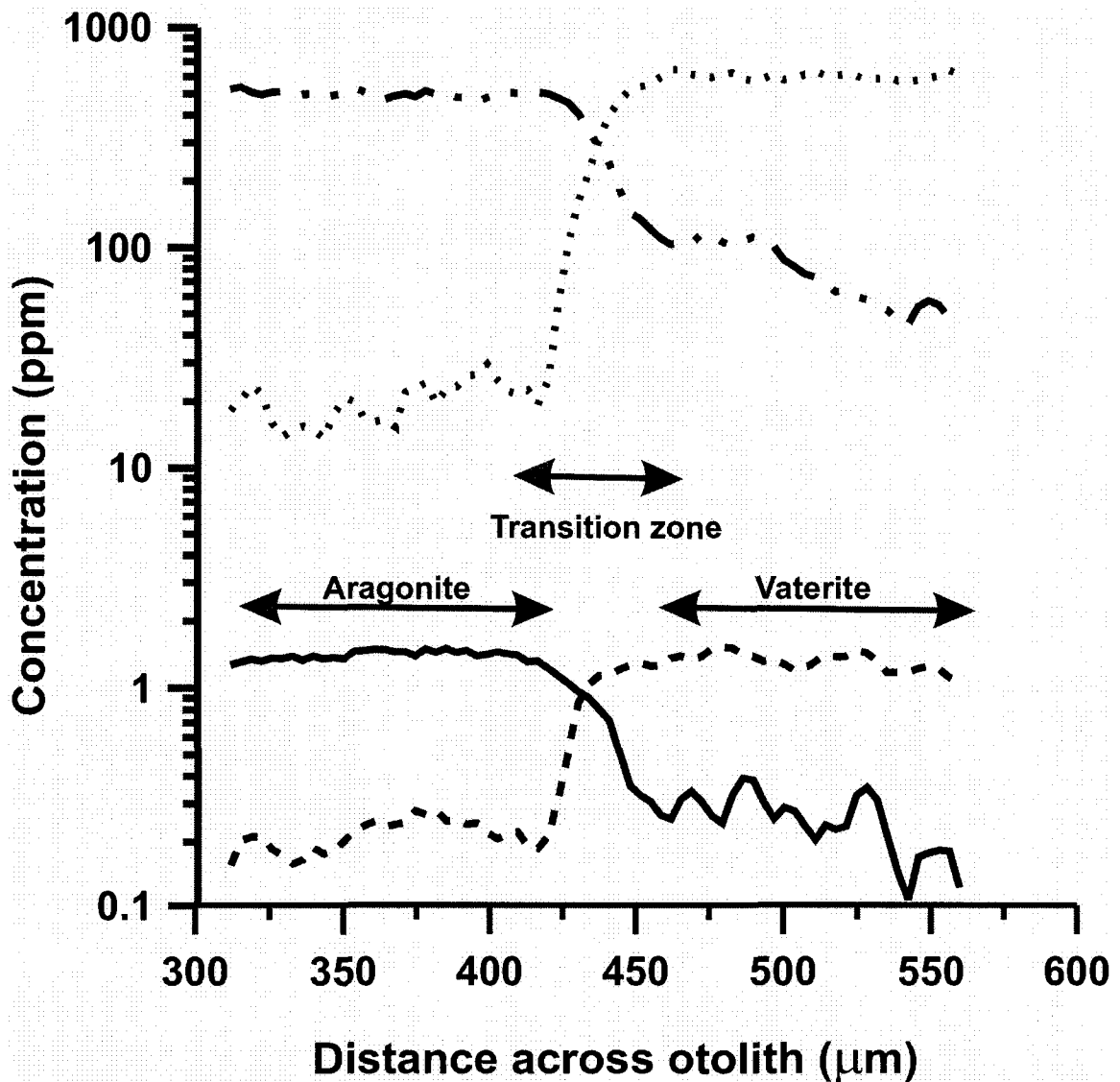


Figure 2.6: Concentrations of metal in aragonite versus vaterite from the hatchery-reared lake trout (*Salvelinus namaycush*) otolith edges (units: mg metal/Kg calcium): (a) lithium (R2 = 0.99, p < 0.001), (b) magnesium (R2 = 0.27; p = 0.07), (c) manganese (R2 = 0.09; p = 0.32), (d) zinc (R2 = 0.02; p = 0.69), (e) rubidium (R2 = 0.26; p = 0.08), (f) strontium (R2 = 0.50; p < 0.01), and (g) barium (R2 = 0.35 p = 0.03). Dashed lines, shown on some plots, are one-to-one lines. Regression equations and regression dashed lines are shown.

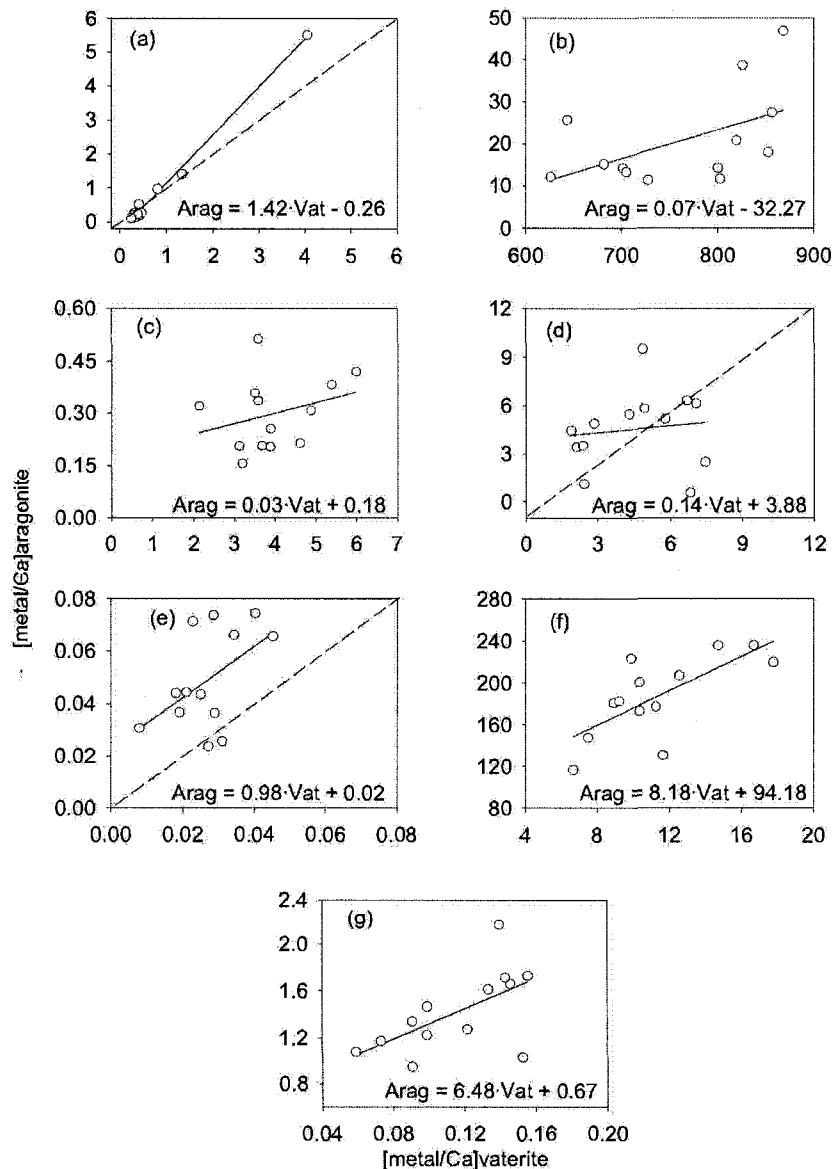
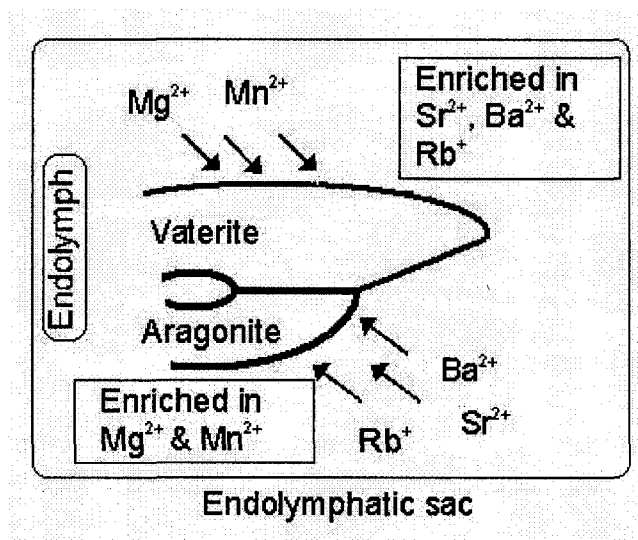


Figure 2.7: Crystallization process of otolith. Arrows portray elements that are mainly incorporated in each crystalline polymorph (vaterite versus aragonite) from the endolymph. Text boxes indicate what is enriched in the residual fluid, after elemental incorporation into the otolith. Differential incorporation of metals into the otolith portions consisting of vaterite versus aragonite would theoretically cause a gradient in the endolymph that might influence future otolith concentration changes.



CHAPTER 3

Mineralogical Approaches to the Study of Biomineralization in Fish Otoliths

3.1 INTRODUCTION

Teleost (bony) fish have three pairs of otoliths (sagittae, asteriscii and lapilli) that are used for balance and hearing. Although otoliths are mainly composed of CaCO_3 (97-99%), other metals also can be incorporated in the crystalline structure as impurities. Otoliths crystallize from fluid (endolymph) within the endolymphatic canal of the inner ear. This fluid predominantly contains ions of calcium, carbonate and bicarbonate, dissolved inorganic carbon (DIC) and trace metals. There also is a small, but non-negligible, presence of proteins and other organic materials in the endolymph and the otolith (Payan et al. 1997).

Otoliths have three properties that have made them valuable for fisheries-related research and management. First, the continual growth of otoliths is recognizable as concentric rings of alternating opaque and translucent zones (Fig. 1), which allows for individuals to be aged on both daily and annual time scales. Second, otoliths are not subject to resorption or chemical reworking, unlike other fish calcified hard parts (e.g., scales, bones). Third, the microchemical composition of otoliths can reflect the ambient chemical environment in which an individual resides. Within the past decade, fishery scientists have used these time-keeping, structural, and micro-chemical properties for numerous fisheries-related purposes, including helping to understand stock (sub-population) structure and mixing, temperature and salinity histories of both modern and ancient oceans, migratory patterns of individuals and populations, and variability in life-history strategies (see reviews by Campana 1999 and Thresher 1999).

Despite the recent, widespread use of otolith microchemistry in fisheries-related investigations, some unresolved issues remain, which have limited use of this tool to its fullest potential. For example, a complete explanation of physiological and chemical processes that determine the micro-chemical composition of otoliths is lacking. Thus, while previous research has identified that metals in the water must pass through many biological barriers (e.g., water-gills, gills-blood system, blood system-endolymph, endolymph-otolith) before being incorporated into the otolith (Campana 1999), our understanding of how metals are partitioned (fractionated) at each barrier remains enigmatic. In turn, this knowledge gap has limited our ability to understand why differences exist between the otoliths and their ambient environment for some elements.

A significant knowledge gap also exists with regard to the processes of otolith nucleation and growth, including how otolith biomineralization is initiated. Our current belief is that a cluster of particles, originally of an organic matrix origin, sets the first stage for otolith biomineralization (Nicolson 2004). Previous studies also have found that the elemental composition of the otolith core can be fundamentally different than in other (non-core) parts of the otolith (Ruttenberg et al. 2005; Brophy et al. 2004). More specifically, the chemistry of the core has been characterized by a manganese enrichment, which could be related to the amount of organic matrix present at the beginning of biomineralization, the presence of another mineral at the core, and/or a maternal transfer during spawning (Brophy et al. 2004, Ludsin et al. 2006).

This current conceptualization of how otoliths grow and biomineralize would suggest that the micro-chemical composition of the otolith core (during egg

sac resorption) would not be representative of the ambient environment. In turn, this could be problematic for fisheries management investigations that attempt to apply otolith microchemical approaches, given that most use the otolith core to define the chemistry of the natal environment (Campana et al. 2000; Secor et al. 2001; Brophy et al. 2003; Warner et al. 2005, Chittaro et al. 2006).

Herein, we document and present examples of: 1) the initial nucleation of growth in otoliths; 2) the first multi-trace element data of endolymph fluid and growing otoliths; and 3) the effect of crystal structure on the microchemistry of otoliths. Ultimately, by increasing our understanding of the mechanisms underlying otolith structure and growth, we seek to improve the ability of scientists to use otolith microchemical investigations for fisheries-related research and management.

3.2 MATERIALS AND METHODS

Fish samples for otolith studies (rainbow trout (*Oncorhynchus mykiss*), yellow perch (*Perca flavescens*), lake cisco (*Coregonus artedii*) and lake trout (*Salvelinus namaycush*)) were provided by Canadian and USA governmental agencies and researchers located in the Great Lakes basin through a number of different projects. Techniques used to prepare otoliths for analysis (sectioning and polishing) and to analyze them by LA-ICP-MS and Raman spectroscopy can be found in Ludsin et al. (2006) (yellow perch) and in Melançon et al. (2005) (all other species, and all Raman analyses).

Heads from eight frozen walleye (*Sander vitreus*) —collected by commercial fishers in western Lake Erie—were used to explore metal partitioning among ambient water, endolymphatic fluid, and otoliths. We collected fluid from both the left and right endolymphatic sacs using 10 μL micropipettes (Kimble©) and extracted the sagittal otoliths from each fish. The fluid was transferred into an acid-washed Teflon PFA container for heavy metals analysis, digested to remove the organic fraction using a mixture of trace metal grade 8N HNO_3 and H_2O_2 (30%), and then diluted with the internal standard (Be, In, Tl) spiked matrix (1% HNO_3) for analysis by ICP-MS. We compared the endolymph chemistry from the two saccular sacs (from the same fish) using a paired *t* test.

3.3 RESULTS AND DISCUSSION

3.3.1: Nucleation of otolith growth

a) Microscopic observations

Transmitted light microscopic observations of the otolith cores for our numerous fish species have demonstrated that sagittal otoliths appear to nucleate around a few (Fig. 3.1) or many (Fig. 3.2) nucleation sites or primordium (also see Campana and Neilson 1985 for a review). These nucleation sites can vary in size both within and among species, ranging in diameter between 1 and 20 μm in the species used in this study. They also are optically clearly different from the surrounding calcium carbonate (aragonite) material, with the primordium appearing much darker. Nicolson (2004) described the beginning of these nucleation sites as clusters of glycogen particles floating in the lumen and then

attaching to the first sensory hair cells. These clusters of particles are then setting the first stage of biomineralization by incorporating organic matrix molecules and starting to crystallize CaCO_3 .

In a cross section through a yellow perch otolith core (Fig. 3.1), four primordia were observed, each no larger than $1 \mu\text{m}^3$. They appeared suspended in the calcium carbonate matrix deposited before the larval fish began to feed (represented by the first growth ring). The first daily ring was deposited approximately $10 \mu\text{m}$ from the nearest primordium leading to a shape that was not concentric. It took the deposition of a few daily growth bands before the rings lose their relationships to the original nucleating sites of growth.

Rainbow trout otolith cores were much larger than the yellow perch otolith cores, being distributed across a band about $100 \mu\text{m}$ wide and $20 \mu\text{m}$ across in plan view, in between the arrows (Fig. 3.2). It shows 6 to 9 superposed primordia that range from 10 to $20 \mu\text{m}$ in diameter, with the first 5 to 10 daily rings clearly growing concentrically around the multiple original nucleation sites. Because of the significant lateral (roughly planar) distribution of the primordia in the rainbow trout otolith core, otolith growth maintains a disc-like form as it grows, unlike the yellow perch which becomes rapidly spherical.

b) Microchemistry of the otolith core

The cores of otoliths are comprised of material deposited prior to active feeding and are considered to represent the portion of the otolith formed at the spawning site while the egg sac is being absorbed (Ruttenberg et al. 2005).

Hence, otolith cores should be fundamentally different than other parts of the otolith in terms of microchemical composition. Indeed, Mn enrichment of the core, attributed to a maternal signature, has been observed by various researchers for many freshwater and marine fish species (Hedges 2002; Brophy et al. 2004; Bartnik 2005; Ruttenberg et al. 2005; Ludsin et al. 2006). Most of them used LA-ICP-MS spot analyses of 30 to 50 μm diameter, which corresponded to simultaneous sampling of all or most of the core material.

A detailed analysis of otolith cores, using a 6 μm laser spot size and laser traverse rate of 4 $\mu\text{m}/\text{s}$, allowed us to obtain much higher spatial resolution data of Mn concentrations. Our LA-ICP-MS results for a yellow perch otolith show a single, very sharp Mn concentration spike in the core centre (Fig. 3.3a), with no changes being apparent for other element such as Ba, Sr and Ca (S. Ludsin, unpublished data). For yellow perch otolith cores, the few primordia were closely spaced and much smaller ($\sim 1 \mu\text{m}^3$ each) than the traversing laser spot diameter (6 μm). Considering a laser sampling depth of approximately 10 μm and a 6 μm spot size, the volume of material being sampled ($V = \pi R^2 h$) by the laser is substantially greater than a single primordium. In turn, our calculated Mn concentration at the centre of the core (207 ppm; Fig. 3.3a) would be significantly underestimated (100 to 300 fold). Some preliminary $\mu\text{-XRD}$ results showed that aragonite was the only mineral present in the core of these yellow perch. However, the synchrotron beam line had a spot size of 10 μm and was too large to show if there was a minor amount ($1 \mu\text{m}^3$) of MnCO_3 in the core.

We also found that the cores of larval lake cisco otoliths were enriched in Mn (Fig. 3.3b). The Mn concentrations exhibit three maxima in the core area and a much broader zone of Mn enrichment that had a maximum concentration calculated at 4130 ppm. The prevalence of multiple, large, and widely dispersed primordia in lake cisco corresponds to what we (and others) have found for another salmonide, rainbow trout (Fig. 3.2).

Based on the coherence of the petrographic and microchemical observations in otolith cores of numerous unrelated species, we suggest that the seemingly anomalous Mn peaks observed are related to the formation, mineralization and micro-distribution of primordia rather than environmental factors or the natal core region in general. The strong Mn enrichment in the primordia could be associated with the large amount of organic matrix present at the beginning of aragonite biomineralization or perhaps the initial formation of a separate mineral phase (e.g., rhodochrosite, MnCO_3), within the primordia. No spectroscopic information is currently available to test these hypotheses; however, our observed very high Mn concentrations in otolith cores does rule out Brophy et al.'s (2004) hypothesis that a calcite precursor is the source of nucleation in otoliths.

The seeding of otolith growth has been studied by several groups: Riley et al. (1997), Pisam et al. (2002), and Nicolson (2004). Previous research, has determined that for zebrafish (*Danio rerio*) larval otolith growth is initiated at 18 to 18.5 hours, post egg fertilization, by the local accretion of precursor glycogen particles at the ends of developing tether hair cells, usually 2 per otolith (Riley et al. 1997). This accretion of precursor particles which fuse to form the early otolith

material is complete by 24 hours. These otolith seed particles are presumably the primordia observed petrographically in otolith cores (Figs. 3.1 and 3.2), which appear to be associated with the Mn enrichment. The localized Mn enrichment must only be associated with the earliest stage(s) of biomineralization in the core. Interestingly certain otoconial deficiencies in mice caused by mutations can be corrected by dietary supplements of Mn and Zn (Riley et al. 1997). This suggests that there may be a link between Mn segregation with the primordia and the beginning of aragonite crystallization in the otolith.

3.3.2: Flux of metals to the growing otolith

*Water-endolymph-otolith equilibrium in Walleye (*Sander vitreus*)*

All post larval otolith growth occurs within the endolymphatic canal of the inner ear, with the otolith crystallizing from a fluid (endolymph) that is chemically connected to the environment (water/food) through the blood system. The endolymph contains ions of Na, Ca, carbonate and bicarbonate, trace metals and organic forms of carbon (e.g., proteins) from which the growing otolith extracts these trace elements. Despite its obvious importance in understanding otolith microchemistry, few studies have considered the relationships between otolith chemistry and endolymph (-water) chemistry (but see Kalish 1991).

Our analysis of eight Lake Erie western basin walleye found all elements, except for Ba, to be statistically identical in both left and right endolymph fluids (paired t test: all $|t| \geq 3.5$). As such, we pooled and averaged the left and right endolymph data for each individual. We also found no relationship between fish age and the endolymph composition for any elements ($R^2 \leq 0.39$; not shown).

However, the fish were harvested at least 3 days before we were able to sample the endolymph and otolith from the frozen heads. Milton & Chenery (1998) found that Na, Mg and Ba concentrations in otoliths were the most affected by otoliths left in the fish head for several weeks, hence our measured endolymph compositions may be somewhat affected by the delayed sampling. The effect would likely be negligible, if present, due to the relatively short period of storage time.

Our results show strong enrichment of Na, K, Zn and Ba from Lake Erie water to the endolymph, all with $K_D (e/w) \gg 1$ (Table 3.1). Sodium, K and Zn are highly regulated elements in fish (Campana 1999), which helps to account for their high K_D s for fresh water fishes (low aqueous concentrations). However, the strong enrichment of Ba is surprising. Other elements including Mg, Ca and Mn (exception of Sr) had similar concentrations in water and endolymph ($K_D (e/w) \approx 1$; i.e., they were not enriched). Partition coefficients between the growing otolith edge (Fig. 3.4) and water for all elements, except Mg, also suggested an enrichment ($K_D (o/w) \gg 1$). The partition coefficients between the otolith and the endolymph ($K_D (o/e)$) were close to 1 for all elements (except Ca and Sr). Calcium and Sr were equally enriched in the otolith relative to the endolymph in which they crystallize ($K_D (o/e) = 4140$ and 3910 , respectively). Barium was much more concentrated than Sr in the endolymph relative to the external water despite the fact that both these elements are generally interpreted to directly reflect water chemistry in otolith microchemistry studies (Bath et al. 2000; Milton. and Chenery 2001; Wells et al. 2003). This deviation may be due to the extremely high strontium $K_D (o/e)$, which can deplete endolymph in Sr compared to Ba (Melançon

et al. 2005). Sodium and K had similar fractionation patterns (i.e., similar $K_D (o/e)$, $K_D (e/w)$ and $K_D (o/w)$ values), presumably because both elements are alkali metals found in and being highly regulated in blood.

The concentrations of K, Ca and Na in the endolymph fluid of individual fish were all strongly positively correlated (all $R^2 \geq 0.9$; Figs. 3.5 a-c). Interestingly, Zn and Cu also showed a similar strong correlation (Figure 3.5d) in endolymph samples from different species. This finding might indicate strong physiological control as these two elements are essential nutrients and may be regulated in fish the same way as Na, K and Ca (Roesijadi 1992). Their cation radii are also similar, 0.88 Å for Zn and 0.87 Å for Cu, suggesting a similar role in the fish's body.

3.3.3: Effect of crystal structure on element partitioning

Simultaneous vaterite-aragonite growth in lake trout otoliths

Previous work has shown that more than one crystal polymorph of CaCO_3 can be found in otoliths (Campana 1983, Gauldie 1986), the most common being aragonite and vaterite. Our microscopic analysis of otoliths from lake trout indicated that aragonite and vaterite can grow simultaneously within the endolymphatic sac (Fig. 3.6). Melançon et al. (2005) showed that aragonite and vaterite can have different growth rates and that generally vaterite growth rates exceeded that of co-precipitating aragonite. They demonstrated that element concentrations were not affected by the growth rate of the polymorphs as elemental results for vaterite>aragonite and vaterite<aragonite were similar for most elements.

The characteristics of the structural forms of CaCO_3 in lake trout sagittal otoliths were investigated by Raman spectroscopy and LA-ICP-MS. The Raman spectra present three distinct characteristics associated with group vibration: lattice mode, symmetric stretching, and in-plane bending (Gans 1971; Truchet et al. 1995). These were used by Gaudie et al. (1997) to distinguish vaterite from aragonite in otoliths of Coho salmon (*Oncorhynchus kisutch*). We used the symmetric stretching of C-O from carbonate anion bonded to calcium, ν_1 , to differentiate vaterite from aragonite. Triplet bands (1075 cm^{-1} , 1081 cm^{-1} and 1090 cm^{-1}) characterized vaterite whereas aragonite has only a single band at 1084 cm^{-1} (Fig. 3.7).

Table 3.2 presents a summary of mean metal concentrations in co-precipitated aragonite and vaterite in adult lake trout otoliths (data derived from Melançon et al. (2005)). There is extreme elemental fractionation between the two crystal polymorphs with aragonite portions of otoliths being characterized by high Sr and Ba and low Mg and Mn, whereas vaterite portions have the opposite trends. Zinc, Li and Rb have approximately equal concentrations for the two phases. Based on these data, the proportions of elements being removed by crystallization of otolith material from the endolymph fluid will be greatly different if one or the other (or both) CaCO_3 polymorphs are forming at a particular time. This result suggests that great care will need to be taken when using and comparing otolith chemistry from species that are known to grow otoliths comprising multiple polymorphs.

3.4 CONCLUSIONS

The three examples, presented in this paper, indicate the importance of mineralogical input and thinking into the understanding of biomineralization processes as well as the need for a much better understanding of the mechanisms of crystal nucleation and growth in these complex systems. There is a pressing need in the study of biomineralization, for more than just the application of geochemical methods to ecological questions. An element like Mn which is clearly influenced by maternal effects and not the environment, should not be trusted for discrimination amongst natal sites in fisheries research.

3.5 ACKNOWLEDGEMENTS

Walleye heads were provided by Presteve Foods Limited, Wheatley, Ontario. Lake Erie lake trout otoliths were graciously provided by Jim Markham, Lake Erie Fisheries Unit, New York State Department of Environmental Conservation (NYSDEC). Cisco larvae from Lake Superior were provided by Jason Stockwell. Rainbow trout fish were provided by Yolanda Morbey from the Ontario Ministry of Natural Resources (OMNR). We thank the Great Lakes Fishery Commission (Fisheries Research Program grant to B. Fryer et al.), the National Sciences and Engineering Research Council (Strategic Research Grant to P. Sale et al. and Discovery Grants to B. Fryer and J. Gagnon), the Ohio Department of Natural Resources-Division of Wildlife, and the University of

Windsor's Great Lakes Institute for Environmental Research for support for this research.

3.6 REFERENCES

- Bartnik, S.E.H. 2005. Population dynamics of age-0 walleye in western Lake Erie. M.Sc. Thesis, University of Windsor, Windsor.
- Bath, G.E., Thorrold, S.R., Jones, C.M., Campana, S.E., McLaren, J.W., and Lam, J.W.H. 2000. Strontium and barium uptake in aragonitic otoliths of marine fish. *Geochim. Cosmochim. Acta.* **64**: 1705-1714.
- Brophy, D., Danilowicz, B.S. and Jeffries, T.E. 2003. The detection of elements in larval otoliths from atlantic herring using laser ablation ICP-MS. *J. Fish Biol.* **63**, 990-1007.
- Brophy, D., Jeffries, T.E. and Danilowicz, B.S. 2004. Elevated manganese concentrations at the cores of clupeid otoliths: possible environmental, physiological, or structural origins. *Mar. Biol.*, **144**: 779-786.
- Campana, S.E. 1983. Feeding periodicity and the production of daily growth increment in otoliths of steelhead trout *Salmo gairdneri*. and starry flounder *Platichthys stellatus*.. *Can. J. Zool.* **61**: 1591-1597.
- Campana, S.E. 1999. Chemistry and composition of fish otoliths: pathways, mechanisms and applications. *Mar. Ecol. Prog. Ser.* **188**: 263-297.
- Campana S.E. and Neilson J.D. 1985. Microstructure of fish otoliths *Can. J. Fish. Aquat. Sci.* **42**: 1014-1032.
- Campana, S.E., Chouinard, G.A., Hanson, J.M., Fréchet, A. and Bratney, J. 2000. Otolith elemental fingerprints as biological tracers of fish stocks. *Fish. Res.* **46**: 343–357.

- Chittaro, P.M., Hogan, J.D., Gagnon, J., Fryer, B.J. and Sale, P.F. 2006. In situ experiment of ontogenetic variability in the otolith chemistry of *Stegastes partitus*. *Mar. Biol.* **149**: 1227-1235.
- Gans, P. 1971. General considerations *In* Vibrating molecules. An introduction to the interpretation of infrared and raman spectra. Edited by Williams Clowes & Sons Limited. London, Colchester and Beccles. pp. 1-25.
- Gauldie, R.W., Sharma, S.K. and Volk, E. 1997. Micro-Raman spectral study of vaterite and aragonite otoliths of the coho salmon, *Oncorhynchus kisutch*. *Comp. Biochem. Physiol. A Comp. Physiol.* **118**: 753-757.
- Hedges, K.J. 2002. Use of calcified structures for stock discrimination in Great Lakes walleye *Stizostedion vitreum*. M.Sc. Thesis. University of Windsor, Windsor, ON Canada.
- Kalish, J.M. 1991. Determinants of otolith chemistry: seasonal variation in the composition of blood plasma, endolymph and otoliths of bearded rock cod *Pseudophycis babatus*. *Mar. Ecol. Prog. Ser.* **74**: 137-159.
- Ludsin, S.A., Fryer, B.J. and Gagnon, J.E. 2006. Comparison of solution-based versus laser-ablation ICPMS for analysis of larval fish otoliths. *Trans. Am. Fish. Soc.* **135**: 218–231.
- Melançon, S., Fryer, B.J., Gagnon, J.E., Ludsin S.A. and Yang, Z. 2005. Effects of crystal structure on the uptake of metals by lake trout *Salvelinus namaycush*. otoliths. *Can. J. Fish. Aquat. Sci.* **62**: 2609-2619.
- Milton, D.A. and Chenery, S.R. 1998. The effect of otolith storage methods on the concentrations of elements detected by laser-ablation ICPMS. *J. Fish Biol.*, **53**: 785-794.

- Milton D.A. and Chenery S.R. 2001. Sources and uptake of trace metals in otoliths of juvenile barramundi *Lates calcarifer*, *J. Exp. Mar. Biol. Ecol.* **264**: 47-65.
- Nicolson, T. 2004. Control of crystal growth in biology: a molecular biological approach using zebrafish. *Cryst. Growth Des.* **4**: 667-669.
- Payan, P., Kossmann, H., Watrin, A., Mayer-Gostan, N. and Bœuf, G. 1997. Ionic composition of endolymph in teleosts: Origin and importance of endolymph alkalinity. *J. Exp. Biol.* **200**: 1905-1912.
- Pisam, M., Jammet, C. and Laurent, D. 2002. First steps of otolith formation of the zebrafish: role of glycogen? *Cell Tissue Res.* **310**: 163-168.
- Riley, B.B., Zhu, C., Janetopoulos, C. and Aufderheide, K.J. 1997. A critical period of ear development controlled by distinct populations of ciliated cells in the zebrafish. *Dev. Biol.* **191**: 191-201.
- Roesijadi, G. 1992. Metallothioneins in metal regulation and toxicity in aquatic animals. *Aquat. Toxicol.* **22**: 81-114.
- Ruttenberg, B.I., Hamilton, S.L., Hickford, M.J.H., Paradis, G.L., Sheehy, M.S., Standish, J.D., Ben-Tzvi, O. and Warner, R.R. 2005. Elevated levels of trace elements in cores of otoliths and their potential for use as natural tags. *Mar. Ecol. Prog. Ser.* **297**: 273-281.
- Secor, D.H., Rooker, J.R., Zlokovitz, E. and Zdanowicz, V.S. 2001. Identification of riverine, estuarine, and coastal contingents of Hudson River striped bass based upon otolith elemental fingerprints. *Mar. Ecol. Prog. Ser.* **211**: 245-253.

- Shannon, R.D. 1976. Revised effective ionic radii and systematic studies of interatomic distances in halides and chalcogenides. *Acta Crystallogr. Sect. A: Found. Crystallogr.* **32**: 751.
- Thresher, R.E. 1999. Elemental composition of otoliths as a stock delineator in fishes. *Fish. Res.* **43**: 165-204.
- Truchet, M., Delhay, M. and Beny, C. 1995. Identification des carbonates de calcium, calcite, aragonite et vaterite par microsonde Raman-Castaing. Application aux biominéralisations. *Analisis*, **23**: 516-518.
- Warner, R.R., Swearer, S.E., Caselle, J.E., Sheehy, M. and Paradis, G. 2005. Natal trace-elemental signatures in the otoliths of an open-coast fish. *Limnol. Oceanogr.* **50**: 1529-1542.
- Wells, B.K., Rieman, B.E., Clayton, J.L., Horan, D.L., and Jones, C.M. 2003. Relationships between water, otolith, and scale chemistries of Westlope Cutthroat Trout from the Coeur D'Alene River, Idaho: the potential application of hard-part chemistry to describe movements in freshwater. *Trans. Am. Fish. Soc.* **132**: 409-424.

Table 3.1: Mean metal concentrations (ppm) in the Lake Erie water (western basin), the endolymph and the growing edges of walleye otoliths. Values of partition coefficients $K_{D(E/W)}$, $K_{D(O/E)}$ and $K_{D(O/W)}$ are also shown.

	Water (n=10)	Endolymph (n=16)	Otoliths (n=16)	$K_{D(E/W)}$	$K_{D(O/E)}$	$K_{D(O/W)}$
Na	19 ±5	1750 ±570	1370 ±330	91	0.47	43
Mg	21 ±1	19 ±10	5 ±3	0.93	1.2	1.1
K	3.9 ±0.6	557 ±190	277 ±46	140	0.32	47
Ca	69 ±6	98 ±34	400432	1.4	4140	5930
Mn	0.04 ±0.01	0.07 ±0.07	0.12 ±0.08	2.0	2.4	4.7
Zn	0.009 ±0.001	3 ±2	3 ±2	370	0.40	150
Rb	N/A	1.1 ±0.4	0.08 ±0.05	N/A	0.074	N/A
Sr	0.9 ±0.4	0.12 ±0.04	159 ±26	0.13	3910	500
Ba	0.048 ±0.003	0.8 ±0.3	1.2 ±0.9	16	4.8	77

Table 3.2: Mean metal concentrations (ppm) in the growing edges of Broodstock lake trout otoliths.

	Cation radii ¹	Aragonite	Vaterite
	Å	(n = 25)	(n = 25)
Mn	0.81	1.0 ±0.2	9.4 ± 0.7
Mg	0.86	16 ±2	596 ± 29
Zn	0.88	11 ±2	8 ± 2
Li	0.90	0.08 ±0.03	0.2 ± 0.1
Ca	1.14	400432	400432
Sr	1.32	780 ±27	45 ± 2
Ba	1.49	7.3 ±0.4	0.39 ± 0.04
Rb	1.66	0.12 ±0.01	0.08 ± 0.01

¹Shannon R.D., 1976

Figure 3.1: Yellow perch (*Perca flavescens*) otolith showing daily growth increments and multiple nucleation sites (primordia) in the core. The core is identified in between the arrows and several primordia have been shown.

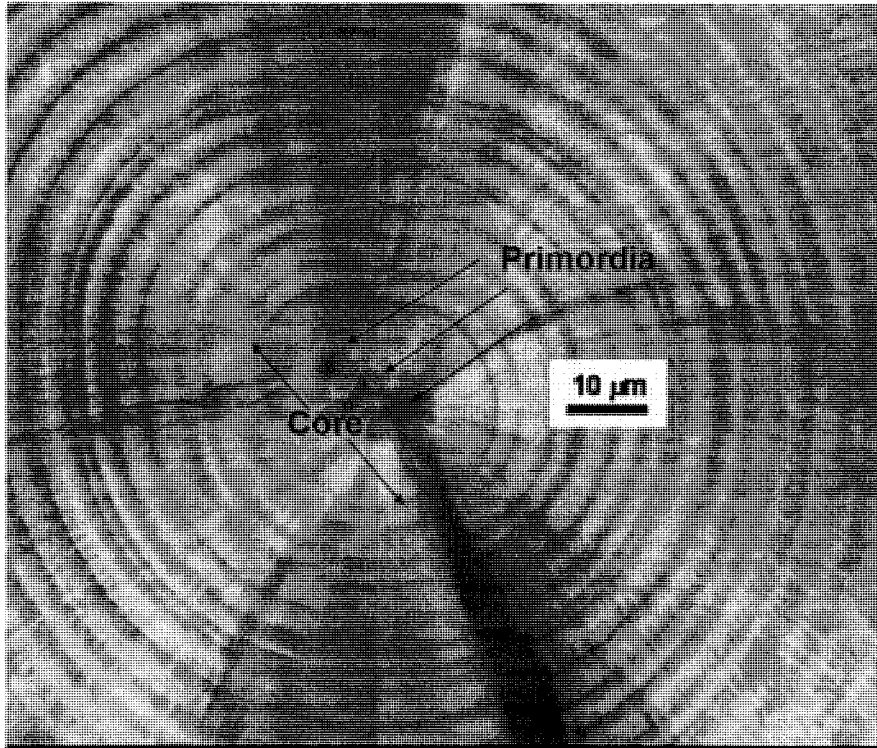


Figure 3.2: Rainbow trout (*Oncorhynchus mykiss*) otolith showing multiple nucleation sites (primordia) in the core as well as subsequent growth initiated around the individual primordia. Some of the primordia are identified with the arrows.

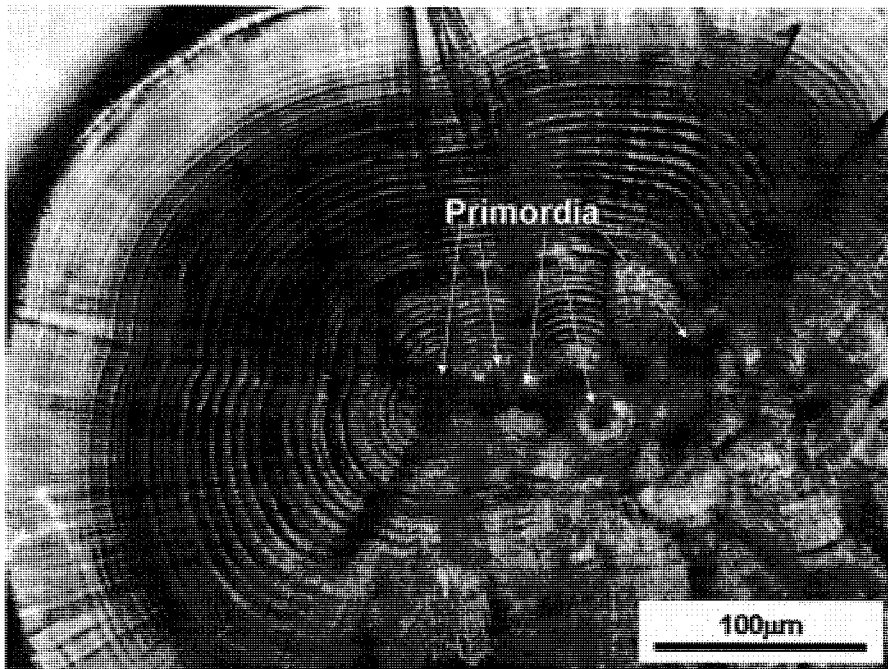


Figure 3.3: Concentration profiles of Mn (ppm) in the otolith cores of (a) Yellow perch (*Perca flavescens*) and (b) cisco (*Coregonus artedii*). Distance is from one edge of the otolith to the other with the laser transect passing through the middle of the core.

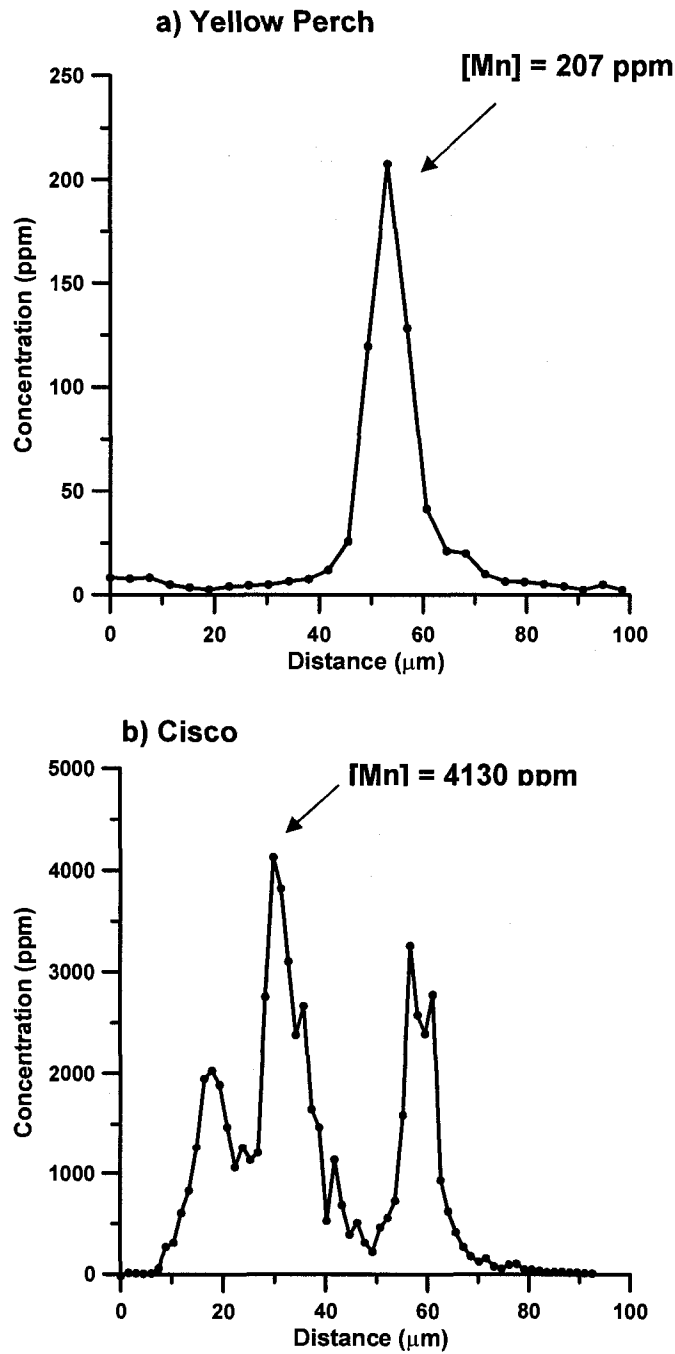


Figure 3.4: Sagittal otolith from age-11 walleye (*Sander vitreus*). Yearly growth bands are indicated by white dots and LA-ICP-MS analyses were conducted on the edge of the year 11 growth band.

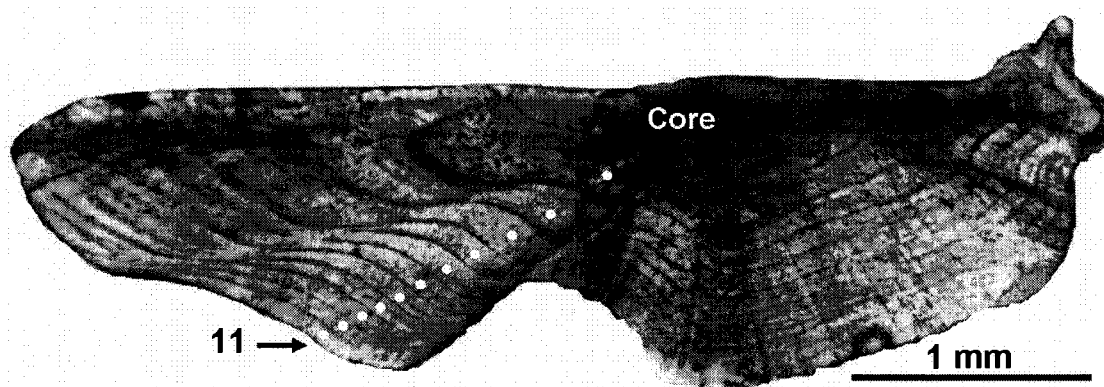


Figure 3.5: Comparison of metal concentrations of the endolymph of walleye a) Ca/K, b) Ca/Na, c) K/Na and d) Zn/Cu

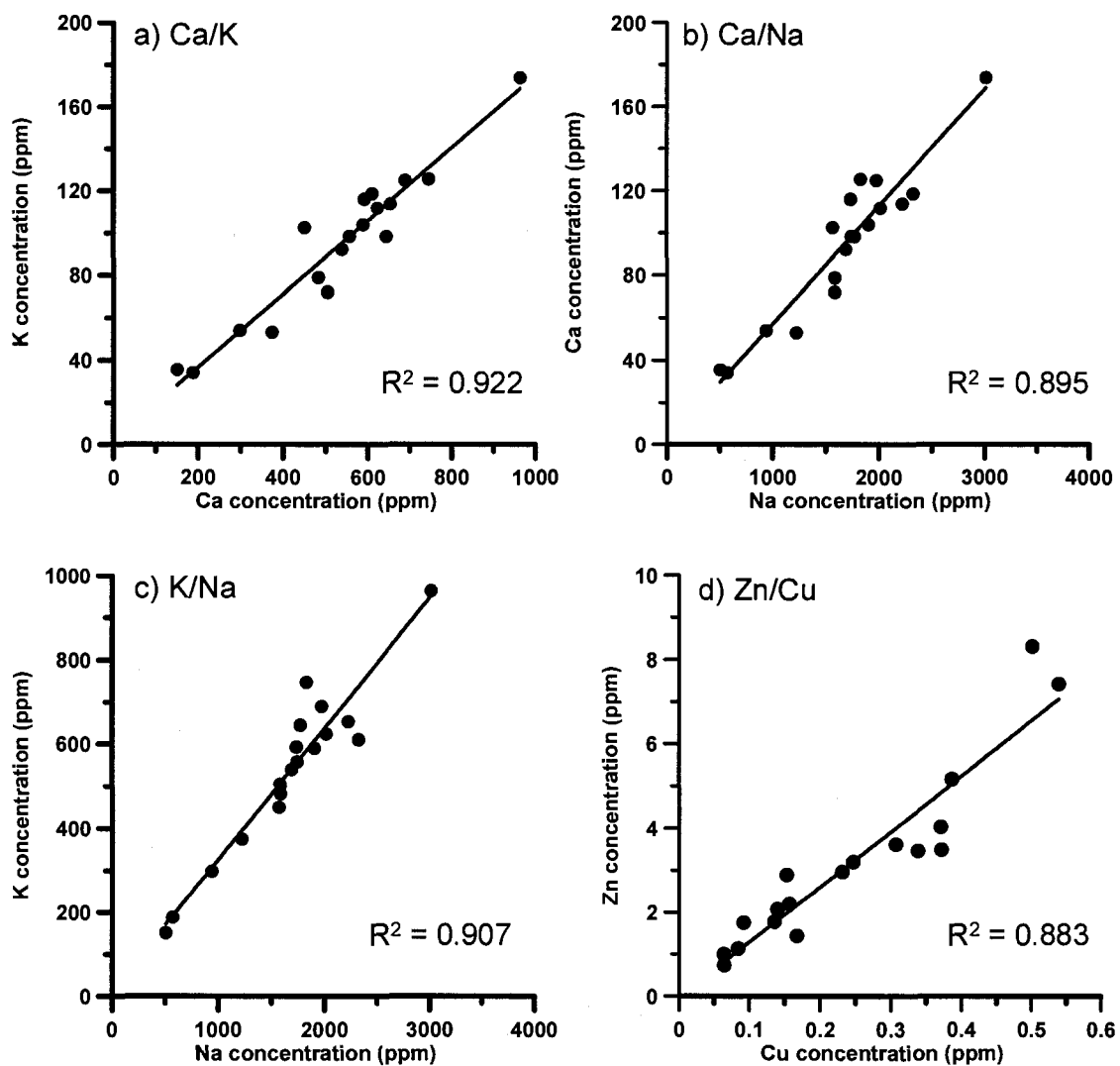


Figure 3.6: Lake trout (*Salvelinus namaycush*) otoliths showing the simultaneous growth of aragonite and vaterite. The 'waviness' of the vaterite growth bands can be easily differentiated petrographically compared to the regular aragonite growth bands.

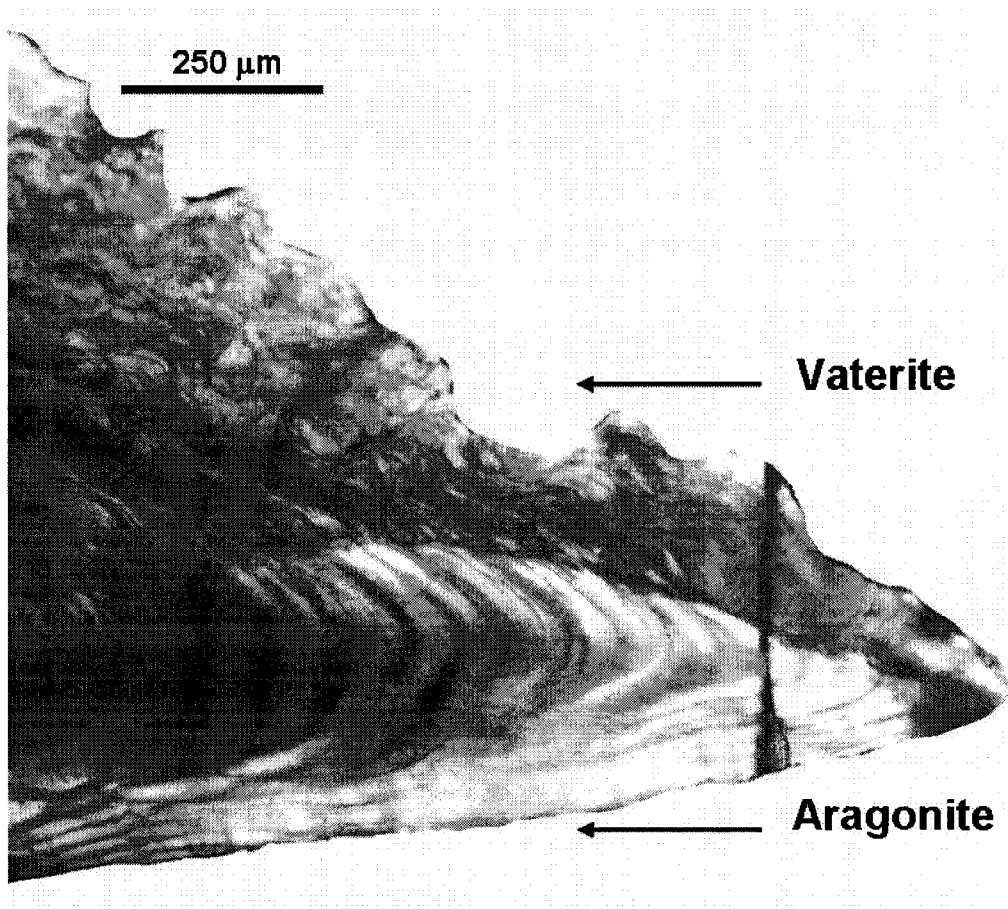
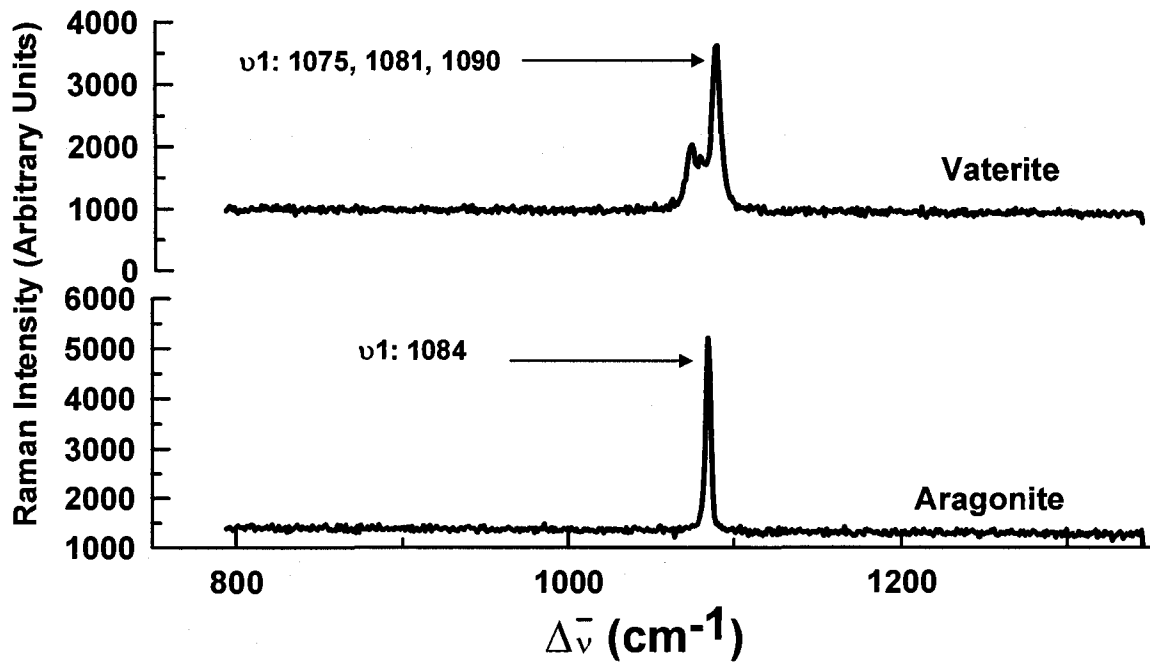


Figure 3.7: Wave numbers from the Raman spectroscopy analysis of aragonite and vaterite in lake trout otolith edges in arbitrary units plotted against Raman shift in cm^{-1} . Vaterite signal is on top and aragonite is at the bottom. Symmetric stretching (ν_1) values are presented on the Raman graph for both polymorphs.



CHAPTER 4

Chemical analysis of the endolymph and the growing otolith: fractionation of metals in freshwater fish species

4.1 INTRODUCTION

Teleost otoliths are calcified structures mainly composed of calcium carbonate (CaCO_3). Considered the ear stones of fish, these function in equilibrium and sound detection. There are three pairs of otoliths: the sagitta, the lapillus and the astericus. These grow in separate compartments (sacculle, utricule and lagena, respectively) filled with a fluid called endolymph. This characteristic differentiates otoliths from other calcified structures (e.g. teeth, bones) as their growth is strictly constrained by the availability of precursors for calcification in the endolymph. This fluid predominantly contains Ca^{2+} , CO_3^{2-} , HCO_3^- , and trace metals (Enger 1964, Payan et al. 1997). There is also a small, but significant, presence of proteins and other organic biomacromolecules in the endolymph and the otolith (Kalish 1989; 1991, Takagi 1997, 2002; Tohse et al. 2004). The sagittae are the largest of the three pairs of otoliths and are normally used to estimate the age of the fish. The daily deposition of a layer of calcium carbonate and proteins marks the continual growth of the otolith and is recognizable as concentric rings of alternating opaque and translucent zones (Degens et al. 1969; Panella 1971). Otoliths are not considered to be subject to resorption. Once an element has been incorporated in the otolith it remains chemically and isotopically inert. Consequently, only ontogenic (physiology of fish) and environmental factors should cause changes in chemical composition (Campana 1999; Thresher 1999). However the relationship between elements in the otolith and how they relate to water composition is complicated by their separation by various boundaries and processes (gills/brachial uptake, cellular

transport, crystallization) where fractionation of trace metals is not well understood.

Fractionation patterns of organic compounds (proteins, triglycerides etc.) and some metals (Na, Mg, K, Ca, Sr) and non-metals (S) were reported in the blood plasma, endolymph and otolith of cod (*Pseudophycis barbatus*) by Kalish (1991). He studied their seasonal variation and found that modest changes in temperature did not dramatically affect metal concentrations in blood and endolymph. Rather it is the physiological changes in the fish during these seasons that were the most important factors in blood and endolymph metal variations which can in turn influence the otolith composition. However, he did not investigate the fractionation of elements between these filters. In a related study, Payan et al. (1999) found that non-uniformity in the composition of the endolymph of trout (*Oncorhynchus mykiss*) and turbot (*Psetta maxima*) influenced the biomineralization process of otoliths. They showed an ionic (K, Na) and proteomic gradient within the endolymph along the proximal-distal axis of the otolith that was partially maintained by the sagittal otolith acting as a physical barrier to the diffusion of ions and proteins. Furthermore, Borelli et al. (2001) found a relationship between organic compounds in the otolith and the surrounding endolymph. Plasma homeostasis, endolymph chemistry and otolith growth in stressed fish have also been studied (Payan et al. 2004, Guibbolini et al. 2006). It was found that fish exposure to Cl_2 (g) decreased the content of Na and Cl in the endolymph and blood plasma, whereas all the other chemicals analyzed (K, PO_4 , Mg and total Ca) remained stable.

Although, many published studies have looked at endolymph composition and how it relates to otolith growth, none report data for trace metals in the endolymph. The only study presenting multi-element analysis of endolymph is a preliminary study we conducted on walleye (*Sander vitreus*) (Melançon S. et al. in review). The only other data available in the literature are for Na, Mg, K, and Ca reported by Kalish (1991) and Payan et al. (1999; 2004).

We do not understand the fundamentals of metal uptake and partitioning between water, blood, endolymph and the otolith despite the fact that otoliths are widely studied and used in a range of environmental applications. There are no published data describing the broad range of metals in blood and endolymph and how they relate to the chemistry of otolith and water.

This research focuses on metal partitioning between otolith and endolymph of two freshwater species: lake trout (*Salvelinus namaycush*) and burbot (*Lota lota*). The two chosen species were collected from the Eastern basin of Lake Erie which is the deepest part (30-60 m) of this large, temperate, dimictic lake. They also have similar feeding behaviours and occupy similar summertime bottom dwelling niches but are from different taxonomic families. The burbot is the only representative of the cod (*Gadidae*) family in North American freshwaters while the lake trout is from the large *Char* group. We also present chemical analyses of water and blood from fish of the same species collected in the same area, in an effort to better understand the fractionation process of trace metals. Assuming steady state, partition coefficients are calculated for metals in the water, blood, endolymph and otolith:

$$K_{D(B/W)} = [\text{Metal}]_{\text{blood}} / [\text{Metal}]_{\text{water}} \quad (1)$$

$$K_{D (E/B)} = [\text{Metal}]_{\text{endolymph}} / [\text{Metal}]_{\text{blood}} \quad (2)$$

$$K_{D (O/E)} = [\text{Metal}]_{\text{otolith}} / [\text{Metal}]_{\text{endolymph}} \quad (3)$$

$$K_{D (O/W)} = [\text{Metal}]_{\text{otolith}} / [\text{Metal}]_{\text{water}} \quad (4)$$

4.2 MATERIALS AND METHODS

4.2.1 Collection of endolymph and otolith extraction

Analyses were conducted on lake trout and burbot collected from the eastern basin of Lake Erie via annual assessment surveys conducted by the New York State Department of Environmental Conservation (NYSDEC) at the Lake Erie Fisheries Unit (see Einhouse et al. 2006 for sampling details). Fish were caught and euthanised over a period of 4 days from 9-12 August 2005. They were all mature and ranged between 4-14 years old. Their length was between 600 and 800 mm and their weight ranged from 2000 to 6300 g.

Study fish were put in coolers on ice, and endolymph and otolith extraction was performed as soon as the fish were brought back on land (within a few hours after death). The skull was opened with a frontal incision behind the eyes and the saccular membrane was exposed (contains endolymph and otolith). The membrane was perforated with a 25 μL syringe (Hamilton 80222) and the endolymph was extracted in the proximal region. We collected both left and right endolymph and otolith from each fish. To reduce trace metal contamination, a 2 inch platinum needle was used (Hamilton 90522). The fluid was transferred into an acid-washed plastic container for metal analysis and diluted with an internal

standard spiked matrix (1% HNO₃ +Be, In, Tl) for preservation until digestions were done. In the laboratory, we evaporated the samples to dryness, added 2 mL of 8 N ultra pure HNO₃ and evaporated overnight (at 100°C). A second digestion step was done using 1 mL of 8 N HNO₃ and 1 mL H₂O₂ (trace metal grade) and evaporated overnight. Lastly, 3 mL of 1 % HNO₃ was added and the Teflon tubes were covered with caps and heated (at approximately 60°C) overnight. Samples were then diluted for analysis and kept in the fridge until SO-ICP-MS analyses.

Sagittal otoliths from this suite of individuals were extracted and stored in small glass vials. Sagittal otoliths were embedded in epoxy resin (West Coast Marine®), sectioned (~800 µm thick) using a Buehler ISOMET™ saw, and polished and cleaned according to protocols in Melançon et al. (2005).

4.2.2 Collection of blood and water

Blood (2006) and water (2007) samples were collected on subsequent annual surveys at the same time of year and locations to provide additional information on element partitioning. Blood from lake trout and burbot were collected from a cardiac puncture. The whole blood samples were mixed with heparin, an anticoagulant, to prevent blood clots and then filtered to remove the solids. The blood was then transferred into plastic vials and kept cool (4°C/F39) until shipped to the lab. In the laboratory, each blood sample was weighed (0.1g) and digested following the same procedure mentioned in the previous section for the endolymph (4.2.1). These samples are used as average blood data and cannot be compared directly to the endolymph-otolith system as they were not

collected at the same time. Surface water samples were collected in acid washed bottles. Two samples were taken at each site over a period of 2 days and refrigerated. The samples were filtered using 0.45-mm viscose filters and acidified to 1% HNO₃ with trace metal grade concentrated nitric acid, for preservation. Samples were then refrigerated until analysis.

4.2.3 Inductively coupled plasma-mass spectrometry

Water, endolymph and blood samples were analyzed using SO-ICP-MS on a Thermo-Elemental® X7® ICP mass spectrometer. All solution samples and standards were spiked with our internal standard solutions (1% HNO₃ +Be, In, Tl) to correct for matrix and drift effects on an individual sample basis. Using SO-ICP-MS, we measured the following isotopes ⁷Li, ²³Na, ²⁴Mg, ²⁵Mg, ³⁹K, ⁴³Ca, ⁴⁴Ca, ⁵⁵Mn, ⁵⁷Fe, ⁶⁶Zn, ⁸⁵Rb, ⁸⁶Sr, ⁸⁸Sr, ¹³⁷Ba, ¹³⁸Ba and ²⁰⁸Pb.

Elemental concentrations of the otoliths were quantified by LA-ICP-MS using a purpose-built laser sampling system comprised of a Continuum® Surelite® I solid state Nd:YAG laser at a wavelength of 266 nm (maximum power: 40mJ; pulse rate: 20 Hz; pulse width: 4-6 ns; laser spot diameter: 32 μm) coupled to the Thermo-Elemental® X7® ICP-MS (peak-jumping mode, 10 ms dwell time per isotope). Analytical protocols are given in Melançon et al (2005) and details concerning measures of precision, limits of detection (LODs), and percentages of samples of above LODs are reported elsewhere (Ludsin et al. 2004). A series of ablations were performed at the growing otolith edges which were in contact with the endolymph and represent the last 30-60 days in the life of

the fish (last ring). Calcium was used as an internal standard to correct for variations in the amount of material ablated (i.e., ablation yield).

4.3 RESULTS

4.3.1 Endolymph and Otoliths

We compared endolymph results from the 2 saccular sacs of the same fish using the paired t-Test. and determined that they were statistically similar for all elements in both species except for Na in burbot (burbot n= 12, all p > 0.07 (except Na = 0.049 which was insignificant after Boneferroni correction; lake trout n= 5, all p > 0.07). This allowed us to pool the left and right data for each fish. Endolymph samples that were two times the standard deviation above or below the mean were rejected. These were suspected to have been contaminated before or during sampling. Since there was no significant difference between left and right endolymph values, 6 additional non-paired endolymph samples from both burbot and lake trout were added to calculate the overall mean metal concentration of the endolymph (Table 1; burbot n= 18; lake trout n= 11). We then compared data between species using the two sample t-Test. All the elements were statistically similar (all p > 0.07) except K, Mg and Ba (all p < 0.008, remained significantly different even after Boneferroni corrections). Burbot and lake trout endolymph were mostly enriched in Na, K and Ca with traces of other metals (Table 4.1).

We investigated the relationship between metals within the endolymph of both fish species (Fig. 4.1). The plots between alkali metals: Na, K, and Rb (Figs. 4.1a, 4.1b, 4.1e) show strong and significant correlations for the burbot (all $R^2 \geq$

0.64, all $p < 0.0001$) but not for the lake trout (all $R^2 \leq 0.09$, all $p > 0.09$) except for Rb and K ($R^2 = 0.72$, $p = 0.001$). We also notice different behaviours of metals within the endolymph for the two fish species when comparing Na/Ca and Mn/Ca (Figs. 4.1c & 4.1d). The Na/Ca plot showed a strong and significant relationship in lake trout ($R^2 = 0.78$, $p < 0.0001$) but not burbot ($R^2 = 0.03$, $p = 0.49$) whereas the Mn/Ca plot has a positive and significant trend in burbot ($R^2 = 0.51$, $p = 0.001$) and not for lake trout ($R^2 = 0.07$, $p = 0.44$). These differences from one species to another seem to indicate that the interactions between metals in the endolymph are not the same in lake trout and burbot. Interestingly, Zn an essential nutrient and Pb (which is not) demonstrate a positive significant relationship (Fig. 4.1f) for burbot ($R^2 = 0.43$; $p = 0.003$) but not for lake trout ($R^2 = 0.29$; $p=0.09$).

Lake trout and other salmonids are known to grow aragonite and vaterite CaCO_3 polymorphs in their otolith crystal structure (Campana 1983; Gauldie 1986, 1996; Gauldie et al.1997). The effects of crystal structure on metal incorporation in otoliths have only been studied by a few researchers (Tomàs and Geffen 2003; Melançon et al. 2005). The microchemistry of the lake trout (aragonite and vaterite) and burbot (aragonite) otoliths was quantified using LA-ICP-MS (Table 4.1). We ablated the growing edge of the otolith, which was in contact with the endolymph sampled at the same time. Most elemental concentrations in aragonitic otoliths of lake trout and burbot were significantly different according to the two sample t-test (all $p < 0.002$) except for Mg and Pb (all $p > 0.22$). Vaterite was only present in lake trout otoliths and results show an enrichment in Mg and Mn and depletion in Sr and Ba compared to the aragonitic

portions (Table 4.1). These differences are mainly due to the distance between the metal and the oxygen in the MCO_3 structure of the polymorphs (for more details see Melançon et al. (2005)). All the elements in vaterite were significantly different than in aragonite for both species ($p \leq 0.0001$) with the exception of Pb ($p = 0.24$).

Investigation of the relationships between metals in the endolymph and the otolith showed some weak linear trends but with insignificant relationships (all $p \geq 0.17$, $R^2 < 0.92$; see Fig. 4.2). Some of the plots showed strong clustering (low variation) depending on the origin of the otoliths (aragonitic of burbot (\blacktriangle) and lake trout (\bullet) and vateritic of lake trout (\blacksquare)). Elements like Na and K (Figs. 4.2a and 4.2c) with similar ion sizes and the same oxidation state (1+) showed similar patterns in the plots: vateritic lake trout otoliths with the lowest elemental otolith concentrations, burbot in the middle and aragonitic lake trout with the highest. While for two other elements of comparable sizes (to Na and K) but of different charge (2+), Ba and Sr (Figs. 4.2f and 4.2g), burbot has the highest otolith concentration (despite a wide endolymph range). Magnesium and Mn (Figs. 4.2b and 4.2d) both have the highest concentration for vateritic lake trout otoliths but with a widespread range in the endolymph for Mg despite a tight range for Mn. The opposite behaviour is observed for the burbot data (a broad range for Mn and tightly clustered for Mg) with the lake trout aragonitic data in the middle. The Zn concentration in the lake trout otoliths (both aragonitic and vateritic) were consistently higher (Fig. 4.2e) compared to burbot otoliths despite similar ranges in endolymph concentrations. Lead concentrations (Fig. 4.2h) show no differentiation between species or crystal polymorph.

4.3.2 Water and Blood

Table 4.2 shows the mean metal concentrations for Lake Erie western basin water and whole blood compositions from lake trout and burbot. Water concentrations are dominated by Ca, Na, Mg, and K with all other metals being less than 1 ppm (Table 4.2). These Lake Erie water samples, which were collected at the same time of year as the endolymph and otoliths, should be broadly representative of the environment in which the fish lived during previous summers.

Burbot and lake trout whole blood composition was, very similar to, but a little more concentrated than the endolymph. We used the two-sample t-Test to compare the blood samples from the burbot and the lake trout. Most of the elements in the blood were statistically similar (all $p > 0.08$) except for Zn, Rb and Sr (all $p \leq 0.003$). Considering the low variation (standard deviation) within each fish species these data should provide representative averages of the blood composition of each fish species at this time of year.

4.3.3 Partition coefficients (K_{Ds})

Mean metal partition coefficients were calculated for water, blood, endolymph and otoliths (Table 4.3 and equations (1) to (4)). Most elements are more enriched in the blood compared to the water for both species with $K_{D (B/W)} \gg 1$ (Fig. 4.3a), except for Sr (≈ 1) and Ca (≈ 3). Endolymph and blood have similar metal concentrations ($K_{D (E/B)} \approx 1$) with only Mn and Pb enriched in the endolymph for the burbot and Mn for lake trout ($K_{D (E/B)} > 1$, Fig. 4.3b). Iron is strongly enriched in the whole blood samples compared to the endolymph due to the presence of red blood cells (RBCs).

The otolith/endolymph partition coefficients were very high for Ca and Sr. In aragonitic otoliths of lake trout and burbot, these two elements were similarly enriched ($K_{D(O/E)} = 6000-9000$) while the vateritic otolith's partition coefficient for Sr was much less so ($K_{D(O/E)} \approx 500$). Other elements are depleted in the aragonitic otolith compared to the endolymph (K and Rb) while others are of similar composition (Na, Mg, Mn, Zn, and Pb). Vateritic otolith partition coefficients showed consistent and large differences compared to the aragonitic ones for Mg, Ba and Mn (Fig. 4.3c). Differences exist between species with burbot Ba $K_{D(O/E)}$ being 7 times that for lake trout (34.5 vs 5.30) and its Mg $K_{D(O/E)}$ was almost twice that for lake trout (4.12 vs 2.75).

Our results show that all elements are enriched in the otolith (aragonitic and vateritic) compared to water with $K_{D(O/W)} \gg 1$ (Fig. 4.3d), except for Mg in the aragonite crystal structure ($K_{D(O/W)} \approx 2$) and Ba in vaterite ($K_{D(O/W)} \approx 4$). Partition coefficients between the otolith and the water, generally in marine environments, are available for a few elements: Ba, Sr, Mg, Mn, La (Bath et al. 2000; Milton and Chenery 2001; Elsdon and Gillanders 2003). In order to compare our values to published ones, we need to divide our $K_{D(O/W)}$ for these two elements by the $K_{D(O/W)}$ of calcium (Equation 5 & Table 4.4).

$$K_{D(O/W)} M / K_{D(O/W)} Ca = D_M \quad (5)$$

Lake trout vateritic partition coefficients have not been reported before and cannot be compared to the existing literature (Table 4.4).

4.4 DISCUSSION

4.4.1 Endolymph chemistry

Previous investigations of endolymph chemistry focused on organic compounds (proteins, glucose, phosphate, triglycerides, etc.) and non-metals (C, CO₂, Cl, S). Metal analyses were seldom incorporated in these studies, with the exception of Na, Mg, K, Ca, and Sr (Payan et al. 1997, 1999, 2002; Guibbolini et al. 2006). Payan et al. (1999) reported data for proximal and distal endolymph samples in rainbow trout (*Oncorhynchus mykiss*) and turbot (*Psetta maxima*). Proximal data for rainbow trout (freshwater) and turbot (seawater), respectively, were 2722 ±213 and 2582 ±94 ppm for Na, 770 ±140 and 1994±78 ppm for K, and 12.2 ±0.9 and 5.3 ±0.6 ppm for Mg. Our elemental concentration results are lower than this data for Na but similar for K and Mg (Fig. 4.1).

Kalish (1991) has also reported metal data (Ca, Sr, Na, K) for water, blood plasma, endolymph and otolith of the marine bearded rock cod (*Pseudophycis barbatus*) and its variation through seasons. He found that all the metals in the endolymph varied significantly with seasons. Most of the elements had two peak concentration times, in September and March-April, except for Sr (only September). Most of the results were presented in graphs without giving a table of values. We have estimated concentration values (ppm) for August from the graphs for comparison to our data set (sampled at that time of year). Kalish's endolymph data for Na, K, Ca, and Sr are approximately, 2620, 2600, 54 and 0.525 ppm respectively. The values for Ca are similar to those we obtained while the values for Na and K are 2 times and Sr are 5 times higher than what we determined for lake trout and burbot endolymph (Table 4.1). Our data is

consistently lower than the ones obtained by Kalish (1991) (see Fig. 4.1), there seem to be important differences in endolymph metal composition between freshwater and marine fish, although we do not know exactly why those differences are so important. We would expect to see some differences as seawater and freshwater have different trace metal compositions and seawater is actively transported in the fish's body whereas freshwater is introduced in the fish by passive transport (Moyle & Cech 2000).

We also noted significant differences in element relationships (Fig. 4.2) from one species to another, however the mean compositions are very similar with only 3 elements out of 11 significantly different (Table 4.1).

4.4.2 Otolith-endolymph relationships

Although lake trout and burbot have very similar endolymph chemistry their aragonitic otoliths have statistically different compositions with the exception of Mg and Pb (Table 4.1). This means that even though the otoliths of lake trout and burbot are crystallizing from endolymph of similar composition, metals are incorporated in the otoliths differently. Previous research studies have also demonstrated that incorporation of metals in otoliths is species specific (Dove et al. 1996; Geffen et al. 1998; Hamer & Jenkins 2007). One explanation of these differences in metal uptake would be the influence of proteins and other organic matter in the endolymph and the otolith. Gauldie (1993) reported that proteins extracted from aragonitic and vateritic otoliths of the blue grenadier (*Macrurus novaezelandiae*) were composed of different sets of amino acid sequences (constituents of proteins). Furthermore, Tomàs et al. (2004) quantified the soluble

proteins in aragonitic and vateritic otoliths of laboratory-reared herring (*Clupea harengus*). Their results suggest that some low concentration soluble proteins, close to the detection limits of the technique, might be undetected and responsible for the crystal polymorph formed. Hypothetically, even if each polymorph has its own set of proteins (Pote and Ross 1991), the same polymorph (i.e. aragonite, vaterite or calcite) in otoliths of different fish species might have varying levels of those proteins from species to species.

Our results demonstrate clearly the species specific effects (Fig. 4.3). Potassium is strongly enriched in lake trout aragonitic otoliths compared to burbot otoliths, possibly indicating a higher concentration of a K-bearing protein in lake trout. Zinc is also highly enriched in lake trout (aragonite and vaterite) otoliths relative to burbot otoliths despite similar ranges of endolymph concentrations. The opposite result is observed for Ba, except for vateritic otoliths, for which crystal structure does not allow excess addition of Ba.

4.4.3 Blood chemistry

It is also important to consider the regulation of elements by the gills (freshwater), the intestine wall (saltwater) and other membranes before they are transported by the blood and ultimately reach the endolymph. Our whole blood data is consistently higher (slightly) than the endolymph for all elements with the exception of Rb, Mn and Pb. Interestingly, although the first two elements are usually not considered to be regulated, our results seem to indicate otherwise for burbot (Figs. 4.2b, 4.2e and 4.2f). When we compare our data with existing blood plasma data from Evans (1993) for a teleost freshwater fish (common carp: *Cyprinus carpio*), his values for Na (2989 ppm), Mg (29 pm) and Ca (84 ppm) are

very close to the ones we obtained but are considerably lower for K (113 ppm) (Table 4.2). The disparity in K may be due to the fact that we analyzed whole blood and not plasma as potassium is transported by red blood cells (Gusev et al. 1995).

4.4.4 Fractionation of metals by fish

In the fisheries community, much attention has been placed on the relationship between water and otolith chemistry (see Campana 1999 for a review) without understanding the mechanisms responsible for elemental fractionation from the water to the otolith. Thus, although previous research has recognized that metals in the water must pass through a series of biological filters (e.g., water, gills, blood system, endolymph, otolith) before being incorporated into the otolith, our understanding of how metals are partitioned (fractionated) at each step remains enigmatic (Campana 1999). The partition coefficients across these filters obtained in this study provide insights on the variability of metal fractionation in fish (Table 4.3).

Interestingly, Mg, Sr and Ba, the trace elements most often used as otolith elemental tracers are the ones with the lowest uptake ($K_{D(B/W)}$) from the water to the blood (Fig. 4.4a). Conversely Rb which is a very large alkali is more strongly fractionated into blood from water than the highly regulated and smaller alkalis, Na and K. It is not surprising that Zn, an essential trace metal, has an extremely high partition coefficient as it is distributed to the body but surprisingly so does Pb (a toxic metal).

Endolymph and whole blood have similar metal concentrations, which is expected, considering that the exchanges between the saccular sac (where the

endolymph is contained) and the exterior fluid are mainly from blood (Payan et al. 1997). Magnesium and Fe are the only elements enriched in the whole blood compared to the endolymph ($K_{D(E/B)} < 0.1$, Fig. 4.4b).

The otolith/endolymph partition coefficients for Ca and Sr are very high ($K_{D(O/E)}$), confirming the major role of Sr as a substitute for Ca in the calcium carbonate structure of the otolith. A species specific effect can also be observed between lake trout and burbot for Ba, Mn and Zn.

4.4.5 Water versus otolith

The relationship between water and the otolith has been broadly studied and is of great interest to the fisheries community. The results of such studies are used to help understand stock (sub-population) structure and mixing, migratory patterns of individuals and populations, and temperature and salinity histories of oceans (see reviews by Campana 1999 and Thresher 1999). Partition coefficients have been calculated for several marine fish (Bath et al. 2000; Zimmerman 2005; Hamer and Jenkins 2007) but not very often for freshwater fish (Wells et al. 2003; De Vries et al. 2005). Our partition coefficients ($D_{(O/W)}$) for Ba and Sr are very close (especially for burbot) to the only other freshwater data available in the literature (Table 4.5 and Equation (5)). Otherwise, our results for Ba are generally lower than the literature ones for wild marine fish (Elsdon and Gillanders 2005; Dorval et al. 2007) but are comparable to those obtained by Bath et al. (2000) and Milton & Chenery (2001) for two marine species under lab conditions. The variation in Ba partition coefficients is large, ranging from 0.0037 to 0.31 indicating diverse fractionation from one fish species to another. Even for

the same species, variation from one study to the other is considerable: 0.099 in 2003 and 0.27 in 2005 (both by Elsdon & Gillanders). We would expect major differences between freshwater and marine fish for D_{Sr} as saltwater has about 100 times the level of Sr than in freshwater (Drever 1982). However this does not translate into greatly different partition coefficients (Table 4.4). Our results are within the range of published values and very close to the other field experiments done with black bream (*Acanthopagrus butcheri*), spotted seatrout (*Cynoscion nebulosus*) and cutthroat trout (*Oncorhynchus clarkia*). Our partition coefficients ($D_{(OM)}$) results for Mn are 0.054 for lake trout and 0.021 for burbot. These are about 20 times lower than the one obtained by Elsdon and Gillanders (2003) and are not comparable at all to the value, 14.8, published by Dorval et al. (2007).

4.5 CONCLUSIONS

This paper investigated the equilibrium between the endolymph and the growing otolith. Our results showed no significant differences between wild lake trout and burbot endolymph metal concentrations but strong differences for the aragonitic otoliths between these species. These findings suggest that fish occupying the same water mass and with similar feeding behaviours do not have specific endolymph signatures. The fact that the aragonitic otoliths of these species differ may be due to the presence of different proteins (and/or organic matrices) which influence metal incorporation in the otoliths.

This is one of the first studies to provide an extended range of trace metal concentrations in blood, endolymph and partition coefficients for freshwater fish. The fractionation of metals from water to otolith is an area of otolith research that

has received relatively limited attention. Past studies have overlooked the importance of metal fractionation in endolymph and blood when addressing otolith microchemistry. Our results illustrate the importance of these parameters for understanding the fundamental processes that affect otolith formation and the need for more research to elucidate the mechanisms affecting metal fractionation.

Our approach assumes a steady-state system which is unlikely to be representative of all the filters we discuss. Further work is required to address these issues and in particular the amount of time required for a fish to “equilibrate” with its environment (kinetics). A major assumption in this study was the use of surface water samples (and only over a one week period) to represent the environment in which these two deeper water species lived. It is however likely that the most important otolith cations (Ca, Mg, Sr and Ba) are still representative.

4.6 ACKNOWLEDGEMENTS

We thank the National Sciences and Engineering Research Council (Discovery Grant to B.J. Fryer), the Lake Erie Fisheries Unit of the New York State Department of Environmental Conservation, the University of Windsor and the Great Lakes Institute for Environmental Research for supporting for this research.

4.7 REFERENCES

- Bath, G.E., Thorrold, S.R., Jones, C.M., Campana, S.E., McLaren, J.W., and Lam, J.W.H. 2000. Strontium and barium uptake in aragonitic otoliths of marine fish. *Geochim. Cosmochim. Acta.* **64**: 1705-1714.
- Borelli, G., Mayer-Gostan, N., De Pontual, H., Bœuf, G., and Payan, P. 2001. Biochemical relationships between endolymph and otolith matrix in the trout (*Oncorhynchus mykiss*) and turbot (*Psetta maxima*). *Calcif. Tissue Int.* **69**: 356-364
- Campana, S.E. 1983. Feeding periodicity and the production of daily growth increment in otoliths of steelhead trout (*Salmo gairdneri*) and starry flounder (*Platichthys stellatus*). *Can. J. Zool.* **61**: 1591-1597.
- Campana, S.E. 1999. Chemistry and composition of fish otoliths: pathways, mechanisms and applications. *Mar. Ecol. Prog. Ser.* **188**: 263-297.
- Degens, E.T., Deuser, W.G., and Haedrich, R. L. 1969. Molecular structure and composition of fish otoliths. *Int. J. Life Oceans Coastal Waters.* **2**: 105-113.
- De Vries, M.C., Gillanders, B.M., and Elsdon, T.S. 2005. Facilitation of barium uptake into fish otoliths: Influence of strontium concentration and salinity. *Geochim. Cosmochim. Acta.* **69**: 4061-4072.
- Dorval, E., Jones, C.M., Hannigan, R., and van Montfrans, J. 2007. Relating otolith chemistry to surface water chemistry in a coastal plain estuary. *Can. J. Fish. Aquat. Sci.* **64**: 411-424.

- Dove, S.G., Gillanders, B.M., and Kingsford, M.J. 1996. An investigation of chronological differences in the deposition of trace metals in the otoliths of two temperate reef fishes. *J. Exp. Mar. Biol. Ecol.* **205**: 15–33.
- Drever, I.D. 1982. The Oceans. *In* The Geochemistry of natural waters. Prentice-Hall, Inc., Englewood Cliffs, New Jersey. pp. 229-249.
- Einhouse, D.W., Markham, J.L., Zeller, D.L., Zimar, R.C., Beckwith, B.J., and Wilkinson, M.L. 2006. NYSDEC Lake Erie Unit 2005 annual report to the Lake Erie Committee. New York State Department of Environmental Conservation, Albany, New York, USA.
- Eldson, T.S., and Gillanders, B.M. 2003. Relationship between water and otolith elemental concentrations in juvenile black bream (*Acanthopagrus butcheri*). *Mar. Ecol. Prog. Ser.* **260**: 263-272.
- Eldson, T.S., and Gillanders, B.M. 2005. Consistency of patterns between laboratory experiments and field collected fish in otolith chemistry: an example and applications for salinity reconstructions. *Mar. Freshwater Res.* **260**: 263-272.
- Enger, P. S. 1964. Ionic composition of the cranial and labyrinthine fluids and saccular D.C. potentials in fish. *Comp. Biochem. Physiol.* **11**: 131–137.
- Evans, D.H. 1993. Osmotic and Ionic Regulation *In* The Physiology of fishes Edited by David H. Evans. CRC Press, London, pp. 315-341.
- Gauldie, R.W. 1986. Vaterite otoliths from chinook salmon (*Oncorhynchus tshawytscha*). *N.Z. J. Mar. Freshwat. Res.* **20**: 209-217.
- Gauldie, R.W. 1993. Polymorphic crystalline structure of fish otoliths. *J. Morphol.* **218**: 1–28.

- Gauldie, R.W. 1996. Effects of temperature and vaterite replacement on the chemistry of metal ions in the otoliths of *Oncorhynchus tshawytscha*. *Can. J. Fish. Aquat. Sci.* **53**: 2015-2026.
- Gauldie, R.W., Sharma, S.K., and Volk, E. 1997. Micro-Raman spectral study of vaterite and aragonite otoliths of the coho salmon, *Oncorhynchus kisutch*. *Comp. Biochem. Physiol. A Comp. Physiol.* **118**:753-757.
- Geffen, A.J., Pearce, N.J.G., and Perkins, W.T. 1998. Metal concentrations in fish otoliths in relation to body composition after laboratory exposure to mercury and lead. *Mar. Ecol. Prog. Ser.* **165**: 225–345.
- Guibbolini, M., Borelli, G., Mayer-Gostan, N., Priouzeau, F., De Pontual, H., Allemand, D., and Payan, P. 2006. Characterization and variations of organic parameters in teleost fish endolymph during day-night cycle, starvation and stress conditions. *Comp. Biochem. Physiol.* **145A**: 99-107.
- Gusev, G.P., Agalakova, N.I., and Lapin, A.V. 1995. Potassium transport in red blood cells of frog *Rana temporaria*: demonstration of a K-Cl cotransport. *J. Comp. Physiol. B.* **165**: 230-237.
- Hamer, P.A., and Jenkins, G.P. 2007. Comparison of spatial variation in otolith chemistry of two fish species and relationships with water chemistry and otolith growth. *J. Fish Biol.* **71**: 1035-1055.
- Kalish, J.M. 1989. Otolith microchemistry: validation of the effects of physiology, age and environment on otolith composition. *J. Exp. Mar. Biol. Ecol.* **132**: 151–178.

- Kalish, J.M. 1991. Determinants of otolith chemistry: seasonal variation in the composition of blood plasma, endolymph, and otoliths of bearded rock cod *Pseudophycis barbatus*. *Mar. Ecol. Prog. Ser.* **74**: 137–159.
- Ludsin, S.A., Fryer, B.J., Yang, Z., Melançon, S., and Markham, J.L. 2004. Exploration of the existence of natural reproduction in Lake Erie lake trout using otolith microchemistry. Fisheries Research project completion report, Great Lakes Fisheries Commission, Ann Arbor, MI.
- Melançon, S., Fryer, B.J., Gagnon, J.E., Ludsin, S.A., and Yang, Z. 2005 Effects of crystal structure on the uptake of metals by lake trout (*Salvelinus namaycush*) otoliths. *Can. J. Fish. Aquat. Sci.* **62**: 2609-2619.
- Milton, D.A., and Chenery, S.R. 2001. Sources and uptake of trace metals in otoliths of juvenile barramundi (*Lates calcarifer*). *J. Exp. Mar. Biol. Ecol.* **264**: 47-65.
- Moyle, P., and Cech., J. 2000. Ionic Regulation *In* Fishes: An Introduction to Ichthyology – fourth edition. Prentice-Hall, Inc., Upper Saddle River, New Jersey. pp. 85-89.
- Panella G.,1971. Fish otoliths: daily growth layers and periodical patterns. *Science.* **173** :1124–1127
- Payan, P., Kossman, H., Watrin, A., Mayer-Gostan, N., and Bœuf, G. 1997. Ionic composition of endolymph in teleosts: origin and importance of endolymph alkalinity. *J. Exp. Biol.* **200**: 1905-1912.
- Payan, P., Edeyer, A., De Pontual, H., Borelli, G., Bœuf, G., and Mayer-Gostan, N. 1999. Chemical composition of saccular endolymph and otolith in fish inner

- ear: lack of spatial uniformity. *Am. J. Physiol.: Reg. Int. Comp. Physiol.* **277**: R123-R131.
- Payan, P., Borelli, G., Priouzeau, F., De Pontual, H., Boeuf, G., and Mayer-Gostan, N. 2002. Otolith growth in trout (*Oncorhynchus mykiss*): supply of Ca^{2+} and Sr^{2+} to the saccular endolymph. *J. Exp. Biol.* **205**: 2687-2695.
- Payan, P., De Pontual, H., Edeyer, A., Borelli, G., Boeuf, G., and Mayer-Gostan, N. 2004. Effects of stress on plasma homeostasis, endolymph chemistry, and check formation during otolith growth in rainbow trout (*Oncorhynchus mykiss*). *Can. J. Fish. Aquat. Sci.* **61**: 1247-1255.
- Pote, K.G., and Ross, M.D. 1991. Each otoconia polymorph has a protein unique to that polymorph. *Comp. Biochem. Physiol.* **98B**: 287-295.
- Takagi, Y. 1997. Meshwork arrangement of mitochondria-rich, Na^{+} - K^{+} -ATPase rich cells in the saccular epithelium of rainbow trout (*Oncorhynchus mykiss*) inner ear. *Anat. Rec.* **248**: 483-489.
- Takagi, Y. 2002. Otolith formation and endolymph chemistry: a strong correlation between the aragonite saturation state and pH in the endolymph of the trout otolith organ. *Mar. Ecol. Prog. Ser.* **231**: 237-245.
- Thresher, R.E. 1999. Elemental composition of otoliths as a stock delineator in fishes. *Fish. Res.* **43**: 165-204.
- Tohse, H., Ando, H., and Mugiya, Y. 2004. Biochemical properties and immunohistochemical localization of carbonic anhydrase in the sacculus of the inner ear in the salmon *Oncorhynchus masou*. *Comp. Biochem. Physiol.* **137A**: 87-94.

- Tomàs, J., and Geffen, A.J. 2003. Morphometry and composition of aragonite and vaterite otoliths of deformed laboratory reared juvenile herring from two populations. *J. Fish. Biol.* **63**: 1383-1401.
- Tomás, J., Geffen, A.J., Allen, I.S., Berges, J. 2004. Analysis of the soluble matrix of vaterite otoliths of juvenile herring (*Clupea harengus*): do crystalline otoliths have less protein? *Comp. Biochem. Physiol.* **139A**:301-308.
- Wells, B.K., Rieman, B.E., Clayton, J.L., Horan, D.L., and Jones, C.M. 2003. Relationships between water, otolith, and scale chemistries of westslope cutthroat trout from the Coeur d'Alene River. Idaho: the potential application of hard-part chemistry to describe movements in freshwater. *Trans. Am. Fish. Soc.* **132**: 409–424.
- Zimmerman, C.E.. 2005 Relationship of otolith strontium-to-calcium ratios and salinity: experimental validation for juvenile salmonids. *Can. J. Fish. Aquat. Sci.* **62**: 88-97.

Table 4.1: Mean metal concentrations in the endolymph and otoliths of burbot and lake trout (units: ppm \pm 1 standard error). Otoliths are divided by crystalline structure (aragonite and vaterite) for lake trout. Burbot only has one type of CaCO₃ polymorph: aragonite.

Metal	Endolymph		Otolith		
	Burbot (n=18)	Lake trout (n=11)	Burbot Aragonite (n=17)	Lake trout Aragonite (n=10)	Lake trout Vaterite (n=3)
Na	1560 \pm 220	1330 \pm 340	2033 \pm 297	2499 \pm 395	1341 \pm 34
K	1410 \pm 270	1100 \pm 190	364 \pm 44	644 \pm 49	242 \pm 25
Rb	1.89 \pm 0.3	2.06 \pm 0.5	0.19 \pm 0.03	0.35 \pm 0.04	0.190 \pm 0.02
Mg	2.84 \pm 0.6	4.89 \pm 3	11.7 \pm 4	13.4 \pm 2	331 \pm 17
Ca	40.6 \pm 5	51.4 \pm 11	400432	400432	400432
Sr	0.099 \pm 0.01	0.093 \pm 0.03	694 \pm 67	544 \pm 90	48 \pm 6
Ba	0.275 \pm 0.1	0.193 \pm 0.02	10 \pm 3	1.0 \pm 0.6	0.066 \pm 0.023
Mn	0.128 \pm 0.05	0.126 \pm 0.05	0.162 \pm 0.09	0.479 \pm 0.3	3.4 \pm 0.8
Fe	2.10 \pm 1	1.51 \pm 0.4	N/A	N/A	N/A
Zn	1.18 \pm 0.3	1.18 \pm 0.6	1.4 \pm 0.6	7 \pm 3	15 \pm 2
Pb	0.091 \pm 0.05	0.082 \pm 0.02	0.119 \pm 0.06	0.166 \pm 0.1	0.178 \pm 0.06

Table 4.2: Mean metal concentrations for Lake Erie western basin water and the blood of lake trout and burbot (units: ppm \pm 1 standard error).

	Water	Blood	
	(n=4)	Burbot (n=5)	Lake trout (n=4)
Na	9.40 \pm 0.1	2670 \pm 254	2620 \pm 202
K	1.26 \pm 0.09	1970 \pm 104	1990 \pm 146
Rb	0.00076 \pm 0.00001	1.96 \pm 0.2	2.42 \pm 0.2
Mg	6.52 \pm 0.1	66.4 \pm 11	67.8 \pm 3
Ca	26.5 \pm 0.4	80.2 \pm 15	102 \pm 21
Sr	0.131 \pm 0.001	0.213 \pm 0.03	0.140 \pm 0.004
Ba	0.0185 \pm 0.0004	0.370 \pm 0.12	0.253 \pm 0.05
Mn	0.00052 \pm 0.00009	0.084 \pm 0.01	0.103 \pm 0.02
Fe	0.271 \pm 0.004	103 \pm 18	129 \pm 14
Zn	0.0012 \pm 0.0006	5.78 \pm 0.2	8.75 \pm 0.7
Pb	0.00011 \pm 0.00005	0.054 \pm 0.2	0.161 \pm 0.2

Table 4.3: Partition coefficient values for Lake trout and Burbot fish (KDs). Partition coefficients between: blood and water (KD(B/W)), endolymph and blood (KD(E/B)), otolith and endolymph (KD(O/E)), and otolith and water (KD(O/W)), for both polymorphs (Arag: aragonite and Vat: vaterite).

	Burbot				Lake trout				
	KD (B/W)	KD (E/B)	KD (O/E)	KD (O/W)	KD (B/W)	KD (E/B)	KD (O/E)	KD (O/W)	KD (O/W)
Na	284	0.585	1.30	216	279	0.507	1.88	1.01	266
K	1560	0.716	0.258	289	1590	0.552	0.583	0.219	512
Rb	2590	0.963	0.099	247	3190	0.853	0.169	0.092	459
Mg	10.2	0.043	4.12	1.80	10.4	0.072	2.75	67.8	2.06
Ca	3.03	0.506	9870	15100	3.85	0.505	7790	7790	15100
Sr	1.63	0.467	6990	5300	1.07	0.670	5820	515	4160
Ba	20.0	0.742	34.5	513	13.7	0.764	5.30	0.343	55.3
Mn	161	1.52	1.27	310	197	1.22	3.37	26.8	812
Fe	380	0.020	N/A	N/A	477	0.012	N/A	N/A	N/A
Zn	4790	0.204	1.17	1140	7250	0.135	5.52	12.4	5410
Pb	500	1.69	1.30	1100	1490	0.510	1.76	2.18	1330

Table 4.4: Comparison with literature values of partition coefficients between the otolith and the water D(O/W) for Ba, Sr and Mn in aragonite for different fish species and type of experiments (laboratory versus in the field). The type of water is indicated by the following letters: S for saltwater, F for freshwater and B for brackish water. Note that data is for aragonitic otoliths with the only data for vaterite in the table presenting an asterisk (*) and is from this study.

Study	Fish	Water	DBa	DSr	DMn	Type of Exp. (°C)
Bath et al. 2000	Spot croaker	S	0.06	0.182	N/A	Lab (20)
Milton & Cheney 2001	Barramundi	S	0.03	0.16	N/A	Lab (28-30)
Wells et al. 2003	Cutthroat trout	F	0.04	0.40	N/A	Field
Elsdon & Gillanders 2003	Black bream	S	0.099	0.131	0.683	Lab (20)
De Vries et al. 2005	Black bream	B	0.058	0.463	N/A	Lab (22)
De Vries et al. 2005	Black bream	S	0.136	0.287	N/A	Lab (22)
Elsdon & Gillanders 2005	Black bream	S	0.27	0.28	N/A	Lab (20)
Elsdon & Gillanders 2005	Black bream	S	0.26	0.52	N/A	Field
Dorval et al. 2007	Spotted seatrout	B	0.31	0.23	14.8	Field
Melançon et al.	Burbot	F	0.034	0.35	0.021	Field
Melançon et al.	Lake trout	F	0.0037	0.28	0.054	Field
*Melançon et al.	*Lake trout	F	0.00024	0.024	0.43	Field

Figure 4.1: Comparison of our proximal endolymph composition (ppm) for Na, Mg, K, Ca and Sr of burbot (black) and lake trout (white) to the literature values for cod's endolymph (horizontal lines) from Kalish (1991), rainbow trout (grey) and turbot (backward slash) proximal endolymph from Payan et al. (1999).

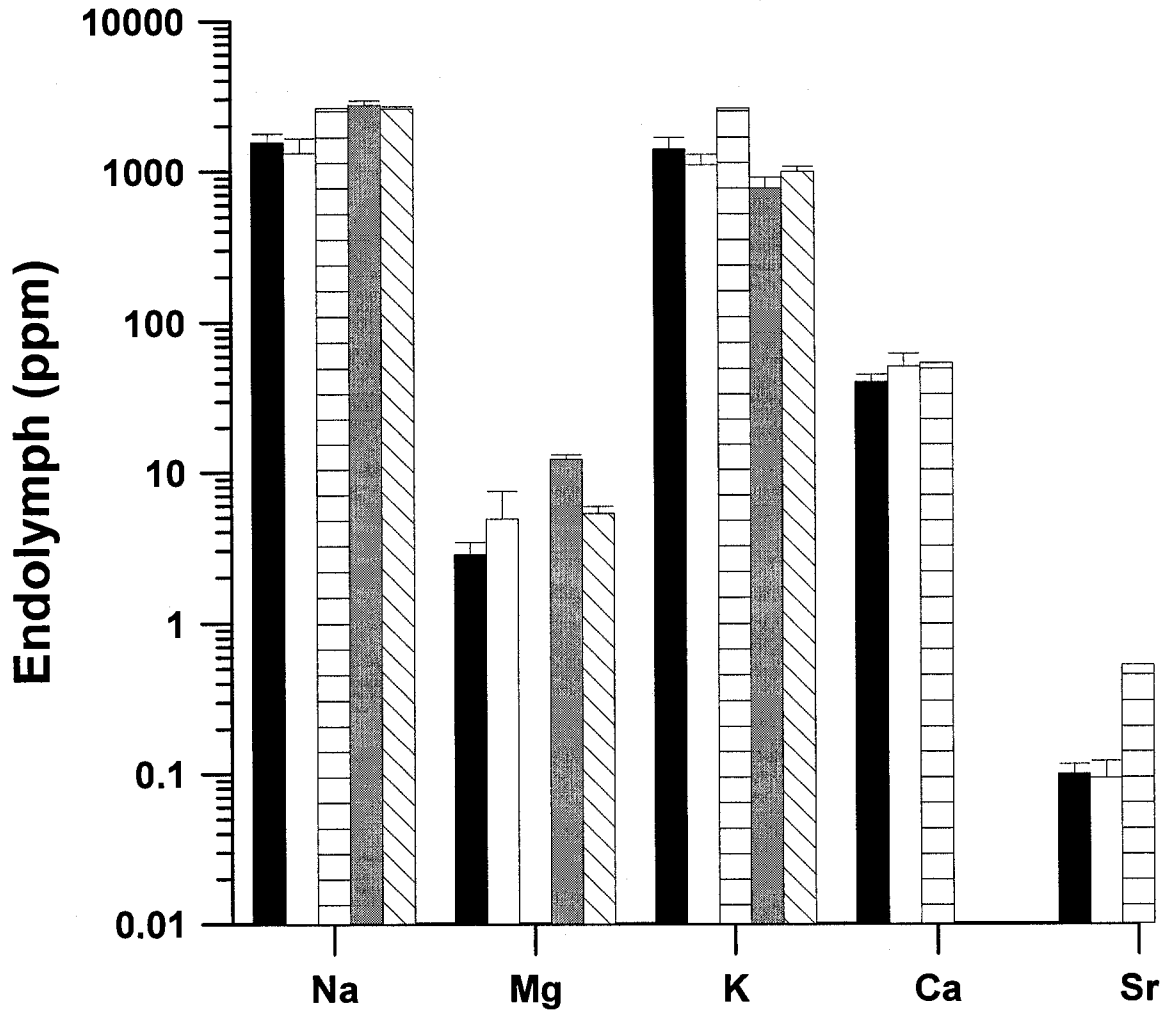


Figure 4.2: Relationship between metals (ppm) in the endolymph of burbot (\blacktriangle) and lake trout (\bullet). (a) Na/K ($\blacktriangle R^2 = 0.67, p < 0.0001$; $\bullet R^2 = 0.09, p = 0.36$); (b) Rb/K ($\blacktriangle R^2 = 0.76, p < 0.0001$; $\bullet R^2 = 0.72, p = 0.001$); (c) Na/Ca ($\blacktriangle R^2 = 0.03, p = 0.49$; $\bullet R^2 = 0.79, p < 0.0001$); (d) Mn/Ca ($\blacktriangle R^2 = 0.51, p = 0.001$; $\bullet R^2 = 0.07, p = 0.44$); (e) Na/Rb ($\blacktriangle R^2 = 0.64, p < 0.0001$; $\bullet R^2 = 0.02, p = 0.71$); (f) Zn/Pb ($\blacktriangle R^2 = 0.43, p = 0.003$; $\bullet R^2 = 0.29, p = 0.09$)

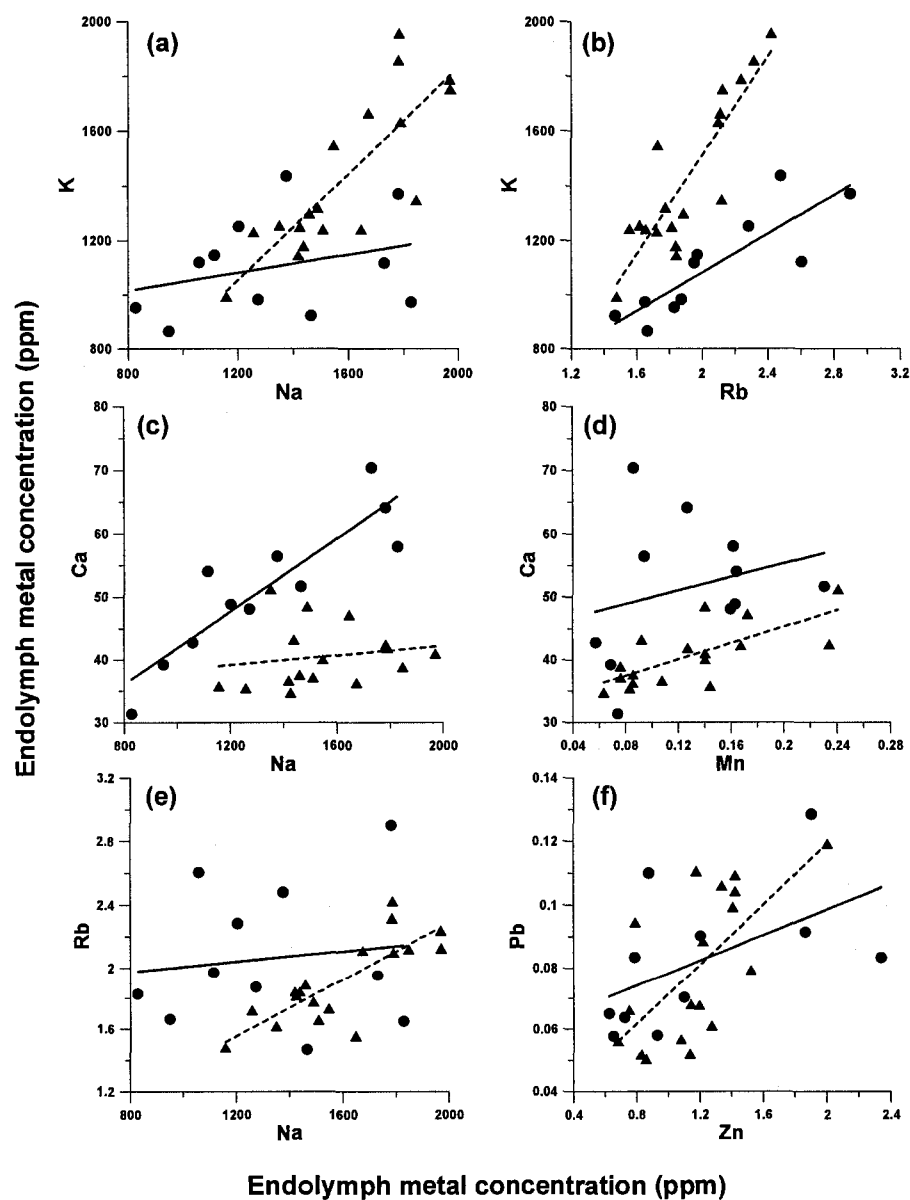


Figure 4.3: Relationship between metals (ppm) in the endolymph and the otoliths of burbot (\blacktriangle) and lake trout, aragonitic otoliths (\bullet) and vateritic otoliths (\blacksquare). (a) Sodium; (b) Mg; (c) K; (d) Mn; (e) Zn; (f) Ba; (g) Sr and (h) Pb

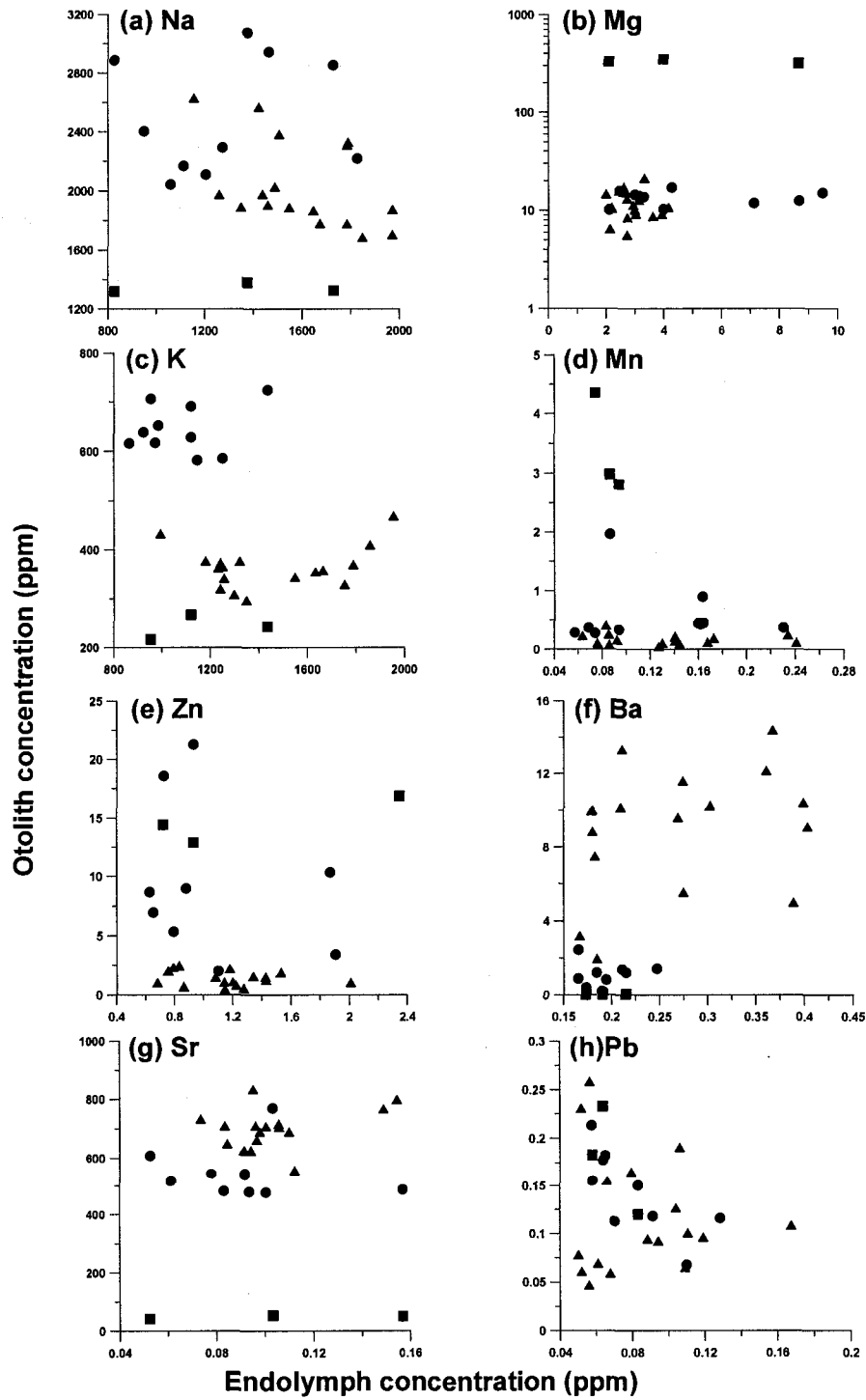
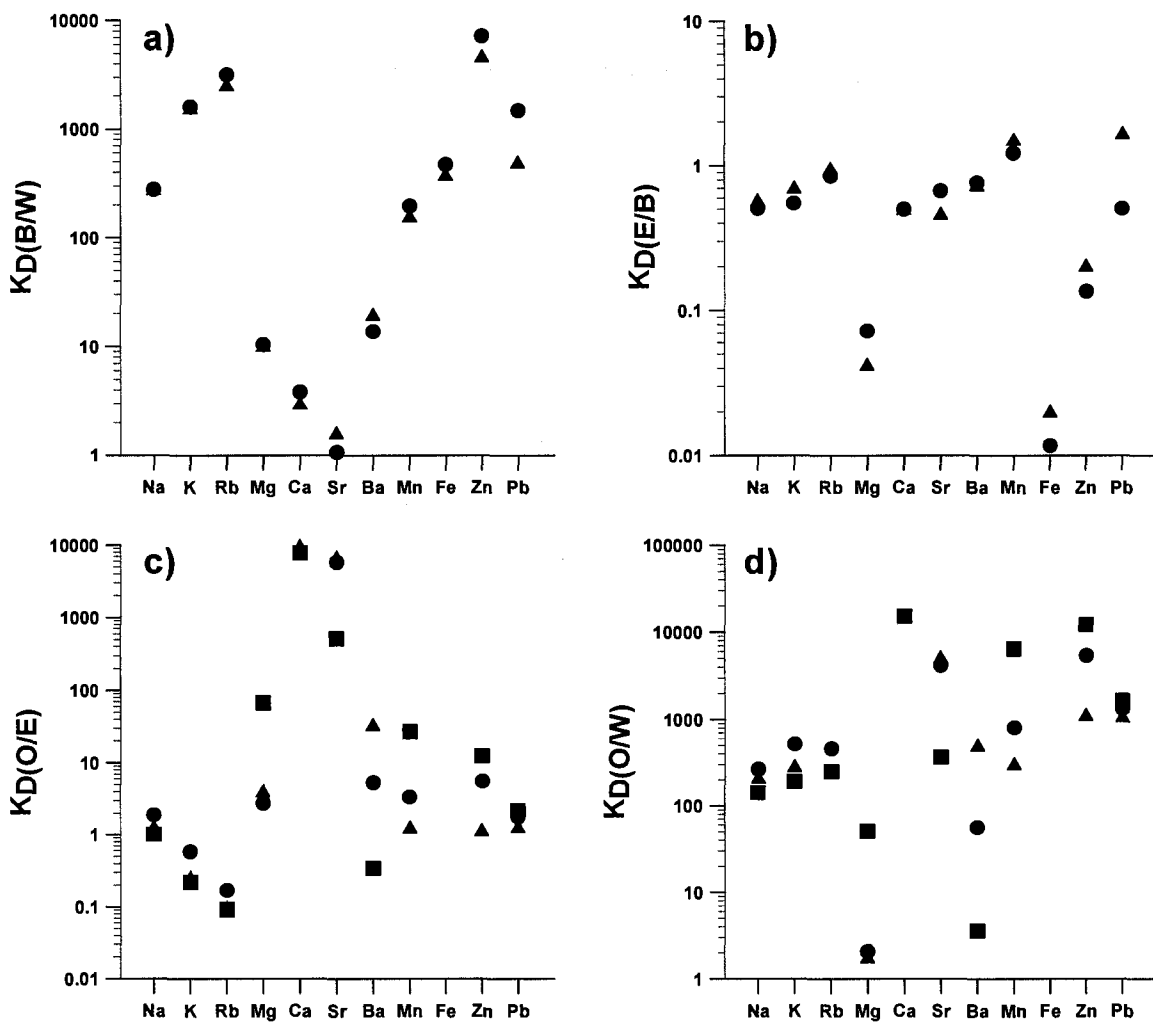


Figure 4.4: Partition coefficients between: a) blood and water ($K_{D(B/W)}$), b), endolymph and blood ($K_{D(E/B)}$), c) otolith and endolymph ($K_{D(O/E)}$), and d) otolith and water ($K_{D(O/W)}$) for burbot (\blacktriangle) and lake trout, aragonitic otoliths (\bullet) and vateritic otoliths (\blacksquare). For a) $K_{D(B/W)}$ and b) $K_{D(E/B)}$ the following symbol (\bullet) is not related to a specific polymorph.



CHAPTER 5

Isotopic labelling of yellow perch (*Perca flavescens*) otoliths by barium and strontium

5.1 INTRODUCTION

Tagging fish and larvae to investigate migration, growth and dispersal has been a subject of research for decades now (see a review by Thorrold et al. 2002). There are two types of tagging methods natural (e.g. gene markers and otolith microchemistry) and artificial, which can be divided in two sub-categories external (e.g. floy and t-bar anchor) and internal (e.g. isotopic, fluorescent and thermal). In order to be useful for fisheries each of these technique must meet the following criteria: lasting effect (as long as the dispersal/migration), easily detectable and administrable, inexpensive, not increase mortality nor modify the fish's natural behaviour (Guy et al. 1996). The marking of larvae is more challenging than juvenile fish considering their small size (often less than 5 mm) and high mortality rates coming from stress of handling. The importance of learning and understanding larval dispersion and population connections are essential to sustain management of fish stocks especially in ecologically protected zones.

Radioactive Sr (^{85}Sr) was used by Vuorinen et al. (1998) to tag pike fry (*Esox lucius L.*). Fish immersion in a Sr spiked solution for three days resulted in a radioactive signature that lasted for 2 months in the fish. They found that marking fish at a concentration $50 \mu\text{Ci/l}$ did not affect their survival but when they doubled that concentration it caused a high mortality rate. They did not look at this radioactive isotope (^{85}Sr) signature in the otoliths.

However, natural strontium isotopes in otoliths have been widely used to reconstruct life histories of salmonides (Barnett-Johnson et al. 2005, Kennedy et

al. 2002; 1997), identify stock structure and natal habitat (Hobbs et al. 2005). Otolith microchemistry of these isotopes is representative of the water isotopic composition (influenced by watershed geology). This technique has been useful when the diversity of geology of the streams where the fish live showed significant differences. Strontium has been widely used as a natural tracer in otoliths but not as an artificial tag.

Thorrold et al. (2006) successfully marked embryonic otoliths through maternal transmission using an enriched barium isotope (^{137}Ba) in clown fish (*Amphiprion melanopus*) and serranid (*Centropristis striata*). The signature of the otolith core was 6 times higher $^{137}\text{Ba}/^{138}\text{Ba}$ than the control otoliths. The level of Ba injected in this study affected the spawning behaviour of the female clown fish that received the two highest doses (4.5 and 23 $\mu\text{g } ^{137}\text{Ba/g}$ female). A few questions remain: how safe is isotopic tagging? Where do these isotopes reside in the fish's body?

In this study, we explore the turnover rates of barium and strontium in the blood, bones, whole bodies and otoliths of yellow perch (*Perca flavescens*). Our research attempts to answer the following questions: 1) are both enriched isotopes, ^{84}Sr and ^{135}Ba , sequestered and/or eliminated at the same rate by the fish 2) are strontium and barium isotope turnover rates in the otolith long enough to be useful as a chemical tracer for fish recruitment 3) how rapidly does a fish equilibrate within its new environment 4) how sensitive is otolith chemistry to environmental change after a perturbation (disturbance of its state of equilibrium).

5.2 MATERIAL AND METHODS

5.2.1 Laboratory experiment

Young of the year yellow perch (*Perca flavescens*) of 3.3-7.7 g body weight and averaging 4.4 ± 1 g were housed in the GLIER Aquatic Facility for a period 11 months (November 2006 to October 2007). They were maintained in two large 1500L flow through tanks fed directly with Detroit River water for 5 months prior to experimentation. Fish were fed once daily with Profishent food ranging from 1 to 4 mm in size (Martin Mills Inc., Ontario, Canada). A total of 100 fish were divided into 4 subgroups based upon isotopic treatment (control, low, medium and high) contained in 2 tanks where temperature was monitored but not controlled and ranged from 15 °C (winter) to 22 °C (summer). Fish in the same tank but from different treatments were physically separated by a net as shown in Figure 1 (same water). Photoperiodicity was achieved using timers to simulate a 12h dark and 12h light cycle. The first tank housed the control and low isotopic fish treatment and the second tank had the medium and high treatment fish. Fish were maintained and handled following the Canadian Council for Animal Care Guidelines. Mortality due to unexpected reasons was less than 10% for the 11 months the fish were housed.

A stock solution of ^{84}Sr and ^{135}Ba was prepared from powdered certified reference materials: $^{84}\text{SrCO}_3$ (82.24%) and $^{135}\text{BaCO}_3$ (93.38%) from Oak Ridge National Laboratory. The final concentration of the stock solution containing both isotopes was approximately 1000 ppm for ^{84}Sr and 7000 ppm for ^{135}Ba . This solution was used to inject the highest dose treatment fish. It was then diluted by

two, with concentrations of 500 ppm and 3500 ppm respectively, for the medium treatment and by ten, 100 ppm and 700 ppm, for the low treatment. Fish from each treatment were injected with their respective solution by subcutaneous injection. To ensure similar handling and stress conditions, the control group was injected with an aqueous solution that did not contain any added ^{84}Sr and ^{135}Ba isotopes. Injections were completed on 28 April 2007 within a 4h time period. The fish were anaesthetised in water containing 5% clove oil and alcohol, weighed and injected with the proper solution at a ratio of $1\mu\text{L}$ of solution per g of fish. Fish ranged from 9.0 to 28.8 g in body weight with an average of 17.7 ± 5 g. The fish were then returned to their initial non-contaminated water tank and maintained alive for the next 5 months. In July 2007, near the experiment's mid point, 2 fish per tank ranging from 31.5 to 61.0 g (average: 46 ± 11 g) were removed for analysis of whole bodies and otoliths only.

Surface water samples were collected weekly and refrigerated until filtration and acidification, this procedure is reported elsewhere (Melancon 2008 - Chapter 4).

5.2.2 Sample extraction and preparation

Study fish were euthanized by anaesthetic overdose (10% clove oil). For our analysis, we randomly chose nine fish per tank for otoliths and blood collection, a subset of five fish were analyzed for total body burden and three for bone isotopic content. The fish tail was quickly severed with a scalpel blade and blood was immediately collected from the caudal vessels using a heparinized

capillary tube (Fisher Scientific 22-362-566) and transferred into pre-weighed acid washed Teflon tubes. Each blood sample was weighed (0.03-0.05 g of whole blood) and digested according to a protocol published by Melancon (2008).

The vomer and the parasphenoid bones were removed from 3 fish per treatment; both bones are from the front part of the roof of the mouth. They were cleaned with 30% H₂O₂ (trace metal grade), sonicated for 5 min, rinsed with Milli-Q water and dried overnight. The bones were analyzed using LA-ICP-MS (sectioned to ~800 µm thick and polished) and ICP-MS (digested). The bone sample (1 mg) was digested in 100 µL of 8N HNO₃, evaporated until dryness (1h) and 10 mL of internal standard matrix was added.

Sagittal otoliths were extracted, dried overnight and stored in small glass vials. One of the paired otoliths was embedded in epoxy resin (West Coast Marine®) and transverse sections (~800 µm thick) were cut using a Buehler ISOMET™ saw, such that each section contained the full growth chronology (including the core). Otoliths were polished and cleaned as described by Melancon et al. (2005).

Individual fish whole bodies were homogenized using an acid washed blender. A body sample of 1 g was placed in a microwave vessel and 10 mL of 16 N HNO₃ (trace metal grade) was added. The samples were digested using a Microwave Accelerated Reactive System® (MARS 5) from CEM Corporation. The digestions were done following a protocol for biological samples in 2 steps. The first step lasted for 70 minutes at 100% power (1200 W) and a pressure of 500 PSI with the temperature ramping up to 210 °C and held for 20 mins. For the

second step, 3 mL of H₂O₂ (trace metal grade) were added to the vessels and put back in the microwave. Samples were heated for a total of 25 minutes at 100% power (1200 W) and 500 PSI. During this stage the temperature was increased to 210 °C and held for 5 mins. Biological certified reference materials from National Research Council Canada, dogfish liver (DOLT-3) or muscle (DORM-2) were analysed for every 11 samples.

5.2.3 Chemical Analysis

Water, blood, bones and digested body samples were analyzed using solution-based-inductively coupled plasma-mass spectrometry (SO-ICP-MS). All data were collected on a Thermo-Elemental® X7® Series II ICP mass spectrometer. Multi-element and single-element in-house calibration standards, spiked with our internal standard solutions (1% HNO₃ +Be, In, Tl) were placed at the beginning, middle and end of sample runs to calibrate the ICP-MS and correct for instrumental drift during the course of the analysis. Additionally, because all samples, including the procedural blanks, were spiked with known concentrations of Be, Th and In, we can correct for matrix effects (drift of sensitivity from the ICP-MS) on an individual sample basis.

Spatially controlled otolith and bone elemental concentrations were analysed using a purpose-built system comprised of a Quantronix Integra C® femtosecond laser operating at the fundamental wavelength of 785 nm (original energy: 0.287 mJ/pulse; energy after pinhole: 0.05 mJ/pulse; pinhole size: 2.5 mm; pulse width: 110 fs; fluence: 13 Jcm⁻²; spot size: 26 μm) coupled to a

Thermo-Elemental® X7® Series II ICP-MS in peak-jumping mode, 10 ms dwell time per isotope except 100 ms for ^{84}Sr and 20 ms for ^{135}Ba (the last 2 isotopes being much less abundant than the others needed more dwell time for precise measurement). We ablated otoliths from the core to the edge, and the bones from one edge to the other.

5.3 RESULTS AND DISCUSSION

5.3.1 Sr and Ba isotopic ratios in water and blood

Water chemistry revealed no change in $^{84}\text{Sr}/^{86}\text{Sr}$ and $^{135}\text{Ba}/^{138}\text{Ba}$ ratios for the duration of the experiment and no significant differences between tanks, control/low and medium/high together (two sample t-test: $p = 0.657$). The average values for these ratios during the 24 week experiment were 0.05329 ± 0.00058 and 0.0815 ± 0.0012 , respectively, showing less than 1% uncertainty in both tanks (Table 5.2). However the amount of enriched Ba and Sr expected to be eliminated by the fish from the gills and the bodies (excretion) is very small. In addition, this amount is then diluted in 1500 litres of flow through water making it nearly impossible for us to pick up an enriched signal by SO-ICP-MS. Natural abundance ratios for $^{84}\text{Sr}/^{86}\text{Sr}$ is 0.0568 and for $^{135}\text{Ba}/^{138}\text{Ba}$ is 0.0919 (calculated from relative abundance ratios), our measured results are slightly lower than expected yet within the experimental error for Sr but not Ba. These variations are likely due uncorrected mass bias effects in the ICP-MS during the experimental run.

Blood samples were collected at day 130 of the experiment and $^{135}\text{Ba}/^{138}\text{Ba}$ ratios are shown in Table 5.2. However, the $^{84}\text{Sr}/^{86}\text{Sr}$ ratios could not be calculated for blood as there was interference on the ^{84}Sr isotope. This interference on the 84 mass probably came from residual proteins in the decomposed organic matrix. Ba isotopic ratios were statistically similar when comparing the 4 treatments (Anova: $p = 0.136$). These results demonstrate no significant differences in enriched Ba isotopes between treatments which imply that this enriched isotope (^{135}Ba) is not circulating 5 months after the injections indicating a complete turnover in the blood.

5.3.2 Otolith, bone and body chemistry

The $^{84}\text{Sr}/^{86}\text{Sr}$ ratios in control fish otoliths show a very stable signal (averaging: 0.0558 ± 0.0022) for the duration of the experiment (Fig 5.2a). However, the $^{135}\text{Ba}/^{138}\text{Ba}$ ratio peaks for some fish of the control group (for 4 fish out of 9) are enriched. Considering the tank setting (Fig. 5.1), this increase in ^{135}Ba is probably coming from the excretion of enriched barium isotope in the water from the bodies of the low level fish. Also, there is a possibility that the control fish were feeding on the feces of the low level fish (hence an increase in ^{135}Ba which was injected at a higher dose than ^{84}Sr).

The low, medium and high treatments exhibit the same typical otolith graph for Ba and Sr (Figs. 5.2b-d) where the enriched isotope ratio begins to rise immediately after the injection. The maximum $^{84}\text{Sr}/^{86}\text{Sr}$ ratio observed in the treated fish increases from low to high treatment from 0.0858 ± 0.0100 to $1.98 \pm$

0.029 (Table 5.2). Interestingly, the same does not apply for Ba as the medium treatment fish have a higher $^{135}\text{Ba}/^{138}\text{Ba}$ ratio average (28.3 ± 4.6) than the high dose treatment otoliths, 25.6 ± 6.1 but with the standard deviation their values overlap (Table 5.2). The medium treatment fish were injected with a solution that was half the concentration of the enriched isotopes injected to the high treatment fish. Despite this fact, we do not observe a significant difference in their otolith composition. There are several hypotheses to explain this behaviour. Our highest dose appears to be so high and potentially toxic to the fish so that it would then try to defend itself against harmful metals and would sequester some of the Ba and decrease its incorporation in the otolith. Several papers have shown that the tripeptide glutathione and other enzymes such as the liver catalase (CAT) were known to increase with metal exposure (Alti and Canli 2008, 2007). Therefore, Ba is not enriched as highly in the endolymph (at the highest dose) and could be present in the bones and other tissues at higher concentrations.

Another factor impacting the level of Ba in the otoliths could be related to the tank setting of the medium/high treatment fish which is the same as the control/low treatments setting (fish feeding on the feces of the higher treatment they are paired with). We also notice that even 5 months after injection, the enriched isotope ratios still have not gone back to the levels of pre-injections ratios for all treatments, except in the controls (Fig. 5.2).

Figure 5.3 shows in more detail one fish from the high level treatment. This otolith demonstrates the differences in Ba and Sr reaction time to the injection. The $^{135}\text{Ba}/^{138}\text{Ba}$ ratio increases right after the injection while the

$^{84}\text{Sr}/^{86}\text{Sr}$ enrichment was delayed for 3-5 days (Fig. 5.3). Investigation on all the fish from the 3 treatments showed that this behaviour is not a consistent phenomenon as Sr enrichment can precede Ba in some fish.

We also noticed differences in time (days) for reaching the maximum in Sr and Ba ratios. For this particular fish, barium's maximum is reached 10 days before Sr peaks (Fig. 5.3). The medium and high treatments showed similar behaviours, having a number of fish with Ba peaking faster than Sr (med: 4; high: 2) as well as the opposite (med: 1; high: 3) and having both ratios reaching their maximum at the same time (med: 4; high: 4). The low level treatment had a majority of fish (8) with their Sr and Ba ratio reaching maximums on the same day. Since Sr and Ba from fish of the lower treatment react the same way while the medium and high treatments show more variations, we can suspect that stress is affecting the metabolism of these fish and is responsible for these discrepancies.

We previously noted that 5 months after injection, Sr and Ba ratios in the otoliths had still not reached pre-injection levels for the low, medium and high treatment (Fig. 5.2). In Figure 5.3, we notice that when we sampled fish in July, the enriched Sr had been reduced from the growing otolith by 97.7 % while Ba was by 94.9%. At the end of the experiment both ratios had been reduced by another 2% of their enriched isotopes in the otolith (Sr 99.4% and Ba 97.1 %).

The analysis of fish bones by LA-ICP-MS (Fig. 5.4) provide some insights on what might be happening in otoliths, as Ba and Sr are highly sequestered in the bones of the high, medium and low level treatments thus are not available for

circulation to the endolymph and otolith (Fig. 5.5). Results for both isotopic ratios of Sr and Ba, are statistically different between the treatments (Anova: $p = 0.003$ and 0.002 respectively). The control fish bones have very stable and consistent ratios, averaging 0.051 ± 0.009 for $^{84}\text{Sr}/^{88}\text{Sr}$ and 0.101 ± 0.025 for $^{135}\text{Ba}/^{138}\text{Ba}$ (Fig. 5.5a) which are near the natural abundance ratios (Table 5.1).

All treatment fish show a clear increase in their bone ratios compared to the control fish bone averages, full and dotted line (see Figs. 5.5b-d). The low treatment has Sr and Ba ratios slightly higher than the control fish while the medium and high treatments are very enriched (Fig. 5.5b). The only difference between the medium and high level treatment relates to the beginning of barium and strontium elimination in the medium level bones. Incorporation of the injected Sr and Ba by the bone further explains why both elements are not more enriched in the otolith as most of it is sequestered in the bones and bodies and thus not circulating in the blood.

The ionic radius of Sr (1.32 \AA) is closer in size to Ca (1.14 \AA) and is probably incorporated in the bone apatite structure ($\text{Ca}_5(\text{PO}_4)_3$) while Ba is a larger cation (1.49 \AA) and may be bound differently (Shannon 1976). Since the endolymph composition comes from ionic transfer from the plasma through the saccular membrane, if both enriched isotopes are not available in the blood they cannot access the endolymph and the otolith (Payan et al. 1997). We suspect the enriched isotopes largely reached the endolymph in a one time pulse shortly after the fish were injected, since the turnover rate of the enriched isotopes in the blood is very fast, and that the otolith then incorporated what was in the

endolymph from that pulse, until it is all eliminated and regains equilibrium with natural Sr and Ba.

Whole body results from all 4 treatments, in July and October, revealed that Sr and Ba ratios were both significantly different for each time (Anova: both $p < 0.0001$). For the control fish, Sr and Ba isotopic ratios in July were the same as the ones in October (Table 5.2). There was a reduction of 15% in the low level fish while the medium and high treatments had decreased approximately 45% in 3 months. In both July and October, the isotopic ratios of Sr and Ba increased from the low to the high treatment. Interestingly, for Ba, the low treatment ratio was 10% of the high treatment ratio and the medium treatment was 50% which is what we would expect according to the injected ratio as the proportions of metals that were injected were retained (Table 5.1).

We calculated the Sr and Ba total body ratio that the fish would have right after the injection using the isotopic mixture equations below (showed for Sr only but calculated for Ba the same way):

$$(^{84}\text{Sr}/^{86}\text{Sr})_{\text{Total Body}} = (^{84}[\text{Sr}]_{\text{Fish}} + ^{84}[\text{Sr}]_{\text{injection}}) / (^{86}[\text{Sr}]_{\text{Fish}} + ^{86}[\text{Sr}]_{\text{injection}}) \quad (1)$$

$$\left(\frac{^{84}\text{Sr}}{^{86}\text{Sr}} \right)_{\text{Total Body}} = \frac{([\text{Sr}]_{\text{fish}} * m_{\text{fish}} * \text{AN}_{84\text{Sr}}) + ([\text{Sr}]_{\text{injection}} * m_{\text{injection}} * \text{AI}_{84\text{Sr}})}{([\text{Sr}]_{\text{fish}} * m_{\text{fish}} * \text{AN}_{86\text{Sr}}) + ([\text{Sr}]_{\text{injection}} * m_{\text{injection}} * \text{AI}_{86\text{Sr}})} \quad (2)$$

Where [Sr] is the concentration (Table 5.3), m is the mass, AN is the natural abundance ratio in the fish and AI is the enriched isotope abundance ratio (Table 5.1). Our calculations for an average fish (weighed at time of injection) in

the high dose treatment gives 0.341 for $^{84}\text{Sr}/^{86}\text{Sr}$ ratio and 10.2 for $^{135}\text{Ba}/^{138}\text{Ba}$. The whole body ratio values in July were 0.331 ± 0.062 for Sr and 7.03 ± 0.86 for Ba (Table 5.2). From the calculated total body maximums, our body ratios in July show a 65% enriched isotope loss for Sr and 55% loss for Ba. At the end of the experiment, the fish bodies were still highly enriched in Sr (15%) and Ba (25%).

Overall, our results indicate that both enriched isotopes of Ba and Sr seem to be going through a similar process when they are injected in the fish's body. The fast elimination of Ba from the blood can be explained by its incorporation in the bone and elsewhere in the fish's body while Sr is not as highly enriched in the bone (Figure 5.6). The partition coefficient between the endolymph and otolith is larger for Sr as it is a major replacement ion for calcium in the CaCO_3 otolith while Ba is usually introduced in the crystal structure in minor amounts (Melancon 2008 -Chapter 4). All of these factors contribute to the reduced incorporation of Sr compared to Ba in the otolith.

5.3.3 Implications

Predicting fish recruitment and larval dispersion and connectivity is a major challenge for fisheries management (Sale et al. 2005). Our results show that both Sr and Ba isotope turnover rates in the otolith would be long enough to be useful as a chemical tracker for fish recruitment. However, once the fish has been injected and an isotopic signature is created in the otolith it takes months before the fish re-equilibrates with its environment. During our 6 month experiment, the otolith enriched isotopic signature for Sr and Ba was reduced by

96-99% but the isotope ratios in the bones and body were still very high. After a perturbation like this, otolith chemistry does not seem to be very sensitive to small scale environmental change. We can speculate that during this time the fish is not in equilibrium with its environment and is just trying to get back to homeostasis. The fact that the fish whole body is highly isotopically enriched is a cause of concern as these fish are important commercially and recreationally. Fish accumulate heavy metals in higher concentrations in their tissues and consumption of these spiked fish might be toxic for humans (Kraal et al. 1995). Unfortunately, there is no regulation or standards on accepted levels of Sr and Ba in the fish, in order to protect human health and the fish.

5.4 ACKNOWLEDGEMENT

We would like to acknowledge the following people: Zhaoping Yang for all her help in preparing the isotopic solutions and ICP-MS analysis, Todd Leadley for setting up the tanks at the GLIER aquatic facility and help during the fish injections and Caroline Dennis for fish dissections and otolith polishing. We thank the National Sciences and Engineering Research Council (Discovery Grant to B.J. Fryer), the University of Windsor and the Great Lakes Institute for Environmental Research for supporting for this research.

5.5 REFERENCES

- Alti, G. and Canli, M. 2008. Responses of metallothionein and reduced glutathione in a freshwater fish *Oreochromis niloticus* following metal exposures. *Environ. Toxicol. Pharmacol.* **25**: 33-38.
- Alti, G. and Canli, M. 2007. Enzymatic responses to metal exposures in freshwater fish *Oreochromis niloticus*. *Comp. Biochem. Physiol.* **145C**: 282-287.
- Barnett-Johnson, R., Ramos, F.C., Grimes, C.B. and MacFarlane, R.B. 2005. Validation of Sr isotopes in otoliths by laser ablation multicollector inductively coupled plasma mass spectrometry (LA-MC-ICPMS): opening avenues in fisheries science applications. *Can. J. Fish. Aquat. Sci.* **62**: 2425-2430.
- Guy, C.S., Blankenship, H.L. and Nielson, L.A. 1996. Tagging and marking. *In*:

- B.R. Murphy & D.W. Willis (eds) Fisheries Techniques, 2nd edn. Bethesda, Maryland: American Fisheries Society, pp. 353–379.
- Hobbs, J.A., Yin, Q., Burton, J.E. and Bennett, W.A. 2005. Retrospective determination of natal habitats for an estuarine fish using otolith strontium isotope ratios. *Mar. Fresh. Res.* **56**: 1-6.
- Kennedy, B.P., Klaue, A., Blum, J.D., Folt, C.L., and Nislow, K.H. 2002. Reconstructing the lives of fish using Sr isotopes in otoliths. *Can. J. Fish. Aquat. Sci.* **59**(6): 925–929.
- Kennedy, B.D., Folt, C.L., Blum, J.D., and Chamberlain, C.P. 1997. Natural isotope markers in salmon. *Nature (Lond.)*, **387**: 766–767.
- Kraal, M.H., Kraak, M.H.S., de Groot, C.J. and Davids, C. 1995. Uptake and tissue distribution of dietary and aqueous cadmium by carp (*Cyprinus carpio*). *Ecotoxicol. Environ. Saf.* **31**: 179–183.
- Ludsin, S.A., Fryer, B.J., Yang, Z., Melancon, S., and Markham, J.L. 2004. Exploration of the existence of natural reproduction in Lake Erie lake trout using otolith microchemistry. Fisheries Research project completion report, Great Lakes Fisheries Commission, Ann Arbor, MI.
- Melancon, S. 2008. Mechanisms controlling the microchemistry and composition of fish otoliths. Ph.D. Thesis, University of Windsor, Windsor.
- Melancon, S., Fryer, B.J., Gagnon, J.E., Ludsin S.A. and Yang, Z. 2005. Effects of crystal structure on the uptake of metals by lake trout *Salvelinus namaycush*. otoliths. *Can. J. Fish. Aquat. Sci.* **62**: 2609-2619.

- Payan, P., Kossmann, H., Watrin, A., Mayer-Gostan, N. and Bœuf, G. 1997. Ionic composition of endolymph in teleosts: Origin and importance of endolymph alkalinity. *J. Exp. Biol.* **200**: 1905-1912.
- Sale, P.F., Cowen, R.K., Danilowicz, B.S., Jones, G.P., Kritzer, J.P., Lindeman, K.C., Planes, S., Polunin, N.V.C., Russ, G.R., Sadovy, Y.J. and Steneck, R.S. 2005. Critical gaps impede use of no-take fishery reserves. *Trends Ecol. Evol.* **20**:74–80.
- Shannon, R.D. 1976. Revised effective ionic radii and systematic studies of interatomic distances in halides and chalcogenides. *Acta Crystallogr.* **A32**: 751.
- Thorrold, S.R., Jones, G.P., Planes, S. and Hare, J.A. 2006. Transgenerational marking of embryonic otoliths in marine fishes using barium stable isotopes. *Can. J. Fish. Aquat. Sci.* **63**:1,193–197.
- Thorrold, S.R., Jones, G.P., Hellberg, M.E., Burton, R.S., Swearer, S.E., Neigel, J.E., Morgan, S.G., and Warner, R.R. 2002. Quantifying larval retention and connectivity in marine populations with artificial and natural markers. *Bull. Mar. Sci.* **70**: 291-308.
- Vuorinen, P. J., Nyberg, K. and Lehtonen, H. 1998. Radioactive strontium (^{85}Sr) in marking newly hatched pike and success of stocking. *J. Fish Biol.* **52**: 268-280.

Table 5.1: Composition of the injections for Sr and Ba ratios and the amount of enriched ^{84}Sr and ^{135}Ba isotopes injected (μg per g of fish).

		Control	Low	Medium	High
Quantity	^{84}Sr	0	0.0759	0.399	0.797
	^{135}Ba	0	0.630	3.32	6.62
Ratios	$^{84}\text{Sr}/^{86}\text{Sr}$	0.0568	22.2	22.2	22.2
	$^{135}\text{Ba}/^{138}\text{Ba}$	0.0919	26.2	26.2	26.2

Table 5.2: Measured values for the average $^{84}\text{Sr}/^{86}\text{Sr}$ and $^{35}\text{Ba}/^{138}\text{Ba}$ ratios in water, fish blood (except for Sr), whole bodies (July and October) and otoliths (July, October and maximum) of yellow perch (*Perca flavescens*). Ratios are calculated considering the sensitivity factor matrix of each isotope and are the average of the number of ratios (\pm standard deviation). N is the number of samples analysed per treatment (except for water where control/low and medium/high were in the same tank). Otolith data was analysed by LA-ICP-MS while all the other parameters were analysed by SO-ICP-MS.

Sample	N	Ratio	Control	Low	Medium	High
Water	24	$^{84}\text{Sr}/^{86}\text{Sr}$	0.05326 \pm 0.00063	0.05326 \pm 0.00063	0.05332 \pm 0.00056	0.05332 \pm 0.00056
		$^{135}\text{Ba}/^{138}\text{Ba}$	0.0814 \pm 0.0012	0.0814 \pm 0.0012	0.0815 \pm 0.0012	0.0815 \pm 0.0012
Blood	9	$^{84}\text{Sr}/^{86}\text{Sr}$	N/A	N/A	N/A	N/A
		$^{135}\text{Ba}/^{138}\text{Ba}$	0.101 \pm 0.021	0.090 \pm 0.001	0.096 \pm 0.002	0.105 \pm 0.018
Whole Bodies	2	$^{84}\text{Sr}/^{86}\text{Sr}$	0.05517 \pm 0.00001	0.0828 \pm 0.0015	0.218 \pm 0.006	0.331 \pm 0.062
-July		$^{135}\text{Ba}/^{138}\text{Ba}$	0.0970 \pm 0.0002	0.773 \pm 0.026	3.49 \pm 0.47	7.03 \pm 0.86
Whole Bodies	5	$^{84}\text{Sr}/^{86}\text{Sr}$	0.0562 \pm 0.0012	0.0719 \pm 0.0034	0.129 \pm 0.020	0.158 \pm 0.017
-October		$^{135}\text{Ba}/^{138}\text{Ba}$	0.0951 \pm 0.0100	0.488 \pm 0.092	2.50 \pm 0.80	3.50 \pm 0.91
Whole Bones	3	$^{84}\text{Sr}/^{86}\text{Sr}$	0.0546 \pm 0.0003	0.0649 \pm 0.0028	0.105 \pm 0.022	0.0932 \pm 0.0101

-October		$^{135}\text{Ba}/^{138}\text{Ba}$	0.0935 ± 0.0207	0.361 ± 0.109	1.47 ± 0.56	1.08 ± 0.14
Otolith Edge	2	$^{84}\text{Sr}/^{86}\text{Sr}$	0.0541 ± 0.097	0.0621 ± 0.0153	0.319 ± 0.076	0.302 ± 0.078
-July		$^{135}\text{Ba}/^{138}\text{Ba}$	0.0969 ± 0.064	0.221 ± 0.184	5.92 ± 4.3	4.20 ± 1.2
Otolith Edge	9	$^{84}\text{Sr}/^{86}\text{Sr}$	0.0558 ± 0.0022	0.0583 ± 0.0020	0.0738 ± 0.0081	0.0786 ± 0.0096
-October		$^{135}\text{Ba}/^{138}\text{Ba}$	0.0979 ± 0.007	0.189 ± 0.07	0.584 ± 0.3	0.619 ± 0.3
Otolith	9	$^{84}\text{Sr}/^{86}\text{Sr}$	0.0858 ± 0.01	0.483 ± 0.110	1.58 ± 0.46	1.98 ± 0.29
-Maximum		$^{135}\text{Ba}/^{138}\text{Ba}$	0.629 ± 0.9	15.3 ± 4.3	28.3 ± 4.6	25.6 ± 6.1

Table 5.3: Average concentrations for Sr and Ba (calculated from ^{86}Sr and ^{138}Ba intensities) in water, fish blood, whole bodies (July and October) and otoliths (July, October and maximum) of yellow perch (*Perca flavescens*) in ppm ($\mu\text{g/g} \pm$ standard deviation). N is the number of samples analysed per treatment (except for water where control/low and medium/high were in the same tank). Otolith data was analysed by LA-ICP-MS while all the other parameters were analysed by SO-ICP-MS.

Sample	N	Isotope	Control	Low	Medium	High
Water	24	Sr	0.114 \pm 0.027	0.114 \pm 0.027	0.114 \pm 0.029	0.114 \pm 0.029
		Ba	0.0116 \pm 0.0006	0.0116 \pm 0.0006	0.0113 \pm 0.0006	0.0113 \pm 0.0006
Blood	9	Sr	0.160 \pm 0.036	0.150 \pm 0.019	0.133 \pm 0.017	0.147 \pm 0.040
		Ba	0.054 \pm 0.015	0.127 \pm 0.239	0.043 \pm 0.034	0.038 \pm 0.010
Whole Bodies	2	Sr	9.36 \pm 2.0	8.52 \pm 0.08	10.5 \pm 1.9	9.30 \pm 3.4
-July		Ba	0.226 \pm 0.020	0.175 \pm 0.011	0.277 \pm 0.015	0.217 \pm 0.034
Whole Bodies	5	Sr	8.70 \pm 1.08	9.29 \pm 1.89	8.10 \pm 1.07	8.45 \pm 3.51
-October		Ba	0.155 \pm 0.037	0.176 \pm 0.044	0.154 \pm 0.036	0.152 \pm 0.067
Whole Bones	3	Sr	127 \pm 62	217 \pm 82	160 \pm 19	202 \pm 76

-October	Ba		1.44 ±1.11	3.06 ±1.26	2.42 ±0.43	2.82 ±2.31
Otolith Edge	9	Sr	533 ±14	530 ±41	495 ±52	460 ±32
-July	Ba		2.19 ±0.40	3.16 ±1.2	2.49 ±0.99	3.16 ±1.4
Otolith Edge	9	Sr	454 ±60	437 ±55	369 ±34	372 ±38
-October	Ba		1.33 ±0.53	1.35 ±0.35	1.37 ±0.33	1.79 ±1.1
Otolith	9	Sr	51.0 ±6.4	55.8 ±7.6	61.8 ±6.5	64.4 ±9.9
-Maximum	Ba		0.124 ±0.033	0.231 ±0.069	0.500 ±0.188	0.547 ±0.228

Figure 5.1: Experimental setting of the tanks. Control and low treatment are in the same tank physically separated by a net. The same setting applies to the medium and high level treatments.

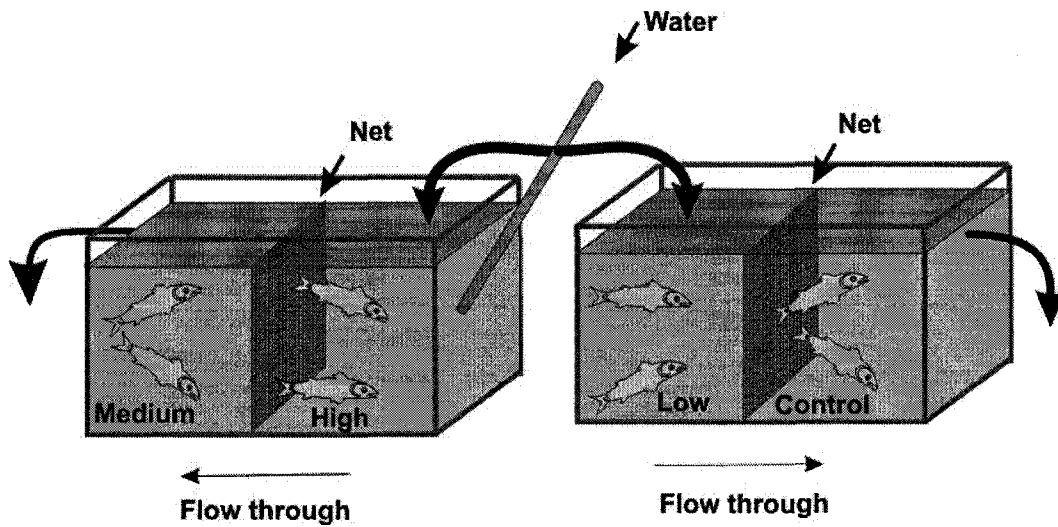


Figure 5.2: Isotopic ratios: $^{84}\text{Sr}/^{86}\text{Sr}$ (\blacktriangle) and $^{135}\text{Ba}/^{138}\text{Ba}$ (\circ) in otoliths of yellow perch (*Perca flavescens*) along the beam transect using laser ablation with inductively coupled plasma mass spectrometry. Distance from the core to the edge of single otoliths from the different treatments a) control, b) low, c) medium and d) high.

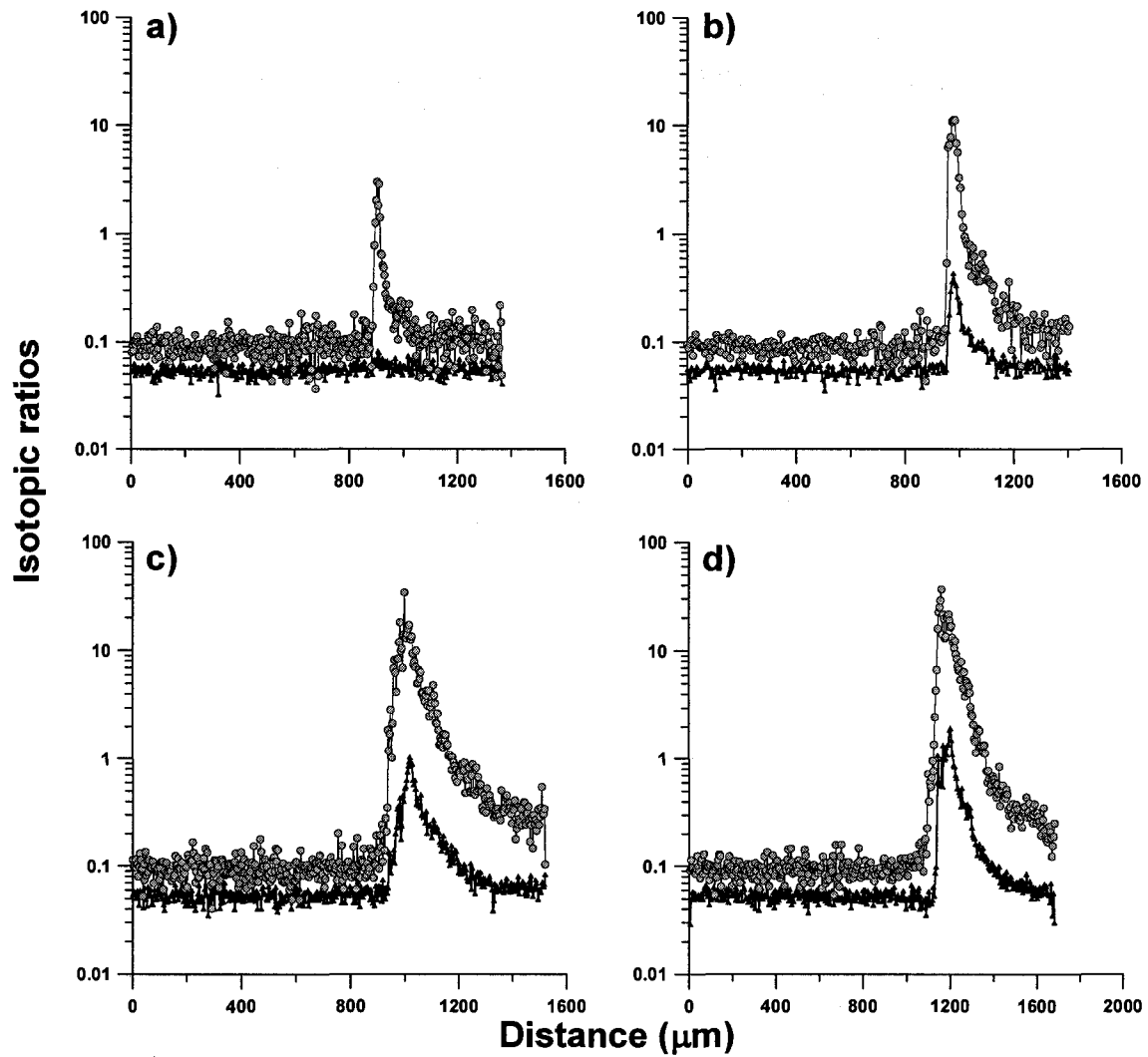


Figure 5.3: An example from the high level treatment of the isotopic ratios: $^{84}\text{Sr}/^{86}\text{Sr}$ (\blacktriangle) and $^{135}\text{Ba}/^{138}\text{Ba}$ (\circ) in otoliths of yellow perch (*Perca flavescens*) against time in days after the injections were administered (Day 0: Inj.). The maximums, fish sampled in July and at the end are shown with appropriate arrows. Dotted line represents average $^{135}\text{Ba}/^{138}\text{Ba}$ ratio in control fish otoliths and full line is the $^{84}\text{Sr}/^{86}\text{Sr}$ ratio

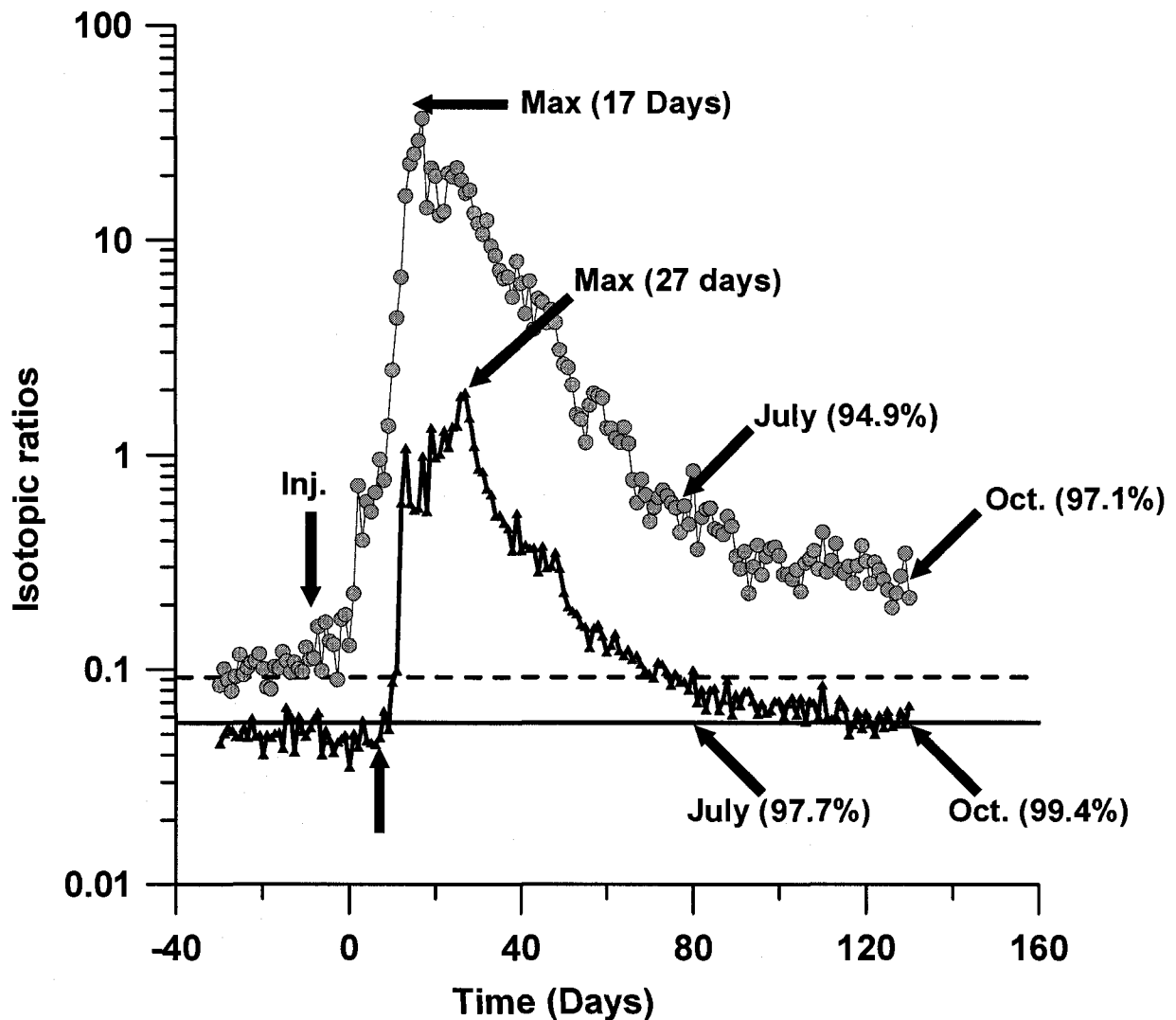


Figure 5.4: Fish bone from the high level treatment, the white arrow represents the path of the laser beam on the bone using LA-ICP-MS

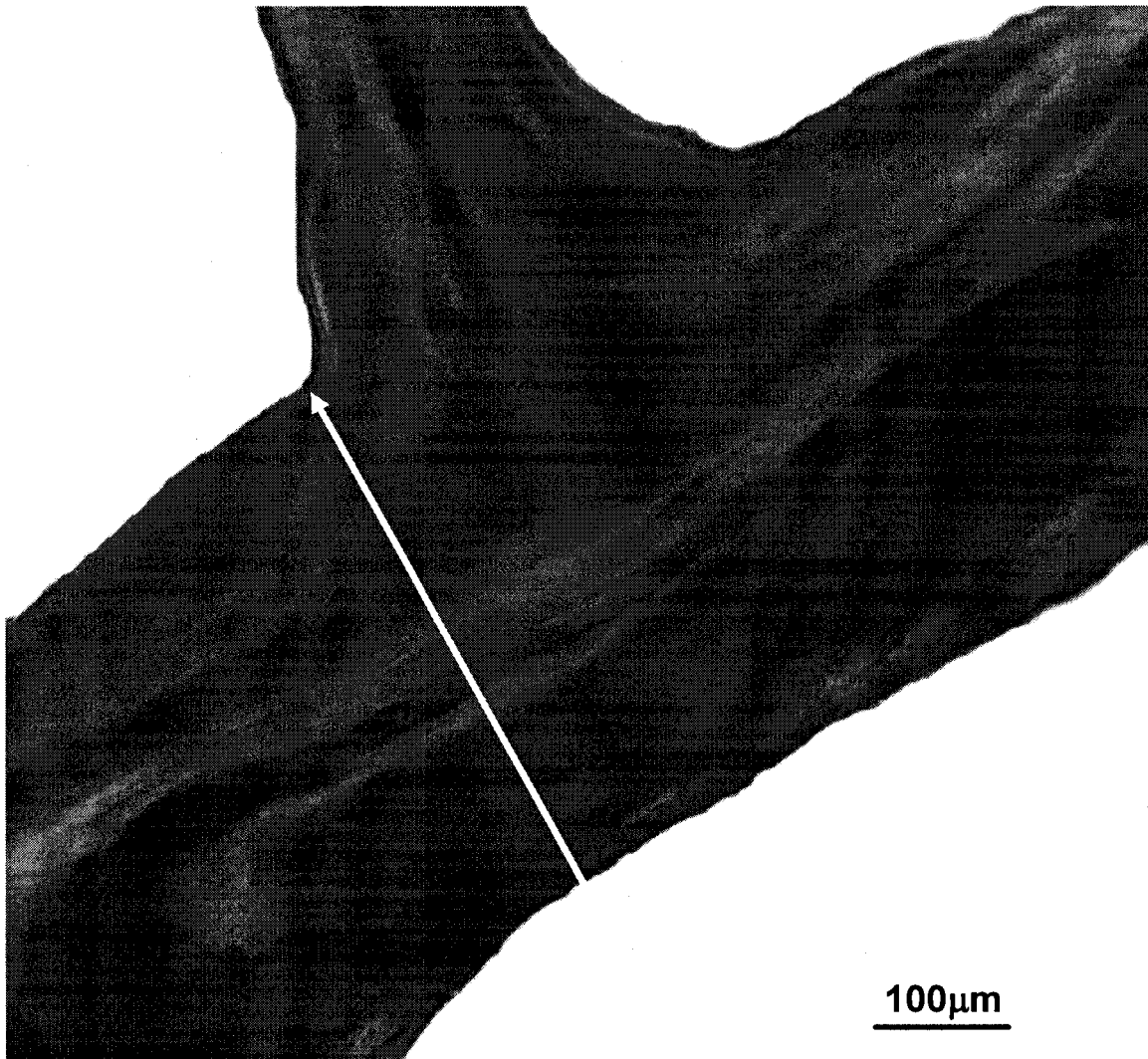


Figure 5.5: Isotopic ratios: $^{84}\text{Sr}/^{86}\text{Sr}$ (\blacktriangle) and $^{135}\text{Ba}/^{138}\text{Ba}$ (\circ) in bones of yellow perch (*Perca flavescens*) along the beam transect using laser ablation with inductively coupled plasma mass spectrometry. Distance is from the one edge of the bone to the other. Each treatment profiled: a) control, b) low, c) medium and d) high. Dotted line represents average $^{135}\text{Ba}/^{138}\text{Ba}$ ratio in control fish bones and full line is the $^{84}\text{Sr}/^{86}\text{Sr}$ ratio.

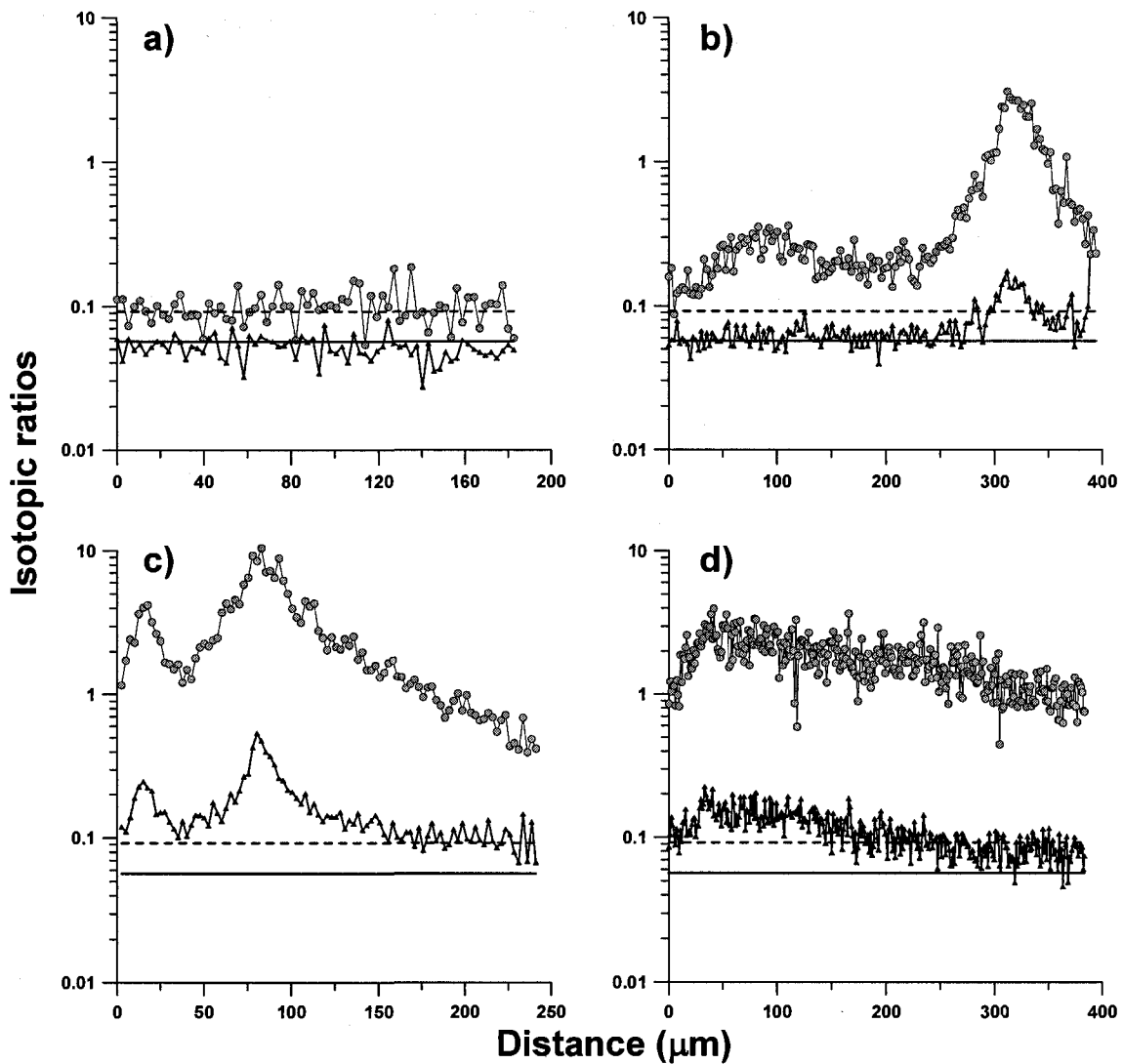
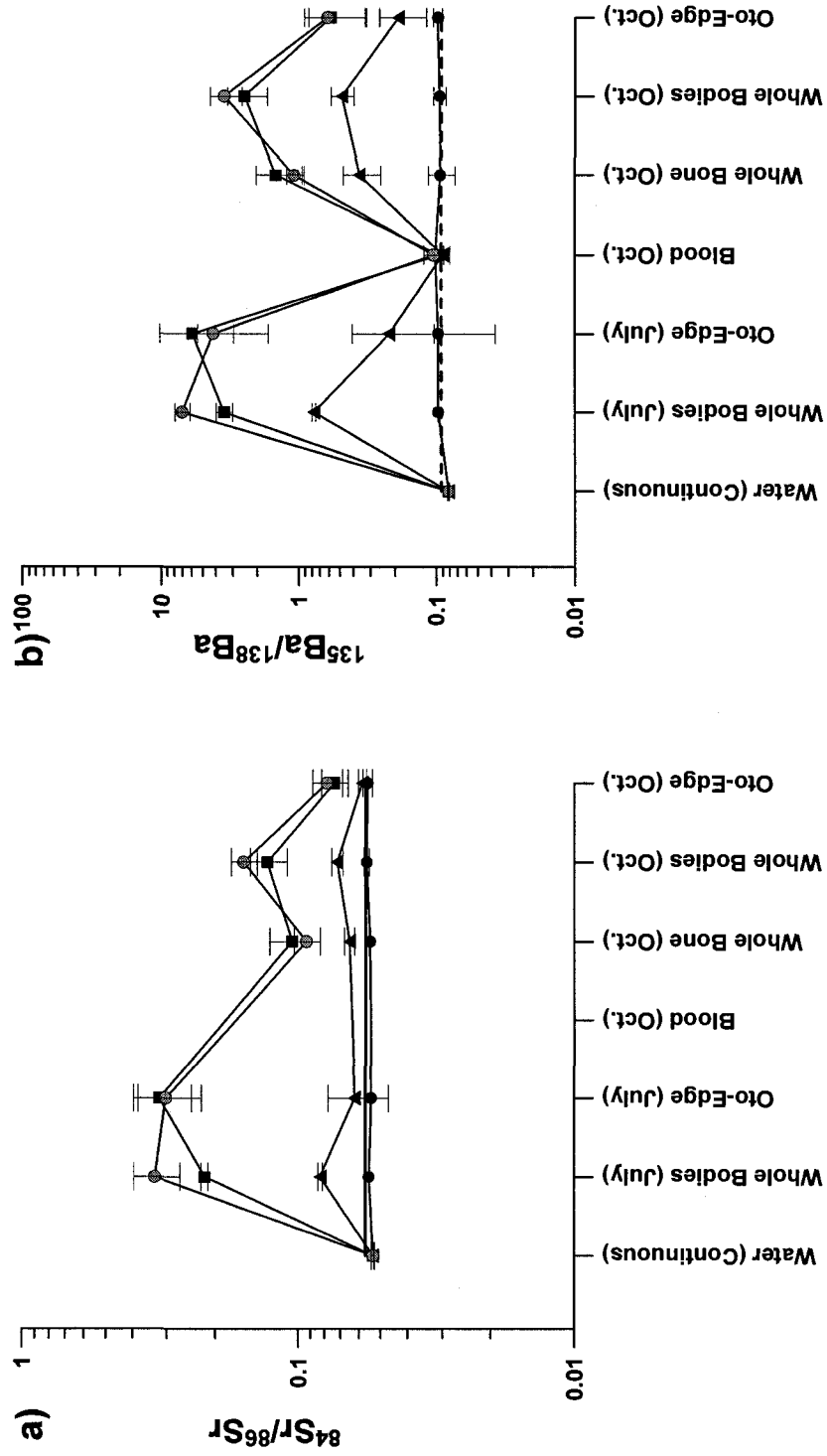


Figure 5.6: a) $^{84}\text{Sr}/^{86}\text{Sr}$ ratios and b) $^{135}\text{Ba}/^{138}\text{Ba}$ ratios in the water, blood (except for Sr), whole bone, whole bodies (July and October) and otolith edge (July and October) for yellow perch. Control (●), low (▲), medium (■) and high treatment (○) are represented. Dotted line represents the natural isotopic $^{135}\text{Ba}/^{138}\text{Ba}$ ratio and full line is the $^{84}\text{Sr}/^{86}\text{Sr}$ ratio.



CHAPTER 6

General Discussion

6.1 INTRODUCTION

Otolith research is a relatively new field, in fact, prior to 1980 only 6 papers were published on this topic (Campana 1999). Within the past decade, otolith time-keeping, structural, and micro-chemical properties have been used for numerous palaeobiology and fisheries-related purposes which include helping to understand stock and sub-population structure and mixing, temperature and salinity histories of oceans, migratory patterns of individuals and populations, and variability in life-history strategies (Thresher 1999). The relationship between otolith and the water is very complex and despite the recent and widespread use of otolith microchemistry in fisheries-related investigations, some unresolved issues have limited the use of this approach to its fullest potential. Most of the research is conducted on the use and applications of otoliths while more research should focus on the mechanisms controlling: otolith growth, polymorphic structure, and inorganic and organic complexes incorporation in the otolith.

6.2 SUMMARY OF THESIS

In my thesis, I tried to address and investigate otolith research areas where information was lacking or had received little attention. In Chapter 2, I explored the mechanisms controlling polymorph growth and how it was affecting metal composition. This was the first study to report spectroscopic and elemental analysis of aragonite and vaterite growing simultaneously and separately in both the core and the edges of the same otolith. My investigations focused on

understanding differential trace metal uptake, including the influence of the metal itself (i.e., ionic radii), the crystalline structure, and the development state of the lake trout (*Salvelinus namaycush*). Analyses of the composition of vaterite and aragonite growing in the same growth ring show that smaller cations like Mg (0.86Å) and Mn (0.81Å) were more abundant in the vaterite hexagonal crystal structure whereas larger cations such as Sr (1.32Å) and Ba (1.49Å) were preferentially incorporated in aragonite (orthorhombic). Similarly, the co-precipitation of aragonite and vaterite in cores and edges allowed us to demonstrate that the uptake rates (as determined by element-specific partition coefficients) for Sr and Ba were greater in aragonite than vaterite, whereas those of Mg and Mn were higher in vaterite than aragonite. Further results on this topic showing how the chemical characteristics of the metal ions (i.e., ionic radii) and the crystalline structure interact to cause differential trace metal uptake between the calcium carbonate polymorphs aragonite and vaterite were shown in Chapter 3.

Researchers believe that clusters of particles originally of an organic matrix origin would presumably set the first stage of otolith biomineralization (Nicholson 2004). Previous studies have found that the otolith elemental core composition is fundamentally different than in other parts of the otoliths (Ruttenberg et al. 2005; Brophy et al. 2004). In Chapter 3, I investigated the biomineralization of otoliths and utilized a mineralogical approach to understand mechanisms of crystal growth and metal incorporation in otoliths. I described the nucleation of otolith growth in the core for several fish species. Microscopic observations have shown that sagittal otoliths appear to nucleate around a few or

many nucleation sites (primordia) and that these sites vary in size depending on the fish species ranging in diameter from 1 to 20 μm . My spectroscopic data showed a high Mn enrichment in the primordia within the core but the reasons for this enrichment are still unclear. Several hypotheses have been suggested such as the presence of an amalgam of bio-metallic macromolecules in the core or possibly another material than calcium carbonate (i.e. rhodochrosite - MnCO_3).

Endolymph composition includes Ca^{2+} , CO_3^{2-} , HCO_3^- , and trace metals. Most of the research done on this fluid has quantified organic compounds but only a few metals: Na, Mg, K, Ca, Sr (Payan et al. 1997; Kalish et al. 1991). In Chapter 3, I provided the first multi-trace element data for endolymph fluid and the growing sagittal otolith of walleye (*Sander vitreus*). In this preliminary experiment, I found large enrichments (Ca and Ba) and depletions (Na, K, Zn and Rb) of elements in the otolith relative to the endolymph. I did a larger scale experiment on the same topic using lake trout (*Salvelinus namaycush*) and burbot (*Lota lota*) endolymph and otoliths (aragonite and vaterite). Water and blood were also sampled during this experiment which allowed me to measure directly the partition coefficients of metals from the water to the otolith. Chapter 4 is one of the rare papers in the literature to publish these kinds of data for freshwater systems (Dorval et al. 2007; Wells et al. 2003). The trace elements (Mg, Sr and Ba) most often used as otolith elemental tracers were the ones with the lowest uptake from the water to the blood. I found that endolymph and whole blood had similar metal concentrations, with Mg and Fe being the only elements enriched in the whole blood. Results showed little significant differences in trace

metal content between wild lake trout and burbot endolymph (except for K, Mg and Ba) but significant differences existed between their aragonitic otoliths. My results suggest two different crystallization processes in these species or the presence of different proteins (and/or organic matrices) which would selectively influence elemental incorporation in the otoliths.

Fish tagging is a popular research area with the use of natural and artificial methods to investigate migration, growth and dispersal (Thorrold et al. 2002). A new and unique attempt at artificial isotopic tagging of otoliths by Thorrold et al. (2006) has brought attention to this field. They successfully marked embryonic otoliths through maternal transmission using an enriched barium isotope. However, they did not track the Ba in the fish's body of the injected fish; they only looked at the Ba signature in the otoliths of the offspring. In Chapter 5 of my thesis, I injected fish with an enriched solution of Sr and Ba isotopes and investigated the effects and elimination of these isotopes on the fish (blood, bones, otoliths and whole body). This is the first investigation of its type, my results indicated that both enriched isotopes of Ba and Sr seemed to be going through a similar process after they were injected in the fish. However, the rates of elimination of these isotopes in the otolith were different which is mainly due to their partition coefficients between the endolymph and otolith ($K_{D O/E}$) being dissimilar. As shown in Chapter 4, the $K_{D O/E}$ of Sr is large as it is an important substitute for calcium in the CaCO_3 structure while Ba is only a minor replacement (Melancon et al. 2005). The blood data shows the fast elimination of Ba which can be explained by its incorporation in the bone and elsewhere in the fish's body while Sr is not as highly enriched in the bone. The final conclusion of

this paper is that both Sr and Ba isotope turnover rates in the otolith would be long enough to be useful as a chemical tracker for fish recruitment. However, after a perturbation like this, otolith chemistry does not seem very sensitive to environmental change as the fish's body is trying to get back to homeostasis and seems to be out of equilibrium with its environment. Lastly, the amounts of enriched isotopes in the fish whole body were high and further investigations should look at the effects on human health as this technique could be use on fish that are important commercially and recreationally.

6.3 CHALLENGES FOR THE FUTURE

There is a clear need for more research on mechanisms controlling microchemistry and composition of fish otoliths. A complete explanation of physiological and chemical processes that determine the micro-chemical composition of otoliths is lacking. Our understanding of how metals are partitioned (fractionated) at each barrier, from the water to the otolith, remains enigmatic. This knowledge gap has limited our ability to understand why imbalances exist between the otoliths and their ambient environment for some elements.

A laboratory experiment that would explore the differences between fish of different age (metabolism) (1) fed with metal-contaminated food versus fish in (2) contaminated water of different levels and another treatment where (3) fish are having both sources of metal exposure and (4) control group without any contamination. There are still significant questions on the origin, food or water, of metals in the fish otolith (Kennedy et al. 2002). To investigate the origin of the

otolith signature, the research should monitor water and sample: blood, endolymph, tissues, organs, bones and otoliths during the experiments. It would also be very interesting to use a species that grows different polymorphs of CaCO_3 in its structure. The analysis of metals as well as proteins and other organic compounds would provide a full description of what might cause changes in the otoliths. The challenge with undertaking that type of experiment resides in having the resources to analyze inorganic and organic compounds (laboratories are usually more specialised in one area), enough tanks to house the different treatments, enough funding to undertake all the analyses, plus finding a species that is easily housed (size of the fish matters) and where a large volume of endolymph can be sampled.

Recent advances in analytical techniques have increased the precision of otolith chemistry results especially for the area of isotopic analysis. The use of the multi collector ICP-MS to track life history of fisheries has been promising (Barnett-Johnson et al. 2005; McCulloch et al. 2005). The use of this instrument to precisely analyse multiple Sr isotopes has the capacity to provide more information than similar elemental studies on freshwater and diadromous fishes (salmon especially). This way broader ecological questions requiring large sample sizes to characterize population dynamics, nursery habitats and stock discrimination can be done.

Some new techniques looking at the atomic scale promise some great imaging for all the different crystallographic structures in the otoliths (e.g. High Resolution Transmission Electron Microscopy (HRTEM) and Time-of-Flight Secondary Ion Mass Spectrometry (TOF-SIMS)).

The identification of proteins associated with the crystallization of different polymorphs is also an area where research is highly restricted by analytical limitations, since the amount of soluble and insoluble proteins in otoliths are very small, 1-5% (Tomás et al. 2004, Pote and Ross 1991). Previous decalcification techniques, using EDTA as a chelating agent, can demetallate the proteins (Borelli et al. 2001). However, Miller et al. (2006) developed a new technique that halted the decalcification reaction which allowed them to extract the intact metal-proteins complexes. This new technique is very interesting as it examines the metals from the protein without incorporating the ones from the CaCO₃ structure or located in the interstitial spaces of the crystal.

Most of the analyses done on the organic matrix in otoliths are done using digested whole otoliths. However, Zhang et al. (2008) recently developed a new in situ Raman microspectroscopy technique that maintained the spatial resolution of the otolith. They investigated the regular variations of major collagens, aromatic amino acids and tryptophan deposition.

One area that remains under studied is the research on the preparation of a new reference material matching the otolith calcium carbonate matrix for laser ablation ICP-MS analysis. Bellotto and Mickleley (2000) found that glass standards had poor sensitivity curves and that they overestimated trace elements from CaCO₃ matrices. In order to remedy this situation, researchers worked on CaCO₃ pressed powder pellet spiked with trace elements (Pearce et al. 1972; Perkins et al. 1991; Bellotto and Mickleley 2000). The production of a homogenous standard has proved difficult to obtain due to the low metal concentration needed for environmental matrices which leaves us with no other

options than using a NIST glass standard as reference material for LA-ICP-MS. However a powdered reference material prepared by Sturgeon et al. (2005) from sagittal red snapper (*Lutjanus campechanus*) otoliths can be use for isotope dilution-ICP-MS as well as one prepared by Yoshinaga et al. (2000) from the emperor red snapper (*Lutjanus sebae*) otoliths.

Finally, otoliths research is truly a multi-disciplinary research field and I think that I pointed out that several issues need to be addressed in all of the following disciplines: chemistry, geology (mineralogy), physiology and biology until we know exactly how otoliths biomineralize, grow and what influences their composition.

6.4 REFERENCES

- Borelli, G., Mayer-Gostan, N., De Pontual, H., Bœuf, G., and Payan, P. 2001. Biochemical relationships between endolymph and otolith matrix in the trout (*Oncorhynchus mykiss*) and turbot (*Psetta maxima*). *Calcif. Tissue Int.* **69**: 356-364.
- Brophy, D., Jeffries, T.E. and Danilowicz, B.S. 2004. Elevated manganese concentrations at the cores of clupeid otoliths: possible environmental, physiological, or structural origins, *Mar. Biol.* **144**: 779-786.
- Campana, S.E. 1999. Chemistry and composition of fish otoliths: pathways, mechanisms and applications. *Mar. Ecol. Prog. Ser.* **188**: 263-297.
- Dorval, E., Jones, C.M., Hannigan, R., and van Montfrans, J. 2007. Relating otolith chemistry to surface water chemistry in a coastal plain estuary. *Can. J. Fish. Aquat. Sci.* **64**: 411-424.
- Kalish, J.M. 1991. Determinants of otolith chemistry: seasonal variation in the composition of blood plasma, endolymph, and otoliths of bearded rock cod *Pseudophycis barbatus*. *Mar. Ecol. Prog. Ser.* **74**: 137–159.
- Kennedy, B.P., Klaue, A., Blum, J.D., Folt, C.L., and Nislow, K.H. 2002. Reconstructing the lives of fish using Sr isotopes in otoliths. *Can. J. Fish. Aquat. Sci.* **59**(6): 925–929.
- Melancon, S., Fryer, B.J., Gagnon, J.E., Ludsins S.A. and Yang, Z. 2005. Effects of crystal structure on the uptake of metals by lake trout *Salvelinus namaycush*. otoliths. *Can. J. Fish. Aquat. Sci.* **62**: 2609-2619.

- Miller, M.B., Clough, A.M., Batson, J.N. and Vachet, R.W. 2006. Transition metal binding to cod otolith proteins. *J. Exp. Mar. Biol. Ecol.* **329**: 135-143.
- Nicolson T. 2004. Control of crystal growth in biology: a molecular biological approach using zebrafish. *Crystal Growth Des.* **4**(4): 667-669.
- Payan, P., Kossman, H., Watrin, A., Mayer-Gostan, N., and Bœuf, G. 1997. Ionic composition of endolymph in teleosts: origin and importance of endolymph alkalinity. *J. Exp. Biol.* **200**: 1905-1912.
- Pote, K.G., and Ross, M.D. 1991. Each otoconia polymorph has a protein unique to that polymorph. *Comp. Biochem. Physiol.* **98B**: 287-295.
- Ruttenberg B.I., Hamilton S.L., Hickford M.J.H., Paradis G.L., Sheehy M.S., Standish J.D., Ben-Tzvi O., Warner R.R. 2005. Elevated levels of trace metal elements in cores of otoliths and their potential for use as natural tags. *Mar. Ecol. Prog. Ser.* **297**: 273-281.
- Sturgeon, R.E., Willie, S.N., Yang, L., Greenberg, R., Spatz, R.O., Chen, Z., Scriver, C., Clancy, V., Lam, J.W. and Thorrold, S. 2005. Certification of a fish otolith reference material in support of quality assurance for trace element analysis. *J. Anal. Atom. Spectro.* **20**(10): 1067-1071.
- Thorrold, S.R., Jones, G.P., Planes, S. and Hare, J.A. 2006. Transgenerational marking of embryonic otoliths in marine fishes using barium stable isotopes. *Can. J. Fish. Aquat. Sci.* **63**:1,193–197.
- Thorrold, S.R., Jones, G.P., Hellberg, M.E., Burton, R.S., Swearer, S.E., Neigel, J.E., Morgan, S.G., and Warner, R.R. 2002. Quantifying larval retention and connectivity in marine populations with artificial and natural markers. *Bull. Mar. Sci.* **70**: 291-308.

- Tomás, J., Geffen, A.J., Allen, I.S., Berges, J. 2004. Analysis of the soluble matrix of vaterite otoliths of juvenile herring (*Clupea harengus*): do crystalline otoliths have less protein? *Comp. Biochem. Physiol.* **139A**:301-308.
- Thresher, R.E. 1999. Elemental composition of otoliths as a stock delineator in fishes. *Fish. Res.* **43**: 165–204.
- Yoshinaga, J., Nakama, A., Morita, M. and Edmonds, J.S. 2000. Fish otolith reference material for quality assurance of chemical analyses. *Mar. Chem.* **69**: 91–97.
- Wells, B.K., Rieman, B.E., Clayton, J.L., Horan, D.L., and Jones, C.M. 2003. Relationships between water, otolith, and scale chemistries of westslope cutthroat trout from the Coeur d'Alene River. Idaho: the potential application of hard-part chemistry to describe movements in freshwater. *Trans. Am. Fish. Soc.* **132**: 409–424.
- Zhang, F., Cai, W., Sun, Z. and Zhang, J. 2008. Regular variations in organic matrix composition of small yellow croaker (*Pseudociaena polyactis*) otoliths: an in situ Raman microspectroscopy and mapping study. *Anal. Bioanal. Chem.* **39**: 777-782.

APPENDIX A

Copyright release

From: "Landriault, Roxanne" <Roxanne.Landriault@nrc-cnrc.gc.ca>

Subject: RE: Permission to reprint an article in a Ph.D. thesis

Date: Mon, 10 Mar 2008 07:40:25 -0400

To: <melanco@uwindsor.ca>

Permission is granted for use of the material, as described below, provided that acknowledgement is given to the source.

Sincerely

Mike Boroczki

Business Manager

NRC Research Press

Tel: 613-993-9108

Fax: 613-952-7656

----- Original Message -----

From: Melançon Sonia

To: cjfas@utoronto.ca

Sent: Saturday, March 08, 2008 9:00 AM

Subject: Permission to reprint an article in a Ph.D. thesis

Hi Ms. Foster

I am currently finishing my Ph.D. thesis and need to get the permission of the National Research Council of Canada to reprint a first author paper that was published in 2005:

Melançon S., B.J. Fryer, J.E. Gagnon, S.A. Ludsin and Z. Yang. 2005. Effects of crystal structure on the uptake of metals by lake trout (*Salvelinus namaycush*) otoliths. Canadian Journal of Fisheries and Aquatic Sciences. 62: 2609-2619.

I don't know if you have a standard procedure for this kind of demand but I am sure a simple e-mail would suffice for the Office of Grad studies here at the University of Windsor.

Thank you in advance,

Sonia

Sonia Melançon MCIC

Ph.D. Candidate, Environmental Chemistry & Toxicology

Great Lakes Institute for Environmental Research (GLIER)

University of Windsor, 401 Sunset Ave., N9B 3P4, Windsor, Ontario, Canada

VITA AUCTORIS

NAME: Sonia Melançon

PLACE OF BIRTH: Montréal, Québec

YEAR OF BIRTH: 1980

EDUCATION: Collège Ville-Marie, Montréal, Québec
1992-1998
Diplôme Études Secondaires International

Collège Maisonneuve, Montréal, Québec
1998-2000
Diplôme Études Collégiales, Sciences de la Santé

Université de Montréal, Montréal, Québec
2000-2003
B.Sc. Chemistry

University of Windsor, Windsor, Ontario
2003-2008
Ph.D. Environmental Sciences